An experimental study of bedload transport in partially ice-covered channels

by

Mina Rouzegar

Thesis submitted to the Faculty of Graduate Studies of
the University of Manitoba
in partial fulfillment of the requirements for the degree of

Doctor of Philosophy

Department of Civil Engineering
University of Manitoba
Winnipeg, Manitoba, Canada

Abstract

The onset of winter in cold climates often leads to the formation of border ice along riverbanks, a phenomenon that can persist for a significant portion of the winter season, thereby affecting river channels' dynamics and geomorphological structure. Understanding the effects of ice cover on sediment transport and bed morphology is crucial, as these elements significantly influence flow resistance and river behavior. While there is extensive literature on sediment transport and bed morphology in open channel flow and several studies in conditions of complete ice cover, research in partially ice-covered channels is sparse.

To address this gap, the current study conducted laboratory experiments at the Hydraulics Research and Testing Facility at the University of Manitoba, Canada. The research aimed to explore the effects of border ice, including the extent of ice cover, variations in flow strength, and the asymmetry of border ice on bedload transport rate and distribution, as well as bed morphology and bedform characteristics. Various experimental setups, ranging from open channel flows to symmetric and asymmetric border ice and fully ice-covered conditions, were analyzed to assess bedform dimensions and bedload transport rates against theoretical models in the literature. This comparison confirmed the reliability of the models in describing bedform features under varying ice conditions. Moreover, despite noticeable differences in bedload transport rates across the channel width, in partially ice-covered conditions, the cross-section-averaged bedload transport rate could still be accurately estimated using conventional equations adapted for open channel and fully ice-covered flows by adjusting for the additional boundary created by the ice in the calculation of the wetted perimeter.

The findings also demonstrate that the presence, positioning, and varying extents of partial ice cover significantly influence bedforms within the channel and the distribution of bedload transport. Notably, the impact of ice coverage is more pronounced at lower flow strengths and diminishes as flow strength increases. This research provides essential insights into the complex interactions between ice cover and sediment transport.

Publications Associated with this Research

Peer Reviewed Publications

Rouzegar M. and Clark S.P. (2023) "Experimental investigation of sediment transport in partially ice-covered channels", International Journal of Sediment Research, 38, 5, 769-779

Rouzegar M. and Clark S.P. (2023) "Sediment transport beneath a simulated partial ice cover: Effects of asymmetric border ice" Water, 15(23)

Peer Reviewed Publications (in revision):

Rouzegar, M. and Clark, S.P. (in revision) "An experimental study into the bedform morphology in partially ice-covered channels", Journal of Cold Regions Science and Technology

Conference Proceedings:

Rouzegar M. and Clark S.P. (2022) "Sediment transport rate estimation in partially ice-covered channels", 26th IAHR International Symposium on Ice, Montréal, Canada – 19-23 June 2022

Rouzegar M. and Clark S.P. (2023) "Experimental investigation of border ice effect on bedform development" 22nd Workshop on the Hydraulics of Ice-Covered Rivers, July 9-12, 2023, Canmore, Alberta, Canada

Rouzegar M. and Clark S.P. (2023) "Experimental Investigation of Asymmetric Border Ice Effect on Sediment Transport" Proceedings of the 40th IAHR World Congress, 21-25 August 2023, Vienna, Austria

Acknowledgments

I would like to express my profound gratitude to my supervisor, Dr. Shawn Clark, for his unwavering support, understanding, guidance, and direction throughout my PhD journey. Shawn, you have taught me to strive to be the best version of myself and have shown fairness and kindness beyond measure. I have thoroughly enjoyed working under your mentorship, and I am continually inspired by your passion for water resources and river ice engineering. Under your guidance, I have experienced significant professional and personal growth.

I am also grateful to my committee members, Dr. Karen Dow and Dr. Masoud Asadzadeh, for their constructive and supportive feedback, which has significantly enhanced the quality of this thesis.

My heartfelt thanks go to my research group and my academic family. This doctoral journey was made easier and enjoyable because of your camaraderie. The years spent with you have been the most memorable, filled with learning and friendship. This healthy atmosphere and wonderful group were made possible by the dedicated efforts and support of Shawn and Karen. I would also like to extend special thanks to Alex Wall for his assistance with the experimental setup.

I would like to acknowledge the generous funding provided by the Natural Sciences and Engineering Research Council of Canada, which was essential for the completion of this research.

Finally, my deepest appreciation goes to my loving and supportive family. To my parents, thank you for believing in me and being a constant source of inspiration and strength. Your unwavering support has been the cornerstone of my achievements, and I would not be here today without you. To my brothers, thank you for always being there and encouraging me to move forward.

Thank you all for being integral to this significant phase of my life.

Table of Contents

List of Figures

List of Tables

Nomenclature

A	cross-sectional flow area
b	flume width
B_l	border ice width-left
B_r	border ice width-right
C	coverage ratio
D	particle diameter
E_{rms}	root-mean-square relative error
Fr	Froude number
g	gravitational acceleration
G	dried mass of sediment
h	flow depth
H	dune height
K_0	a constant for a given flow rate
k_n	unit conversion factor
L	dune length
m_i	parameter related to ice roughness
m_b	parameter related to bed roughness
n	Manning's roughness
N	number of experimental measurements
P	wetted perimeter
q_b	volume of bedload transport per unit width of the channel
Q	flow rate
R_h	hydraulic radius
S	slope friction slope (equal to water surface slope and bed slope under uniform conditions)
T	sampling time
$\bar{u}$	average streamwise velocity
u_*	shear velocity

V	volume of dried sediment
V_{avg}	average velocity
w	sediment fall velocity
z	distance from bed
α	empirical coefficients
β	empirical coefficients
γ	specific weight of water
Δ	s-1 (s = specific gravity of sediment)
ΔB	roughness shift
θ	dimensionless flow strength
θ_c	critical dimensionless flow strength
θ_L	dimensionless flow strength in the leftt section
θ_M	dimensionless flow strength in the middle section
θ_R	dimensionless flow strength in the right section
κ	von Karman constant (0.41)
ν	kinematic viscosity
ρ	water density
ρ_s	sand bulk density
τ	average shear stress
τ_b	boundary shear stress
τ_c	critical shear stress for the median bed material size from the Shields curve
ϕ	dimensionless bedload transport rate
ϕ_L	dimensionless bedload transport rate in the left section
ϕ_M	dimensionless bedload transport rate in the right section
ϕ_R	dimensionless bedload transport rate in the right section

Chapter 1 Introduction

1.1 Background and Motivation

As air temperatures plummet in northern regions, the formation of ice on rivers heralds the arrival of winter, marking a critical transition from flowing waters to a frozen state. This phenomenon, while seemingly minor, carries significant implications on both human activities and natural ecosystems. For example, communities often depend on the formation of ice roads as critical infrastructure for transportation and accessing isolated locations. Furthermore, the presence of ice surfaces facilitates a range of recreational activities during the winter months, including skating, hockey, and ice fishing, which are integral to cultural and social practices in these areas. The impact of ice on flow conditions is particularly noteworthy, as it affects the mobilization and deposition of sediments. This dynamic significantly influences the geomorphology of water bodies, dictating erosional patterns and sediment accumulation that ultimately shape the aquatic landscape.

In alluvial rivers of cold climates, the interplay between sediment dynamics and ice cover- especially during dramatic shifts in flow conditions- plays a pivotal role in altering riverbeds, yet this complex relationship remains underexplored. The initial stage of ice formation often begins with border ice along the banks due to lower velocities, with the border ice growing laterally inwards towards the channel centreline. This process results in a partial ice cover, complicating the turbulent flow analysis. Consequently, the coexistence of open water and ice intricately impacts sediment transport, rendering its analysis more challenging. This research includes laboratory experiments to model the sediment movements in partially ice-covered rivers. The following sections summarize the general description of border ice formation, its effect on the flow characteristics of rivers, and the interaction between sediment movement and the presence of ice.

1.1.1 Border ice formation

Upon the advent of subfreezing air temperatures, the riverbanks cool faster than the flowing water, leading to the freezing of the water-saturated bank material. The shallow water depths adjacent to the banks result in lower water velocities, facilitating the formation of a supercooled layer on the water surface. Ice formation initiates at the water's edge, extending from the bank into the river. In conditions of low water velocity, this border ice initially appears as long, slender ice formations oriented against the current. These structures eventually form a thin ice sheet aligned parallel to the channel banks. As this border ice establishes itself, it expands both outwards into the river and downwards, becoming thicker (Clark, 2013).

Border ice growth in rivers occurs through two primary mechanisms: thermal growth and frazil ice accretion. Thermal growth is driven by heat loss at the air-water interface, causing the ice to expand both vertically and laterally from the riverbanks, predominantly in conditions of low water velocity. This type of growth results in a smooth, outward expansion of border ice towards the channel's centerline, often described as forming in "warm" water conditions relative to the colder, frazil ice-laden waters. Frazil accretion, on the other hand, involves the aggregation of frazil ice particles or flocs at the edge of the existing border ice, a process that can occur in areas of the river where frazil ice is present in the flow, typically in colder water conditions (Clark, 2013).

These processes of border ice formation can happen independently or concurrently, influenced by local environmental conditions such as water temperature, flow velocity, and the presence of frazil ice. As border ice forms, it undergoes vertical thickening akin to stationary ice cover, extending laterally into the river through either thermal growth or frazil accretion. This dual growth mechanism leads to the development of a wedge-shaped ice sheet that extends from the shoreline, with the ice being thickest near the shore and tapering off as it grows outward (Clark, 2013).

Thermal growth starts near the banks where water velocities are low, allowing the ice to gradually extend towards the channel's center until the flow velocity exceeds a certain threshold (Peters, 2015). Theoretical analyses by Matousek (1984) suggest that such formation requires vertical water velocities to be lower than the rise velocity of ice particles, influenced by various factors, including streamwise velocity and heat transfer. Both heat loss to the atmosphere and specific local flow conditions, such as slush ice concentration, significantly impact this process of border ice accumulation (Newbury, 1986).

1.1.2 Hydraulic characteristics of partially ice-covered rivers

As ice begins to form along the riverbanks, the added resistance from the ice cover leads to a decrease in discharge beneath the ice while the discharge in the remaining open-water sections of the river increases. With the eventual formation of a complete surface ice cover, resistance spreads to the central part of the river as well, resulting in a reduced discharge in the middle and a compensatory increase in discharge along the edges. This progressive freezing of the river's surface causes a dynamic shift in the velocity distribution across the river's cross-section, illustrating the impactful role of border ice in altering the channel's flow dynamics during the freezing process.

1.1.2.1 Velocity

1.1.2.1.1 Cross-sectional average velocity

In the analysis of channel flow, a logical starting point frequently involves considering fundamental characteristics like depth and average velocity under conditions of uniform flow. Among the various models available, the Manning equation stands out as a widely recognized formula for estimating the average velocity in a channel derived from empirical observations. The current form of Manning's equation is presented as follows.

$$V_{avg} = \frac{k_n}{n} R_h^{2/3}\sqrt{S} \qquad [1.1]$$

Where:

V_{avg} = average velocity

k_n = unit conversion factor

n = Manning's roughness

R_h= hydraulic radius

S = friction slope (equal to water surface slope and bed slope under uniform conditions)

When an ice cover exists at the free surface, it introduces a no-slip condition to the flow, alters the roughness coefficient, expands the wetted perimeter, and increases the overall flow resistance. As resistance rises, it results in a diminished flow rate for the same water level, or conversely, to sustain the same flow rate, a higher water level is needed.

Manning's roughness coefficient is intended to account for the effect of the overall channel flow resistance. This coefficient is influenced by a variety of factors, such as bed texture, vegetation presence, and variations in the channel's cross-section shape and slope (Ashton, 1986). Moreover, n can exhibit variations across different locations and periods, a characteristic frequently observed in natural watercourses. Such variability becomes especially significant in the winter season when dynamic ice cover formation can alter channel characteristics.

Ice formation across a water channel creates a new boundary, distinct from the open water, characterized by its specific roughness profile. This ice roughness can vary significantly, from the smooth surface of thin skim ice to the complex, irregular structures formed during ice jams. To capture this variability in hydraulic models, particularly when employing Manning's equation, it is essential to use a composite roughness coefficient that accounts for the diverse roughness conditions along the channel.

The principle of conveyance in divided channels allows for the estimation of the depth-averaged velocity distribution in a channel experiencing a certain extent of border ice encroachment. This approach asserts that the overall conveyance of the channel is equivalent to the cumulative conveyance of its individual segments. When applying this to a channel with border ice, the channel is effectively divided into three distinct zones: those under left border ice cover, those under right border ice cover, and those that are ice-free. Subsequently, by assessing the conveyance for each distinct section, the flow distribution across the channel can be determined.

1.1.2.1.2 Velocity distribution

In real-world scenarios, the velocity within a channel differs from one location to another. It is common to observe lower velocities adjacent to the solid boundaries within open channel flows, with velocities increasing towards the channel's central area. Across the flow depth, velocity profiles at specific points are commonly depicted through logarithmic or power-based relationships. Key formulations include the log-law, velocity-defect law, and Cole's law of the wake. Although these models are theoretically limited to specific portions of the velocity profile, empirical evidence suggests their utility in capturing velocity patterns across most of the flow's depth (Nezu & Nakagawa, 1993). The log-law equation for rough channels is provided below. The roughness shift should be set to zero to adapt this equation for smooth channels.

$$\frac{\bar{u}}{u_*} = \frac{1}{\kappa} ln\left(\frac{u_* z}{\nu}\right) + 5 - \Delta B \qquad [1.2]$$

Where:

$\bar{u} =$ average streamwise velocity

u_*= shear velocity

ν = kinematic viscosity

κ = von Karman constant (0.41)

z = distance from bed

ΔB = roughness shift

According to the log law, the velocity reaches its maximum at the water's surface, growing steadily as one moves away from the riverbed. Yet, in the dynamics of open channel flow, the peak velocity is commonly found not at the surface but rather between 5% and 25% of the depth below it (Chow, 1959). This phenomenon is frequently ascribed to the presence of secondary currents (Nezu & Nakagawa, 1993).

In rivers completely covered by ice, the no-slip condition enforced by the ice cover reduces the velocity at the ice's underside to zero, causing the point of maximum velocity to move closer to the riverbed. The position of this maximum velocity is influenced by the ice roughness compared to that of the channel bottom; a rougher ice surface results in the maximum velocity occurring closer to the bed. Theoretically, if the ice cover has the same roughness as the riverbed, the highest velocity point will be positioned midway between the riverbed and the ice's underside (Peters, 2015). The vertical streamwise velocity profile is articulated using an advanced two-parameter power law (Teal et al., 1994; Tsai & Ettema, 1994). This methodology enhances the conventional power-law approach typically employed in open channel flow analyses by incorporating a unified curve to represent the complete velocity profile. This curve takes into account the specific roughness conditions of both the ice cover and the riverbed, providing a comprehensive view of the velocity distribution (Teal et al., 1994). The two-parameter power law developed by Tsai and Ettema (1994) is outlined as follows:

$$\bar{u} = K_0 \left(\frac{z}{h}\right)^{1/m_b} \left(1 - \frac{z}{h}\right)^{1/m_i} \quad [1.3]$$

Where:

K_0 = a constant for a given flow rate

m_i = parameter related to ice roughness

m_b = parameter related to bed roughness

h = water depth

Error! Reference source not found. illustrates the normalized streamwise velocity d istribution for open channel flows and fully and partially ice-covered conditions. The figure depicts only half of the channel, as the flow demonstrates symmetry. In the case of partially ice-covered rivers (Fig 1.1c), channel cross-section can be considered as three distinct zones: open, transitional, and covered, reflecting the influence of partial ice cover on the velocity profile. Each zone exhibits unique velocity characteristics: the covered zone mirrors the velocity profile typical of fully ice-covered channels, the open zone aligns with traditional open channel flow profiles, and the transitional zone presents an intermediary velocity profile, distinct from both the fully covered and entirely open scenarios (Peters et al., 2017).

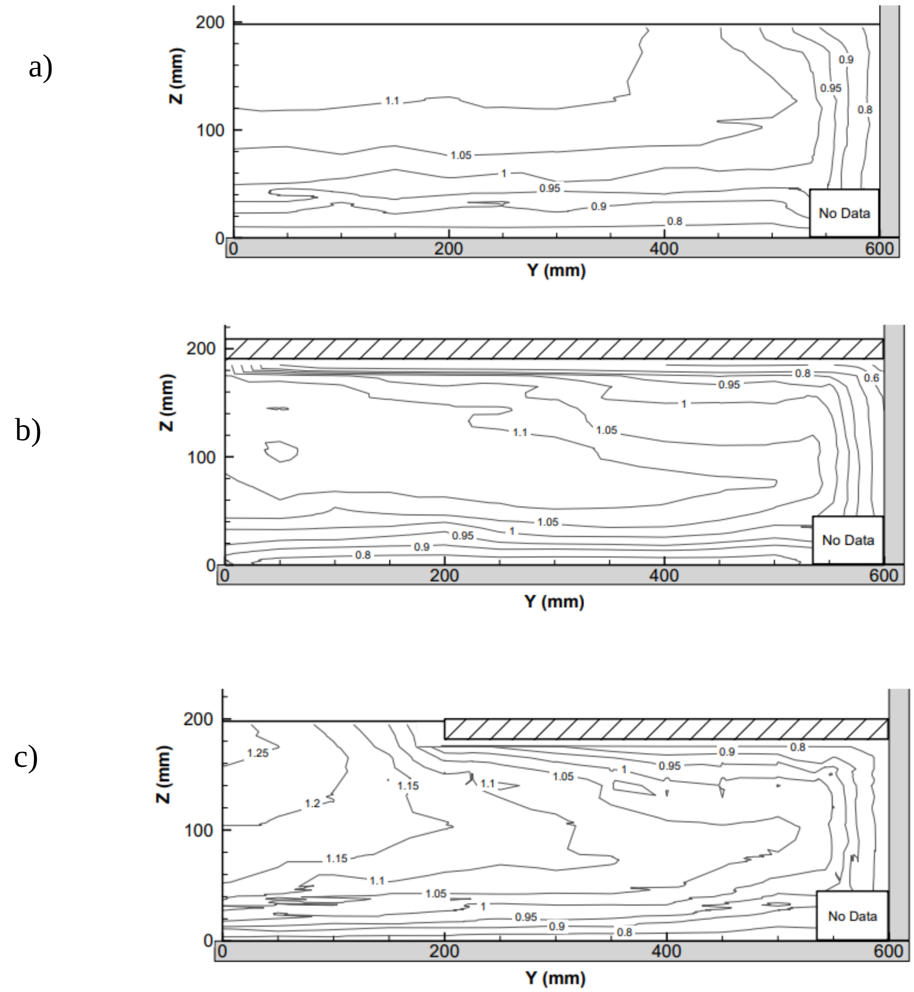

Figure 1.1. U/U$_{avg}$ contours for a) open channel, b) fully ice-covered, and c) partially ice-covered flow (Peters et al., 2017).

1.1.2.2 Shear stress

1.1.2.2.1 Average shear stress

A comprehensive understanding of shear stress distribution within channels is pivotal for the exploration of interconnected phenomena such as sediment transport. The ability to accurately characterize sediment transport is essential for assessing critical areas like scour analysis, riverbank stability assessment, the impact on aquatic habitats, and suspended sediment concentration dynamics (Sturm, 2010).

Directly at the boundary interface, the fluid velocity equates to that of the boundary itself, a principle referred to as the no-slip condition. This fundamental principle results in the generation of a shear force on the channel boundary due to the fluid motion (Munson et al., 2013). A momentum analysis conducted on a uniform flow section within the channel indicates that the average shear stress across the channel can be mathematically formulated as:

$$\tau = \gamma R_h S \qquad [1.4]$$

Where:

τ = average shear stress,

γ = specific weight of water,

The approaches used to ascertain average shear stress in open channels are similarly effective for channels with ice covers. It is important to highlight that the wetted perimeter, a critical factor in calculating hydraulic radius, differs between partially ice-covered, fully ice-covered, and open channel flows.

1.1.2.2.2 Shear stress distribution

It should be noted that the shear stress along the channel's wetted perimeter exhibits spatial variability, resulting in certain areas experiencing shear stress above or below the average. One approach to calculate the shear stress at a specific point along the channel bed is to fit the local velocity profile to the log law. In this context, the shear velocity u_* is utilized as an adjustable parameter to align the observed velocity profile with the theoretical one predicted by the log-law. Upon determining u_*, this parameter can then be utilized to compute the local boundary shear stress at the specified location using the following equation:

$$\tau_b = \rho {u_*}^2 \qquad [1.5]$$

Where:

τ_b = boundary shear stress

ρ = water density

Research on open channel flow demonstrates that shear stress distribution exhibits its maximum values at the channel's center, reducing to minimal levels at the edges, where it sharply falls to zero at the interface of the water surface and the river bank. It is important to note that the spatial distribution of shear stress across a channel's cross-section for ice-covered flow may differ significantly. The distribution model by Nezu and Nakagawa (1993) diverges from the open channel distribution with a central peak, presenting a local minimum at the center and two maxima positioned closer to the walls. However, this configuration is not always the case. The work of Knight et al. (1984) demonstrated that in many instances, the shear stress distributions in fully ice-covered flows resemble those observed in open channel flows, with variances in the intensity and positioning of local maxima. That is, numerous studies still identify the highest shear stresses at the midpoint of the channel, as initially mentioned.

Peters (2015) demonstrated that in channels with border ice cover, the shear stress distribution across the bed largely mirrored that of open channels, with the lowest shear stress at the corners and the highest at the channel center. However, experiments with high Froude numbers, 50% coverage, and rough bed conditions deviated from this pattern, exhibiting a local minimum at the centerline and maximum shear stress points located near the ice cover's edge. This observed distribution aligned more closely with the theoretical model for shear stress in fully covered channels. The reason for the deviation observed in these three specific experiments remains unclear, particularly since the experiment involving a fully covered channel did not demonstrate this pattern. Moreover, the degree of ice coverage seemed to have little impact on the shear stress distribution across the channel bed.

1.1.3 Sediment transport

The initiation of sediment motion within alluvial channels occurs when the exerted shear stress exceeds the sediment's threshold value. This movement is typically categorized for descriptive simplicity into three primary modes: bedload, saltation, and suspension, differentiated by the ratio of the sediment's fall velocity (w) to the shear velocity as (Raudkivi, 1998):

$$\left.\begin{array}{ll} 2 < \frac{w}{u_*} < 6 & \text{bedload} \\ 0.6 < \frac{w}{u_*} < 2 & \text{saltation} \\ \frac{w}{u_*} < 0.6 & \text{suspension} \end{array}\right\}$$

In the current study, the ratio $\frac{w}{u_*}$ falls within the range of 2 to 6. As a result, the focus of this research is on bedload transport. Bedload transport, occurring under relatively minor shear stress excess, involves sediment moving along the bed primarily through sliding and rolling. This mode of transport maintains continuous contact with the bed, with particles moving intermittently (Raudkivi, 1998). The volume of bedload transport per unit width of the channel, a key metric in sediment transport studies, is denoted as q_b and expressed in units of volume over area per time. This metric is influenced by a variety of factors, including the boundary shear stress and the physical properties of the sediment (García, 2007).

Numerous formulas have been established in the broader context of sediment transport, mainly describing the relationship between the dimensionless bedload transport rate and the dimensionless flow strength. Chein and Wan (1999) proposed an empirical formula that links dimensionless bedload transport rate to dimensionless flow strength, as seen in Equation [1.6]. Following this, Knack and Shen (2015) conducted a comprehensive review of various studies to empirically ascertain suitable values for α and β, which were found to be 25 and 2.1, respectively.

$$\phi = \alpha(\theta - \theta_c)^{\beta} \qquad [1.6]$$

$$\phi = \frac{q_b}{(\Delta\, g D^3)^{1/2}} \qquad [1.7]$$

$$\theta = \frac{\tau_b}{\Delta\, \rho\, g\, D} \qquad [1.8]$$

Where:

ϕ = dimensionless bedload transport rate

θ = dimensionless flow strength

θ_c = critical dimensionless flow strength

α and β = empirical coefficients

Δ = s-1 (s = specific gravity of sediment)

D = the particle diameter

g = gravitational acceleration

Sediment movement on the bed is influenced by various forces such as lift, drag, and gravity. Ice cover can alter these dynamics by creating turbulence and reducing water drag on the bed, mainly due to the additional resistance from the ice cover leading to higher water levels and lower average velocities for the same flow rate. This can cause sediment transport rates to vary and significantly impact channel morphology (Ettema & Daly, 2004). Conventional equations typically applied to free-surface flow conditions can be adapted to estimate bedload transport within ice-covered channels by characterizing the flow strengths using the bed shear stress (Knack & Shen, 2015).

1.1.4 Bed morphology

When sediment particles are set in motion, their unpredictable erosion and sedimentation patterns introduce slight disturbances in the bed surface's elevation. These slight changes in the bed's surface structure, known as bedforms, can often span the entire riverbed width. The flow resistance, which is significantly influenced by the configuration of these bedforms, plays a crucial role in determining the water surface elevation in alluvial channels. Shifts in the resistance due to changes in bedform configurations lead to adjustments in the stage-discharge relationship, thereby presenting challenges in accurately determining river flow volumes based on water level measurements (Julien, 1995).

The formation, growth, and movement of bedforms are central to sediment transport processes (Venditti et al., 2016). Studying these structures is vital not only for analyzing current river channel behavior but also for shedding light on the geomorphological characteristics of ancient river systems that no longer exist on Earth or other planetary bodies. This understanding is instrumental in predicting the characteristics of dune features based on observed flow properties and inferring historical flow conditions from dunes preserved in geological records.

The relationship between flow properties and dune dimensions is critical for quantifying flow resistance and estimating scour depths, as dune sizes directly indicate roughness height. Moreover, numerous sediment transport equations integrate these dimensions to model sediment dynamics (Bradley & Venditti, 2017). Two critical parameters of bedforms, their height, and length, play significant roles in numerous experimental bedform equations. These parameters are illustrated in the figure below.

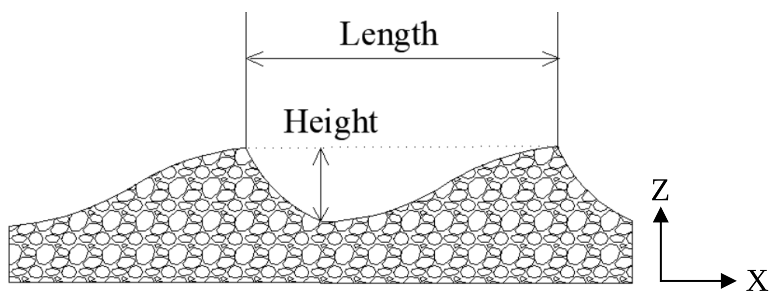

Figure 1.2. Schematic of bedform height and length definition.

The historical development of relations that link various flow parameters to dune dimensions, often called scaling relations, has been significant. These scaling relations are structured around several key variables: the depth of the flow, which is often equated with boundary layer thickness and typically assumed to be the flow depth in rivers (Yalin, 1964); the depth and grain size of the sediment (Julien & Klaassen, 1995); the transport stage (Allen, 1978; Karim, 1995; van Rijn, 1984); and combinations of transport stage and Froude number (Gill M.A., 1971; Karim, 1999).

Yalin's contributions from 1964 are particularly noteworthy, providing recognized dune scaling relations that link bedform dimensions primarily to the flow depth. These relations were established through dimensional analysis, utilizing unpublished and published flume observations and select field data (Barton & Lin, 1995; Lane & Eden, 1940; B. Singh, 1960; Vanoni & Brooks, 1957). Yalin's work resulted in the following empirical formulas:

$$\frac{\mathrm{H}}{\mathrm{h}} = \frac{1}{6}\left(1 - \frac{\tau_c}{\tau_b}\right) \quad [1.9]$$

Where H is dune height, h is flow depth, τ_c is critical shear stress for the median bed material size from the Shields curve. Subsequently, the equation was simplified to:

$$\mathrm{H} = \frac{\mathrm{h}}{6} \quad [1.10]$$

Yalin (1964) also suggested an empirical formula to estimate dune length (L), expressed as:

$$\mathrm{L} = 5\mathrm{h} \quad [1.11]$$

Furthermore, these scaling relationships have been expanded by researchers like Flemming (1988), who suggested an empirical equation relating bedform height to length based on a comprehensive analysis of deep-sea, tidal, and river bedforms (Equation [1.12]). This and other similar equations by researchers like Chen et al. (2012) and Lefebvre et al. (2016), with varying coefficients, provide a robust framework for understanding bedform dynamics (Bradley & Venditti, 2017).

$$\mathrm{H} = 0.0677\ \mathrm{L}^{0.8098} \quad [1.12]$$

Furthering the field's development, Bradley and Venditti compiled a comprehensive dataset of dune dimensions and flow characteristics from a wide array of sources, including both laboratory flume experiments and field studies. Their work verified that dune height and length follow a power law relationship specifically expressed as Equation [1.13], which is consistent with Flemming's established relationship.

$$\mathrm{H} = 0.0513\ \mathrm{L}^{0.7744} \quad [1.13]$$

1.2 Literature Review

1.2.1 Partially ice-covered flow

The formation of border ice from riverbanks introduces additional resistance under the ice cover, causing decreased flow in the covered areas and increased flow in the open areas of the channel. The expansion of border ice, leading to complete surface coverage, enhances this resistance in the channel's central part. This alteration affects the flow dynamics, causing a decrease in the central flow as Tsang (1970) observed. The dynamic impact of border ice on flow distribution continues throughout the freeze-up period, with the growth of border ice incrementally increasing the channel's wetted perimeter (Clark, 2013). The impact of border ice on flow redistribution has been the subject of limited studies.

Tsang (1970) explored how an ice cover alters velocity distribution through field studies on the Nottawasaga River, revealing that velocity profiles in open water are similar to those of open channel flow, increasing from zero at the bed to the maximum at the surface. Under ice, the velocity profile resembles an ice-covered channel, with zero velocity at the bed and ice, reaching a maximum in between.

The depth-averaged velocity distribution in a channel impacted by border ice can be estimated by applying the principle of conveyance in divided channels. This principle asserts that the channel's total conveyance is the sum of the conveyances of its individual subsections. Hirayama (1986) applied this approach to the Yubetsu River in Japan, observing a shift in flow towards the open water section as border ice expanded. This shift in flow distribution was also noted by Majewski and Baginska (1988) during an ice jam on the Vistula River, where they observed significantly lower velocities beneath the border ice compared to the increased velocities in the open water sections.

In laboratory experiments, Majewski (1992) investigated the influence of border ice on channel hydraulics, experimenting with varying coverage and roughness levels. The findings indicated an increase in the velocity gradient across the open water section with wider border ice expanses. The divided channel conveyance principle was applied to calculate the channel's velocity distribution, with the channel divided into distinct sections and the total discharge computed by summing the discharges of all sections. While there were some differences in quantitative results, the qualitative insights remained consistent, indicating a substantial reduction in flow beneath the ice cover compared to the open channel section.

Miles (1993) monitored velocity profiles at three sites throughout winter, measuring velocities beneath the ice at various depths and distances from the bank towards the ice edge. Due to accessibility and safety issues, velocities in the open channel section were estimated. Findings suggested that border ice creates an additional solid boundary, increasing the wetted perimeter and thus resistance to flow, reducing conveyance capacity. Velocity reduction was less pronounced, moving from the bank towards the ice edge. Various methods were employed to predict lateral velocity distribution, incorporating different equations and concepts to estimate composite roughness values.

Peters et al. (2015, 2017, 2018) conducted experimental studies at the University of Manitoba focusing on the hydraulic dynamics induced by border ice in a rectangular setup. Their work highlighted the profound effect of border ice's presence and physical characteristics, particularly its extent and surface roughness, on the flow redistribution within a channel. Notably, the studies demonstrated that roughness significantly alters flow dynamics by decreasing water velocity in proximity to the roughened ice edges and increasing the shear stress exerted on these areas. They also introduced a systematic framework to categorize the channel cross-section into open, transitional, and ice-covered areas.

In a detailed experimental study led by Kimiaghalam et al. (2017) in a controlled laboratory setting, water velocities were measured within a smooth rectangular flume under simulated smooth border ice conditions. The measurement of these velocities was facilitated by the use of an Acoustic Doppler Velocimeter (ADV), providing the necessary data to compute the average shear stress and the spatial distribution of boundary shear stresses using the established logarithmic law. Additionally, various methods like energy transportation, momentum and continuity equations, flow net analysis, and geometric techniques were employed to estimate shear stress distributions. While there was consistency in average shear stress calculations across these methods, discrepancies emerged in the boundary shear stress estimates, particularly along the channel sidewalls. The flow net approach was notably more aligned with logarithmic law predictions. In 2018, Kimiaghalam et al. simulated a partially ice-covered flow in a trapezoidal channel. The study explored variations in streamwise water velocity and boundary shear distribution, analyzing the effects of differing ice coverage and surface roughness.

Essel et al. (2021) undertook a comprehensive study involving experimental observations and three-dimensional (3D) computational modeling to examine turbulent flows in channels under simulated partial ice cover conditions. Their findings revealed that partial ice covers and secondary currents near the channel walls significantly reshaped the channel's mean velocity profiles, Reynolds stress distributions, and turbulence production. The 3D simulations highlighted that these alterations in turbulence characteristics were predominantly shaped by pronounced counter-rotating secondary flows in the center of the channels with partial ice coverage, alongside eight smaller secondary flows at the channel's corners. These central flows were observed to interact with the smaller corner flows, establishing a dynamic interconnection between the open water areas and the areas under ice cover, significantly impacting the channel's overall flow dynamics.

Nyantekyi-Kwakye et al. (2021) employed particle image velocimetry to meticulously examine turbulent flows beneath simulated partial ice coverage conditions. This innovative approach allowed for an in-depth analysis of velocity patterns, which served as a foundation for testing the efficacy of several bed shear stress models that are conventionally used for open channel flows. The research compared the performance of established models, including the Ludwieg–Tillmann, quadratic stress law, and Prandtl's seventh power law, against the traditional logarithmic law model in predicting bed shear stress variations under different degrees of ice coverage.

1.2.2 Sediment transport and bed morphology in ice-covered rivers

Extensive research has been dedicated to formulating equations that capture the complexities of sediment transport and the ensuing morphological changes in riverbeds under open channel flow conditions. These models are instrumental in predicting key parameters such as sediment transport rates, suspended sediment concentrations, and the characteristics of bedforms, thereby offering profound insights into river geomorphology (Knack, 2011). The dynamics of sediment motion at the riverbed are primarily governed by forces such as lift, drag, and gravity. Ice cover introduces additional complexity, generating turbulence and diminishing the water's drag effect on the bed, primarily attributed to the extra resistance from the ice cover that elevates water levels and reduces mean flow velocities (Ettema & Daly, 2004). Ice cover also modifies the vertical distribution of streamwise velocities, typically resulting in reduced sediment transport rates compared to open channel flows. Nonetheless, as hypothesized by Ettema and Daly (2004), ice cover may also induce lateral flow redistribution, thereby variably influencing sediment transport rates across different sections of the channel depending on the thalweg's positioning. Despite the acknowledged impact of ice cover on sediment transport dynamics, empirical investigations into its quantitative effects remain sparse.

Field investigations, such as those conducted by Lawson et al. (1986), have provided comparative analyses of sediment concentration data across winter and summer periods, highlighting seasonal variations. Wuebben (1986, 1988) explored the dynamics of sediment transport and bedform development under conditions of a floating cover, demonstrating the potential applicability of open water sediment transport theories to the sub-ice flow layer dominated by bed resistance. Complementing this view, flume experiments conducted by Shen and Wang (1995) demonstrated that bedload transport under ice-covered conditions could be conceptualized within the frameworks established for equivalent open-channel flows. Similar inferences were drawn by Ettema et al. (2000), who compared the flume data of Sayre and Song (1979), Smith and Ettema (1995) and Ettema et al. (1999) with established sediment transport formulations by Einstein (1950) and Meyer-Peter and Muller (1948). Ettema and Daly (2004) provided an in-depth qualitative exploration, proposing a series of dimensionless parameters anticipated to influence sediment transport and bedform dimensions under ice-covered conditions. Zabilansky et al. (2007) conducted real-time scour measurements under ice using Time Domain Reflectometry (TDR) across three sites, demonstrating that ice covers, particularly when unable to adjust vertically to discharge changes, can significantly accelerate riverbed erosion. Their laboratory tests, simulating open water, floating ice, and restrained ice conditions, mirrored these findings. Specifically, under restrained conditions with increased discharge, the velocity near the smoother riverbed increased, enhancing shear stress and subsequently intensifying bed erosion.

Recent observations have highlighted the significance of anchor ice rafting in transporting sediment under ice-affected conditions. Kempema and Ettema (2010) described anchor ice formation and rafting in the Laramie River, noting that anchor ice can form on various substrates, including cobble, gravel, and sand. Their study revealed that anchor ice, when released, can raft significant amounts of sediment downstream, including large particles that are not typically mobilized by peak discharge flows. Kempema and Ettema's findings suggest that anchor ice can transport much larger sediment particles than those moved by bedload transport alone, indicating a unique and potent form of sediment mobilization may occur during winter low-flow periods.

Further explorations of the interactions between ice processes and fluvial sediment dynamics have been conducted by Turcotte et al. (2011) and Ettema (2008), which emphasize the profound impact of ice cover on river morphology. However, the difficulties associated with fieldwork under such conditions have resulted in limited detailed empirical data, thus restricting in-depth quantitative analysis. Kämäri et al. (2015) studied the impact of river ice cover on sediment dynamics using a one-dimensional hydrodynamic model on the Kokemäenjoki River in Southwest Finland. Their findings indicated that a smooth, thermally-formed ice cover significantly reduces riverbed erosion and turbidity compared to ice-free conditions with similar discharges. Additionally, long-term field data revealed that ice cover notably decreases suspended sediment concentrations, lowering the river's overall sediment load. Pajunen et al. (2024) investigated sediment transport in a subarctic river using one-dimensional morphodynamic models and image-based data, comparing low-flow open-channel conditions in autumn to ice-covered conditions in winter. Simulations indicated a marked reduction in sediment transport under ice compared to open water, with erosion predominating in open water and deposition in ice-covered conditions. Additionally, increasing ice thickness subsequently increased flow velocity and shear forces, enhancing bedload transport. The use of image-based datasets for sediment analysis proved more reliable for model calibration in ice-covered conditions, suggesting a potential for broader application in sediment transport studies, particularly in icy environments.

The exploration of the impacts of ice cover on sediment transport and river bed alteration through numerical modeling has been relatively limited but noteworthy. Studies by researchers such as Carr and Tuthill (2012), Kolerski and Shen (2015), Manolidis and Katopodes (2014), Zhang et al. (1994), and Knack (2011) have made significant contributions to this field. A particularly notable advancement was made by Knack and Shen (2018), who developed a comprehensive coupled model that integrates sediment transport and riverbed morphological changes with hydro-thermal-ice dynamic processes. The model stands as a significant leap forward in understanding the interplay between ice cover and sediment dynamics. However, the validation of this model poses a challenge due to the limited availability of laboratory or field data that quantitatively document changes in riverbed morphology under ice-covered conditions, underscoring a gap in the current body of knowledge and highlighting an area for future research endeavors.

1.3 Research Objectives

As evidenced in the previous sections, understanding sediment transport, bed dynamics, erosion, and deposition is critical when designing new in-stream structures. A multitude of models have been specifically developed to assess these factors under open water conditions. These models are fundamental in predicting key variables such as suspended sediment concentrations, sediment transport rates, and changes in riverbed morphology. Accurately modeling these parameters is essential for a comprehensive understanding of river geomorphology and is integral to effective river management and engineering.

Significantly, in colder climates, many rivers experience partial border ice cover for extensive periods during the winter. This ice cover can substantially influence river dynamics, potentially altering sediment transport processes and riverbed morphology. Despite some existing research on the effects of ice on sediment dynamics, the specific impact of border ice on these processes remains underexplored. Border ice, forming along the edges of a river, can alter flow patterns and sediment distribution. The interaction between ice cover and sediment dynamics remains underexplored and poorly understood in river engineering and environmental management. There is a clear need for more comprehensive studies that focus specifically on how border ice affects sediment transport in rivers. Such research would not only fill a critical knowledge gap but also contribute to the development of more accurate predictive models and management strategies for rivers in cold regions, ensuring their ecological stability and the effectiveness of engineered river structures. The objectives of this research are as follows:

Objective 1: Explore the influence of border ice on bedload transport rates and distribution and formulate an equation to quantify bedload transport rate in rivers with partial ice cover.

Objective 2: Investigate how asymmetric border ice affects bedload transport rates and distribution.

Objective 3: Examine the impact of border ice (both symmetric and asymmetric) on bedform characteristics.

1.4 Organization of Thesis and Contribution of the Author

Chapter2

Chapter 2 presents laboratory experiments examining the influence of border ice on sediment transport rate and distribution, directly addressing Objective 1 of the thesis. This chapter is an adapted version of a publication in the International Journal of Sediment Research titled "Experimental investigation of sediment transport in partially ice-covered channels" authored in collaboration with Dr. Shawn Clark from the University of Manitoba.

The primary author, Mina Rouzegar, independently designed the methodology, conducted the experiments, analyzed the results, and authored the manuscript under the guidance of co-author (Dr. Shawn Clark). The final manuscript was accepted on June 16, 2023.

Chapter3

In Chapter 3, laboratory experiments are detailed to explore the impact of asymmetric border ice on sediment transport rates and distribution, directly aligning with Objective 2 of the thesis. This chapter is an adapted version of a published paper in the Water journal titled " Sediment transport beneath a simulated partial ice cover: Effects of asymmetric border ice" co-authored with Dr. Shawn Clark of the University of Manitoba.

The primary author, Mina Rouzegar, independently designed the methodology, conducted the experiments, analyzed the results, and authored the manuscript under the guidance of co-author (Dr. Shawn Clark). The final manuscript was accepted on November 25, 2023.

Chapter4

In Chapter 4 of the thesis, laboratory experiments were conducted to explore the influence of symmetric and asymmetric border ice on bedform features, directly addressing Objective 3. This chapter is an adapted version of a manuscript submitted to the journal Cold Regions Science and Technology titled "An experimental study into the bedform morphology in partially ice-covered channels," co-authored with Dr. Shawn Clark from the University of Manitoba, submitted on April 4, 2024.

The primary author, Mina Rouzegar, independently designed the methodology, conducted the experiments, analyzed the results, and authored the manuscript under the guidance of co-author (Dr. Shawn Clark).

Chapter 5

Chapter 5 provides a summary of the major findings and contributions of this research. It also introduces suggested areas for future exploration.

Chapter 2 Paper 1: Experimental investigation of sediment transport in partially ice-covered channels

2.1 Abstract:

It is important to understand the effects of ice cover on sediment transport in cold climates, where sub-freezing temperatures affect water bodies for a significant part of the year. The literature contains many studies on sediment transport in open channel flow, and several studies on sediment transport in completely ice-covered flow. There has been little or no research on sediment transport in partially ice-covered channels. In the current study, laboratory experiments were done in a rectangular flume to quantify the impact of border ice presence on the sediment transport rate. The effects of ice cover extent and changing flow strengths on sediment transport distribution also were investigated, and the results were compared to those for fully ice-covered and open channel flow. The ice coverage ratios considered were 0 (representing the open water condition), 0.25, 0.50, 0.67, and 1 (representing fully ice-covered flow). The partial ice cover was found to impact the sediment transport distribution within the channel. The effect of ice coverage extent on sediment transport distribution was more significant at lower flow strengths and became negligible at higher flow strengths. The conventional equations for sediment transport in open channel flow and fully ice-covered flow that relate the dimensionless bedload transport rate to the flow strength were found to be applicable to estimate the total cross-section-averaged bedload transport for partially ice-covered flow when modified appropriately. Empirical coefficients for these equations were determined using the experimental data.

Keywords: Sediment transport, Bedload, Ice-covered channel, Border ice

2.2 Introduction

It is essential to understand the impacts of ice cover on the hydraulic, sediment transport, and geomorphological characteristics of rivers in northern climates because sub-freezing air temperatures affect water bodies for a significant part of the year. Early-winter ice formation can take the form of border ice, which forms along the river banks due to the low water velocities in this area. A partial ice cover results from lateral border ice growth from each side of the river. It can cause flow redistribution and change the water velocity profile in the channel cross section (Peters et al., 2017). Impacts from the developing border ice cover vary temporally as the ice grows inwards towards the channel thalweg. The duration of the partial ice cover is a function of both the local hydraulic and meteorological conditions and could vary from days to weeks or even longer. Observations on the Dauphin River, Manitoba, Canada, have noted the development of mid-winter open water leads that formed within a consolidating ice cover (Wazney et al., 2018). The hydraulic conditions would likely have been similar to those of a developing border ice cover, and these conditions persisted for weeks. In some cases, the presence of a partial ice cover is, therefore, something that should not be ignored when trying to understand the full sediment budget of a river.

Many studies have investigated open channel and completely ice-covered flow; however, research on partially ice-covered flow is limited. Understanding border ice formation and the impact of its presence on the hydraulic characteristics of rivers, sediment transport, and geomorphology will fill current knowledge gaps and improve the potential for numerical models to accurately simulate morphodynamic changes in rivers that experience partial ice cover (Peters, 2015).

There are many equations that deal with sediment transport and associated bed changes for open water conditions. These equations are used to predict suspended sediment concentrations, sediment transport rates, and bed form type and size, and have an important role in understanding river geomorphology (Knack, 2011). Bed sediment motion results from the forces exerted on bed particles (lift, drag, gravity). The presence of ice cover can generate turbulence and decrease water drag on the bed (Ettema & Daly, 2004). This is mainly due to the additional boundary resistance imposed by the ice cover that causes an increased water level and lower average velocity for the same flow rate. The ice cover presence also vertically redistributes the streamwise flow velocity. These two effects typically cause an overall decrease in the sediment transport rate in comparison to open channel flow. On the other hand, Ettema and Daly (2004) hypothesized that ice cover presence laterally redistributes the flow, causing either an increase or decrease in the sediment transport rate at specific spanwise locations depending on the location of the thalweg (ice cover usually concentrates the flow along the thalweg). The presence of rough ice and/or a rough bed can cause more complicated redistribution in flow velocity and shear stress (Peters et al., 2018). Consequently, flow response to ice cover presence is variable in different situations, making it difficult to draw a conclusion about its effects on a river's bed and banks. Analyzing partially ice-covered rivers is even more complicated because of the simultaneous existence of open water and ice cover. Also, field data under partial ice cover conditions is limited because of the temporary duration of border ice growth and the low strength of thin ice, causing safety concerns for data collection (Nyantekyi-Kwakye et al., 2021). Numerical modeling on partial ice cover also is scarce since there is insufficient benchmark data for model validation. As such, advancements in partial ice cover research have mainly come from experimental measurements (Essel et al., 2021; Kimiaghalam et al., 2017; Majewski, 1992; Peters, 2015).

Relatively few studies have investigated the effect of ice presence on the sediment transport rate; however, Ettema and Daly (2004) provided a thorough, qualitative assessment on the topic. They developed a set of dimensionless parameters hypothesized to affect sediment transport in the presence of an ice cover. Lawson et al. (1986) did fieldwork in which suspended and bedload concentration data were measured during the winter and then compared to summer period data. Wuebben (1986, 1988) investigated sediment transport and bedforms under floating cover conditions and showed that open water theories might be applied to the lower flow layer of the ice-covered condition, where the bed resistance governs the flow (Knack & Shen, 2015). Flume experiments in 1995 done with a floating cover and low-density chips have also shown that bedload transport in ice-covered channels can be described by conventional relations for the equivalent open channel flow (Shen & Wang, 1995). Ettema et al. (2000) made similar suggestions for the sediment transport rate. They compared the flume data of Sayre and Song (1979), Smith and Ettema (1995), and Ettema et al. (1999) with both the Einstein (1950) and the Meyer-Peter and Muller (1948) formula.

Knack and Shen (2018) proposed a numerical model for sediment transport and bed change in alluvial channels with a full ice cover.

The literature shows that the effect of a partial ice cover, and more specifically, the different extents of partial ice cover on sediment transport, have not yet been investigated. The current study aims to quantify the sediment transport rate using simulated border ice in a controlled laboratory setting and investigate the effect of different extents of border ice cover on the sediment transport rate and distribution.

2.3 Methodology

The physical experiments were done in the Hydraulics Research & Testing Facility at the University of Manitoba. A rectangular flume (Figure 2.1) 14 m long, 1.2 m wide was constructed using high density overlay (HDO) plywood with a bed slope of 0.26%. Discharge was measured in the flume's supply pipe using a Dynasonic ultrasonic flow meter (±1% accuracy) which led to a head tank that had a greater width and depth than the flume to help dissipate turbulence produced by the discharge pipe. Water then flowed through a honeycomb flow straightener to condition the flow. The flume bed at the upstream end was lined with gravel of varying diameter to help facilitate rapid boundary layer development in order to promote fully developed flow conditions over a greater length of the flume. Fully developed flow was confirmed by measuring vertical profiles of streamwise velocity at varying distances along the flume length using a Nortek Vectrino acoustic Doppler velocimeter. Five 39.4 mm diameter manometer tubes were installed on the flume wall to measure the water surface profile using a point gauge with an accuracy of ± 0.2 mm. A 70 mm thick layer of uniform silica sand with a median diameter (d_{50}) of 1.3 mm was placed throughout the flume length. Steel rails were installed along the length of the flume walls, upon which a leveling device on rollers was installed to ensure that the sand bed was smooth and flat at the start of each experiment. The sand bed slope could be changed by adjusting the slope of the flume rails and adding or removing sand as required. A rigid step (width = 1.2 m, length = 0.6 m, height = sand height) was installed at the downstream end of the flume to separate the movable sand from the sediment trap, located downstream of the step to collect sediment and measure the sediment transport rate. The sediment trap was divided into three separate bins in the streamwise direction using two long sections of aluminum angle. This division of sediment trap facilitated the measurement of the sediment transport rate near the channel walls and within the center section separately. The downstream water level was controlled by a bottom-mounted, hinged gate.

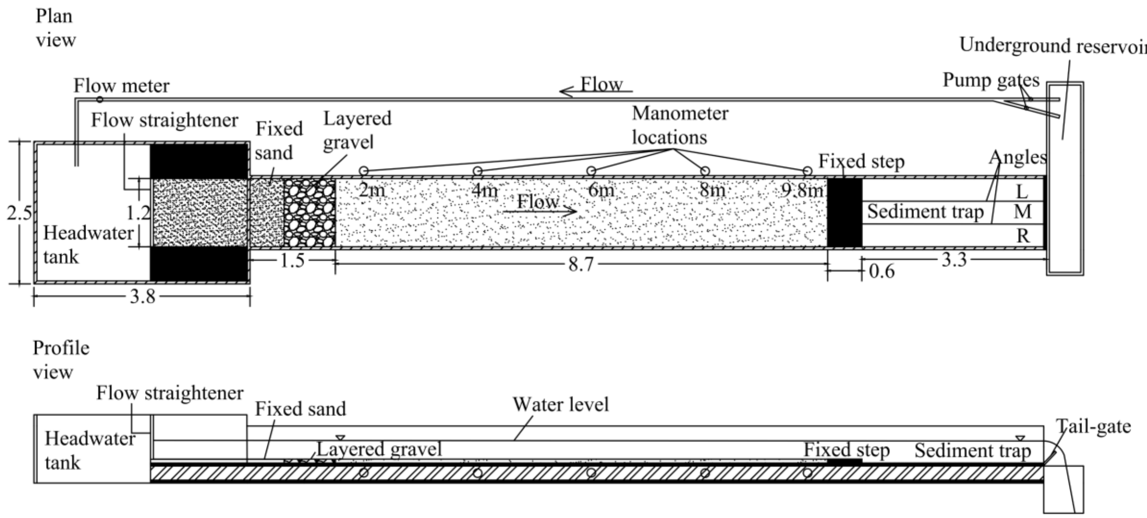

Figure 2.1. Schematic diagram of the experimental setup (all dimensions in meters).

Bubble wrap was used to simulate a smooth partial ice cover (Figure 2.2). Three lines were drawn along the bubble wrap, at the appropriate distance to represent the three different ice coverage ratios used in the current study. The bubble wrap was nailed to the flume wall at the appropriate elevation along the appropriate line to set the desired ice coverage ratio and prevent lateral movement of the simulated ice for each partially ice-covered test. For fully ice-covered conditions, the bubble wrap was nailed to the upstream end of the flume. Bubble wrap and a thermally grown border ice cover have similar hydraulic roughness; however, they are different in terms of rigidity. While bubble wrap is a relatively soft material that can be easily deformed, border ice is relatively rigid and less flexible. Furthermore, the simulated border ice was quite thin, which is more similar to border ice formed early in the winter rather than ice that has thickened considerably over time. Additional details and pictures of the experimental setup can be found in Rouzegar and Clark (2022).

a) b)

Figure 2.2. Simulated ice-covers for a) partially ice-covered flow and b) fully ice-covered flow.

An initial test was done to measure the critical shear stress of the bed material by observing the point of incipient motion for this bed material and back-calculating the corresponding applied shear stress. The measured value was found to be nearly identical to the value obtained using the Shield's diagram. Subsequent bedload transport experiments were designed to ensure that the critical shear stress was exceeded.

The sediment transport experiments were done under uniform flow conditions by adjusting the discharge and water depth to the desired value for each test. A composite Manning's n value of 0.012 was experimentally determined using the observed water surface profiles over a range of partially and fully ice-covered flow conditions. Also, Manning's composite roughness was assumed to be constant for all the tests since it did not change considerably from the open channel flow to the partially covered condition (Peters, 2015). A consistent procedure was followed to reach a uniform flow in the lab. The bed was flattened at the desired slope, and the tailgate was raised to initially prevent flow before starting each experiment. The flume was slowly filled using a sump pump at the downstream end (i.e., filling the flume rather than conveying water through the flume) to prevent disruption of the bed with a first flush of water through the flume. Then, the main pump was turned on, and the inlet valve was slowly opened to create a steady, low-velocity initial flow condition. This initial inflow was set such that no sediment transport occurred. Finally, the flow was gradually increased to the desired value and held constant. Uniform flow was then established by adjusting the tailgate height. The water surface slope and flow depth were measured in all the experimental runs. The approach was consistent with other studies (e.g., Khosravi et al., 2020). The duration of each test was set considering the sediment transport rate such that tests with a larger sediment transport rate had a relatively shorter duration and tests with lower sediment transport rate had relatively longer durations. The test conditions, including the duration of each experiment, are listed in Table 2.1.

At the end of the experiment, sand in the left (L), right (R), and middle (M) sections of the sediment trap was collected separately, dried in an oven at a temperature of 110 ± 5 °C (230 ± 9 °F), cooled in the air at room temperature for 1 ± 1⁄2 hour, and the mass was determined with an accuracy of ±0.2 g (ASTM C-128-15, 2015). The sediment volume was obtained considering that bulk density was 1.5 g/cm^3 ($\rho_s = \frac{G}{V}$), where G is the collected and dried mass of sediment [g], V is the volume of dried sediment [m^3], and ρ_s is the sand bulk density. Then, the volumetric rate of bedload transport per unit width (q_b) was calculated as follows (Khosravi et al., 2020; Nezu & Rodi, 1986; Tsai & Ettema, 1994):

$$q_b = \frac{V}{\mathrm{b}T} \quad [2.1]$$

where T is the sampling time [s] and b is the flume width.

In short-duration experiments, the effect of not supplying sediment throughout the experiment can only be noticed at the upstream end of the channel, and does not influence the morphology in the downstream sections of the channel or the channel's sediment transport rates (Binns & da Silva, 2009; Khosravi et al., 2020). The test durations in the current set of experiments were all set to ensure the foregoing conclusion held true.

To investigate the effect of border ice extent and flow strength on sediment transport rate, tests were done for five different ice coverage ratios including 0 (open water), 0.25, 0.50, 0.67, and 1 (fully covered); as well as five different dimensionless flow strengths (0.05, 0.06, 0.07, 0.085, 0.1). Two different sand bed slopes (0.1%, 0.26%) were used to facilitate this range of flow strengths. For each coverage ratio, one test was repeated to confirm that the experiments were repeatable. Also, five additional tests were done at a constant discharge over the same range of coverage ratios. As the ice coverage ratio increased, the water surface elevations increased which impacted the dimensionless flow strengths. These five additional tests were undertaken to simulate the manner in which a river might freeze over via border ice growth in the early winter under a constant discharge. The elevation of the simulated border ice was adjusted manually for each experiment. This is somewhat different than the process that might happen in nature, where a thin border ice cover might naturally deflect upwards as the water level rises. In nature the border ice could also temporarily become flooded with a rising water level; however, this flood water is likely to quickly freeze and serve to thicken the border ice from above in addition to the thermal ice thickening that occurs from below.

Table 2.1. Experimental conditions (note: C = coverage ratio, Q = flow rate, Fr = Froude number).

C	Dimensionless flow strength (θ)	Q (m^3/s)	Water depth (cm)	Slope (%)	Fr	Measured dimensionless bedload transport rate	Bedload collection time (min)
0	0.05	0.06	10	0.10	0.52	0.001	180
0	0.06	0.09	13	0.10	0.52	0.006	80
0	0.07	0.13	16	0.10	0.53	0.017	45
0	0.085	0.05	7	0.26	0.80	0.022	45
0	0.10	0.07	8	0.26	0.78	0.029	20
1	0.05	0.13	20	0.10	0.37	0.001	180
1	0.060	0.18	26	0.10	0.36	0.006	80
1	0.064	0.21	28	0.10	0.38	0.011	45
1	0.085	0.10	13	0.26	0.57	0.024	45
1	0.10	0.13	16	0.26	0.55	0.033	20
0.25	0.05	0.08	13	0.10	0.47	0.001	180
0.25	0.06	0.12	17	0.10	0.47	0.007	80
0.25	0.07	0.16	20	0.10	0.47	0.016	45
0.25	0.085	0.06	8	0.26	0.73	0.028	45
0.25	0.10	0.08	10	0.26	0.70	0.031	20
0.50	0.05	0.10	16	0.10	0.42	0.001	180
0.50	0.06	0.14	20	0.10	0.43	0.008	80
0.50	0.07	0.20	24	0.10	0.43	0.023	45
0.50	0.085	0.08	10	0.26	0.63	0.017	45
0.50	0.10	0.10	12	0.26	0.64	0.036	20
0.67	0.05	0.11	17	0.10	0.40	0.003	180
0.67	0.06	0.16	22	0.10	0.41	0.008	80
0.67	0.07	0.21	26	0.10	0.42	0.024	45
0.67	0.085	0.08	11	0.26	0.61	0.020	45
0.67	0.10	0.11	13	0.26	0.62	0.044	20
0	0.07	0.13	16	0.10	0.53	0.017	45
1	0.05	0.13	20	0.10	0.37	0.001	180
0.25	0.064	0.13	18	0.10	0.48	0.009	80
0.50	0.059	0.13	19	0.10	0.42	0.004	80
0.67	0.055	0.13	20	0.10	0.40	0.002	80

2.4 Results and Analysis

For each test, the average shear stress along the entire wetted perimeter was calculated using Equation [2.2], where τ = the average shear stress, γ = the specific weight of water, R_h = the hydraulic radius, and S = the water surface slope. The shear stress at the channel bed (τ_b) was then calculated by multiplying the average shear stress (τ) by 1.2 (Equation [2.3]) as suggested by Peters (2015) who used a log-law fitting procedure for similar hydraulic conditions in the same experimental setup.

$$\tau = \gamma R_h S \qquad [2.2]$$

$$\tau_b = 1.2\tau \qquad [2.3]$$

The dimensionless bedload transport rate (ϕ) and the dimensionless flow strength (θ), given in Equations [2.4] and [2.5], were calculated for each test using:

$$\phi = \frac{q_b}{(\Delta\, g D^3)^{1/2}} \qquad [2.4]$$

$$\theta = \frac{\tau_b}{\Delta\, \rho\, g\, D} \qquad [2.5]$$

where g = gravitational acceleration, D = the particle diameter, and Δ = s-1 (s = specific gravity of sediment).

The hydraulic radius was calculated using Equation [2.6], where A = the cross-sectional flow area; and P = the wetted perimeter. The wetted perimeter and area for open, partially ice-covered, and fully ice-covered flow is shown in Figure 2.3. In the current study only symmetric simulated border ice covers were used, and the extent of the ice cover was quantified by the coverage ratio, C, defined as the ratio of the top width covered by ice to the total top width.

$$R_h = \frac{A}{P} \qquad [2.6]$$

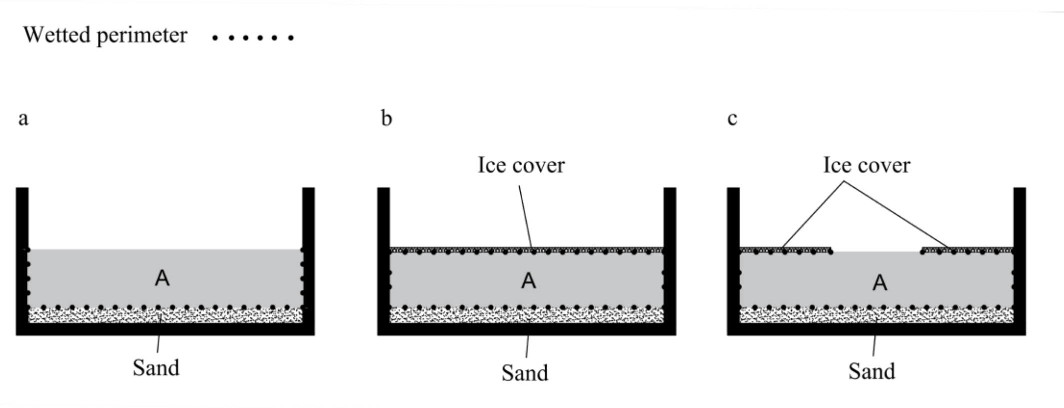

Figure 2.3. Wetted perimeter for a) open channel flow, b) fully ice-covered flow; and c) partially ice-covered flow.

Chein and Wan (1999) suggested an empirical equation relating ϕ to θ (Equation [2.7]) where θ_c is the critical dimensionless flow strength and α and β are empirical coefficients. Knack and Shen (2015) used a range of studies to empirically determine appropriate values of α and β (yielding $\alpha = 25$ and $\beta = 2.1$).

$$\phi = \alpha(\theta - \theta_c)^\beta \qquad [2.7]$$

Figure 2.4 shows the dimensionless bedload transport rate from the current set of experiments compared with previous studies for open channel flow and fully covered flow. The Knack and Shen (2015) equation is in close agreement with the data from the previous studies. There were some limitations in the current experimental setup, such as pump capacity, measurable water depth, and measurable amount of sand, causing a limited range of flow strengths to be included in the experimental data. It should be noted; however, that border ice formation during freeze-up is inhibited by very high water velocities, so the limited data range was viewed as sufficient.

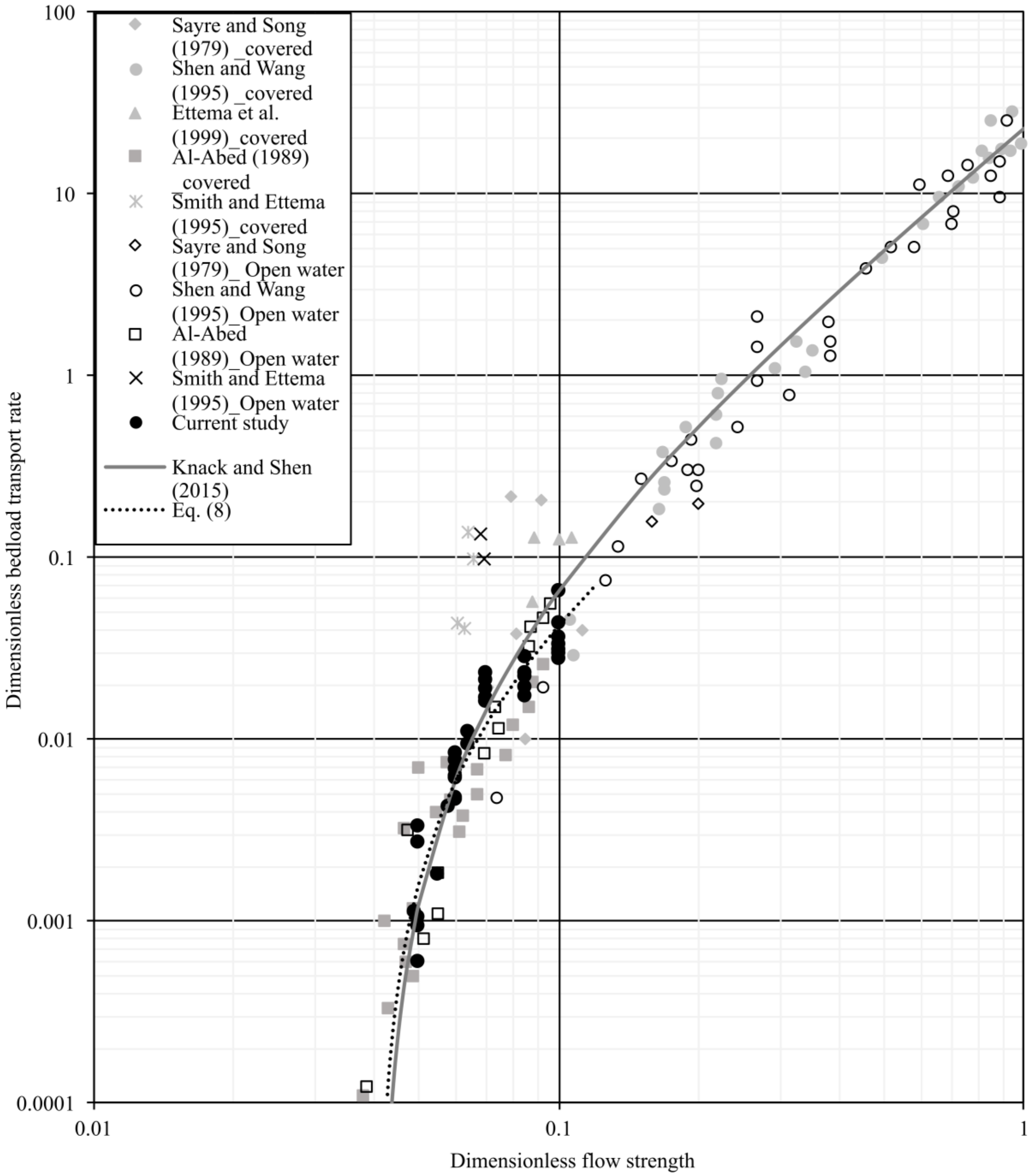

Figure 2.4. Comparison of experimental data and fitted equation to previous studies.

All data points from the current study were plotted, and the best-fit line using $\phi = \alpha(\theta - \theta_c)^{\beta}$ was drawn on the graph, with coefficients α and β (Equation [2.8] determined by minimizing the root-mean-square relative error as defined by Equation [2.9]). The E_{rms} calculated for this dataset is equal to 0.189, which is acceptable compared to previous studies (Knack & Shen, 2015) (Figure 2.4).

$$\phi = 6.07(\theta - 0.041)^{1.75} \quad [2.8]$$

$$E_{rms} = \sqrt{\frac{1}{N}\sum_{i=1}^{N}\left[\log\left(\frac{\phi_{calculated}}{\phi_{measured}}\right)\right]^2} \quad [2.9]$$

where N = the number of experimental measurements, $\phi_{calculated}$ = the value obtained by using Equation [2.8].

Uncertainty analyses of the experimental data were undertaken for the two main parameters using the method proposed by Coleman and Steele (1999). The resulting measurement uncertainty of θ and ϕ were found to be 5% and 2.5%, respectively.

For a constant discharge, an increase in the ice coverage ratio causes an overall increase in water depth and an overall decrease in water velocity and a commensurate decrease in flow strength. This is demonstrated in a series of tests with a constant discharge of Q = 0.13 m^3/s shown in Figure 2.5. The measured dimensionless bedload transport rate clearly decreases in response to increasing the coverage ratio.

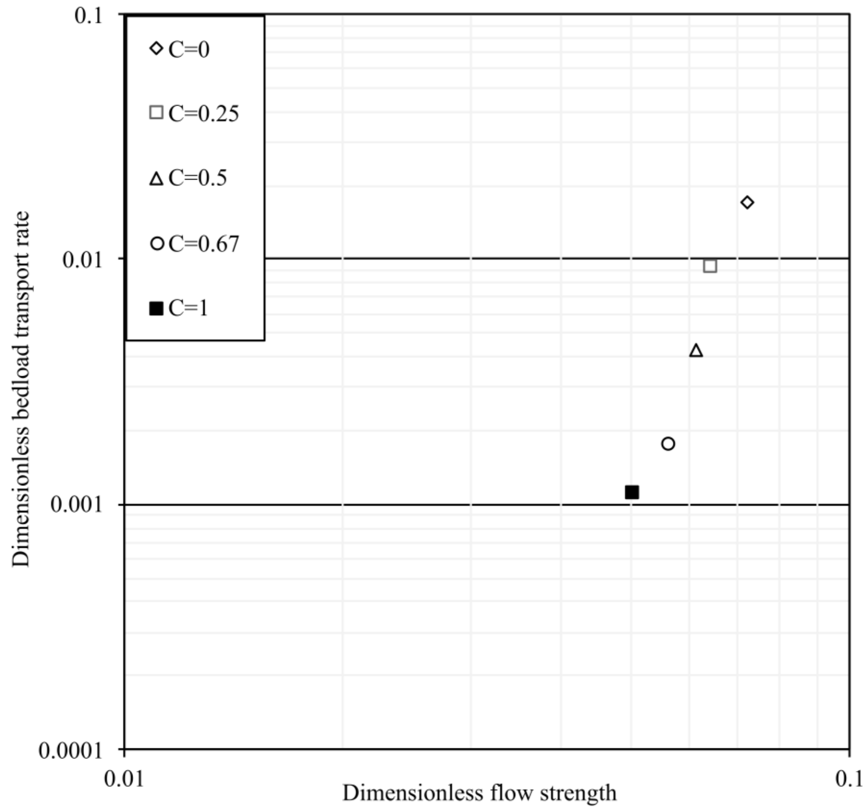

Figure 2.5. Effect of coverage ratio on bedload transport rate for a constant discharge of Q = 0.13 m^3/s.

The sediment trap was divided into three sections to investigate the effect of different extents of border ice on the dimensionless bedload transport rate. The values of ϕ and θ for each section are denoted with subscripts L, R, and M for the left, right, and middle sections, respectively; while the values of dimensionless flow strength and bedload transport rate for the entire cross-section have no subscript. The values of the section area, A, and wetted perimeter, P, used in the calculation of R_h for each section are defined in Figure 2.6.

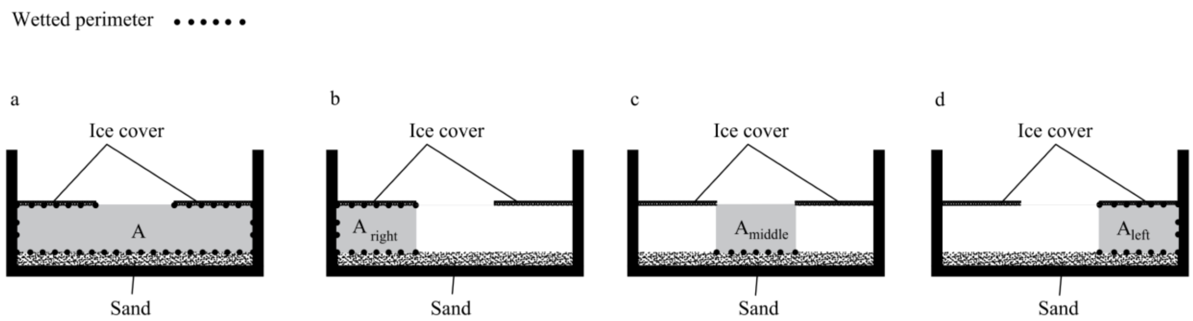

Figure 2.6. Wetted perimeter and area for the a) cross section, b) right section, c) middle section, and c) left section. Note the view is looking upstream.

The ratio of $(\phi_R + \phi_L)/ \phi_M$ was defined to help illustrate the change of the bedload transport rate in the side sections relative to the middle section. Understanding the shear stress distribution in a channel is necessary to analyze sediment transport. Shear stress distributions reported by Peters et al. (2017) were used to explain the sediment transport redistribution due to the ice cover presence. Also, for each coverage ratio, the velocity profile was measured using Nortek Vectrino II profiling acoustic Doppler velocimeter (ADV), and the bed shear stress distribution was calculated by fitting the log-law to each velocity profile. The results matched those of Peters et al. (2017) very well (Figure 2.7). In the case of open channel flow, if the bed shear stress distribution were perfectly uniform along the channel bed, $(\phi_R + \phi_L)/ \phi_M$ would equal two. However, the side-wall effects cause nonuniform sediment transport in the cross section during the open channel flow experiments. It is worth mentioning that the side-wall effects existed in all tests, including open channel, fully ice-covered, and partially ice-covered flow. The exact shape of the shear stress distribution is not constant in all the channels, and many factors like cross-sectional shape and aspect ratio, the sinuosity of the channel, and the boundary roughness distribution can affect it. Previous studies have indicated that the shear stress along the bed is zero in the corners and is the highest in the center of a rectangular channel (Oslen & Florey, 1952).

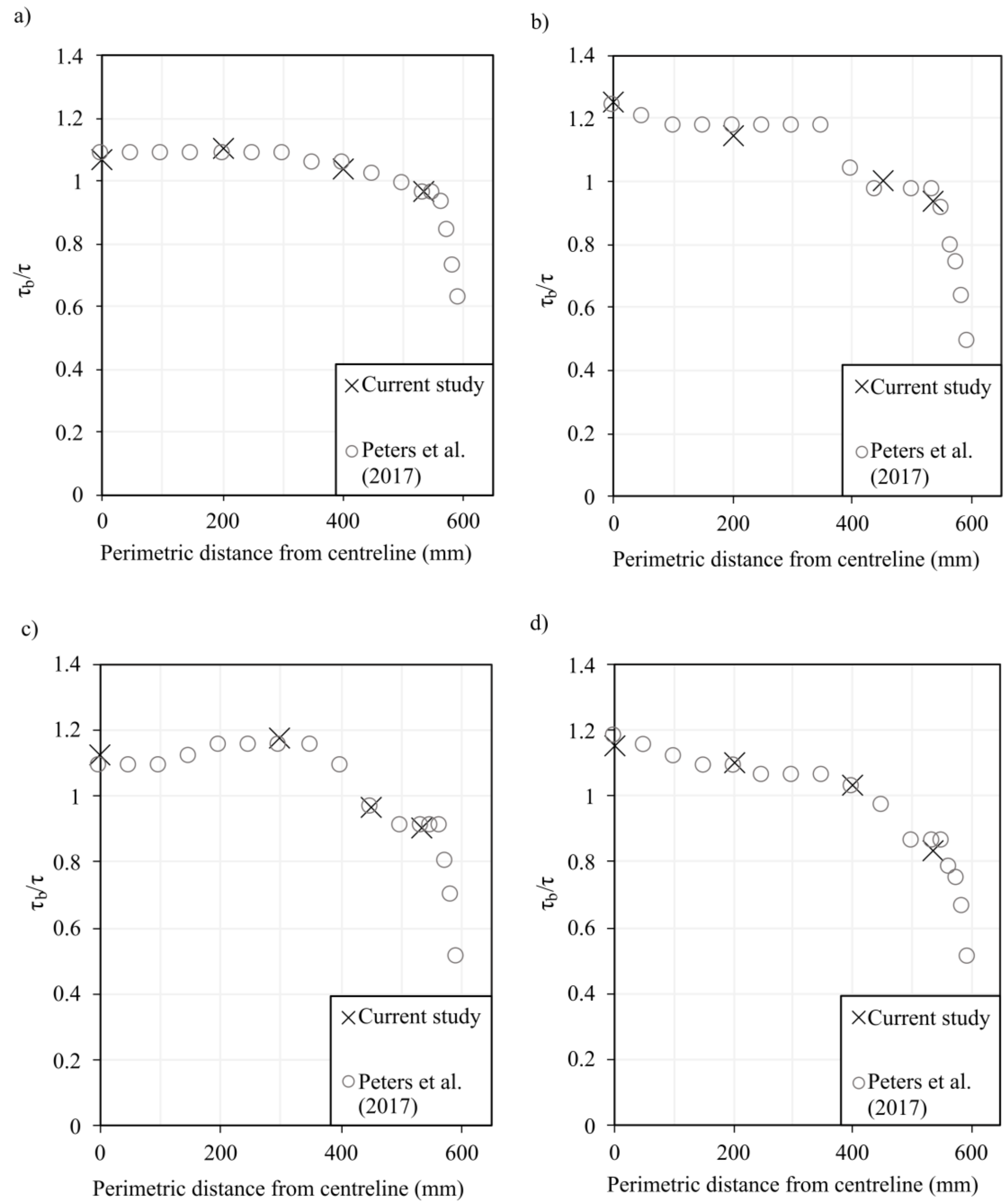

Figure 2.7. Dimensionless shear stress distribution for a) coverage ratio = 0, b) coverage ratio = 0.25, c) coverage ratio = 0.5, d) coverage ratio = 0.67.

The observed bedload transport rate in the current experiments was minimum in the corners and was highest in the center of the channel. A typical sediment transport distribution, showing the sediment collected in the sediment trap for one of the open channel tests, is shown in Figure 2.8. For this specific example, $(\phi_R + \phi_L)/\ \phi_M$ had a value of 1.18. These results show that side-wall effects did occur during the experiments, including the open channel flow experiment. The side-wall effects would have been similar for all experiments, which allows the incremental impact on sediment transport that is caused by a partial ice cover to be assessed.

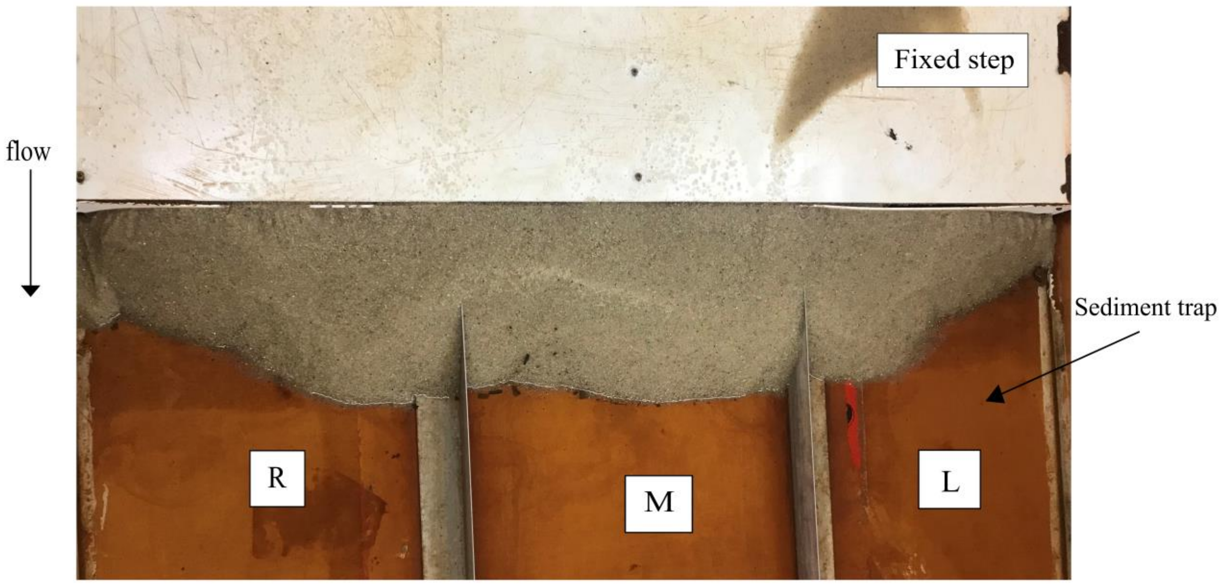

Figure 2.8. Typical open channel sediment transport distribution (plan view).

The shear stress distribution along the channel bed changes by adding full ice cover. Nezu and Nakagawa (1993) reported a shear stress distribution that did not have a maximum value at the center of the channel and instead had two maxima, each located approximately half the distance from the wall to the center. However, in the distribution presented by Knight et al. (1984), the global maximum shear stresses were at the center of the channel. In the current set of experimental results, $(\phi_R + \phi_L)/\phi_M$ of the fully ice-covered flow was equal to or less than that of open channel flow for a constant flow strength (Figure 2.9).

The shear stress distribution for partially ice-covered flow is even more complicated. Peters et al. (2017) presented a shear stress distribution for partially ice-covered channels with a coverage ratio of 0.25, 0.5, and 0.67. For most tests the minimum shear stress was in the corner, and the maximum shear stress was in the center of the channel. However, two tests did not follow this trend; the high Froude number experiment (Froude number = 0.5) and the 0.5 coverage ratio experiment, which instead had a maximum shear stress value beneath the edge of the ice and a local minimum value at the centerline.

Comparison of $(\phi_R + \phi_L)/\phi_M$ for different flow strengths and coverage ratios is shown in Figure 2.9. At a constant flow strength the open channel and fully ice-covered flow experiments had the most uniform sediment transport distribution across the channel as demonstrated by the relatively high values of $(\phi_R + \phi_L)/\phi_M$. It is worth noting that high values of dimensionless flow strength had more uniform sediment transport distributions with values of $(\phi_R + \phi_L)/\phi_M$ that were closer to 2. The presence of border ice caused a significant decrease in $(\phi_R + \phi_L)/\phi_M$, with larger coverage ratios even further decreasing the bedload transport rate in the side sections. This effect was more pronounced at lower flow strengths than at higher flow strengths. These results clearly demonstrate that border ice can cause a shear stress redistribution along the riverbed that promotes greater relative sediment transport in the middle of the channel and reduced relative sediment transport closer to the banks.

Peters et al. (2017) suggested that the shear stress distribution remains relatively constant for the different coverage ratios; however, their experiments were limited to dimensionless flow strengths in excess of 0.1. The current experiments are not necessarily in disagreement with this statement since the values of $(\phi_R + \phi_L)/\phi_M$ have a tendency to converge at high flow strengths. Also of interest is the fact that $(\phi_R + \phi_L)/\phi_M$ for C = 0.5 is greater than that for C = 0.67 in some of the current experiments. This may correspond to the observation by Peters et al. (2017) that the bed shear stress distribution peaked directly below the ice cover for C = 0.5 with a local minimum along the channel centerline.

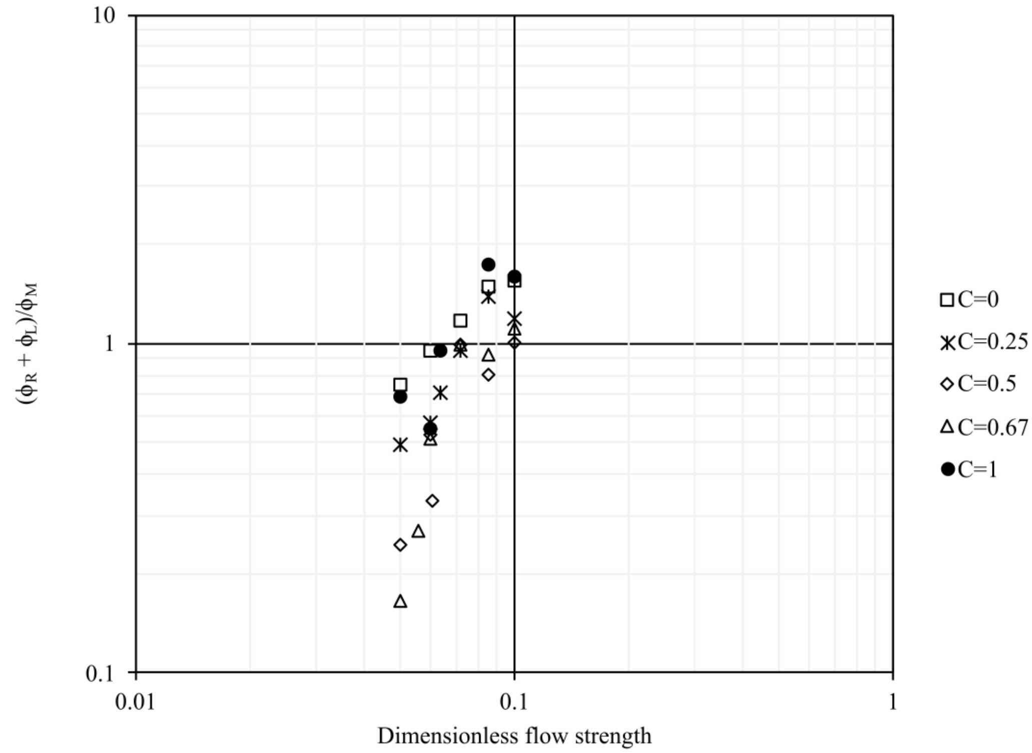

Figure 2.9. Effect of border ice coverage ratio on dimensionless bedload transport rate in the three sections of the sediment trap (R-M-L).

Figure 2.10 shows the detailed data upon which the ratios presented in Figure 2.9 were based. The rows of Figure 2.10 correspond to sets of experiments with the same coverage ratio. For a specific coverage ratio (or row of the figure) the plot in the left-hand column shows the how the total dimensionless bedload transport rate increases with increasing dimensionless flow strength. The figure in the right-hand column further separates out the experimental results into the left, middle, and right hand sections, (i.e. (θ_L, ϕ_L), (θ_M, ϕ_M), (θ_R, ϕ_R)). In each group of points, $\theta_L = \theta_R < \theta_M$, which means that the two points on the left-hand side shows the dimensionless bedload transport rate in the side sections, and the point on the right-hand side depicts the middle section. In all cases, the applied shear stress and bedload transport rate were higher in the middle section than the side sections. At high dimensionless flow strengths the rate of bedload transport in the middle section was only slightly higher than the sides; whereas at low dimensionless flow strengths the relative bedload transport rates in the sides were significantly less than the middle.

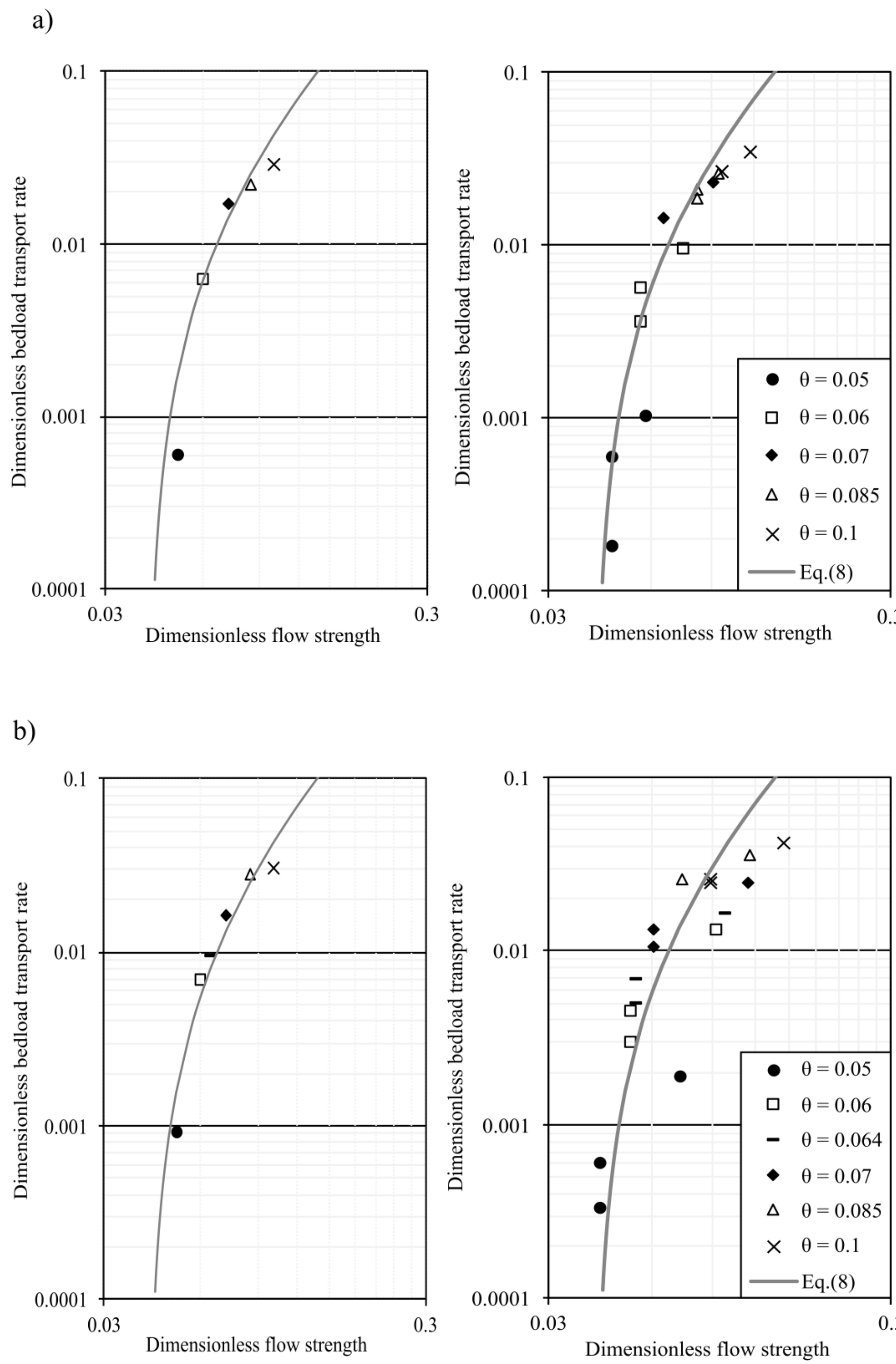
a)
0.1
0.01
0.001
0.0001
0.03
0.3
Dimensionless bedload transport rate
Dimensionless flow strength
θ = 0.05
θ = 0.06
θ = 0.07
θ = 0.085
θ = 0.1
Eq.(8)
b)
θ = 0.05
θ = 0.06
θ = 0.064
θ = 0.07
θ = 0.085
θ = 0.1
Eq.(8)

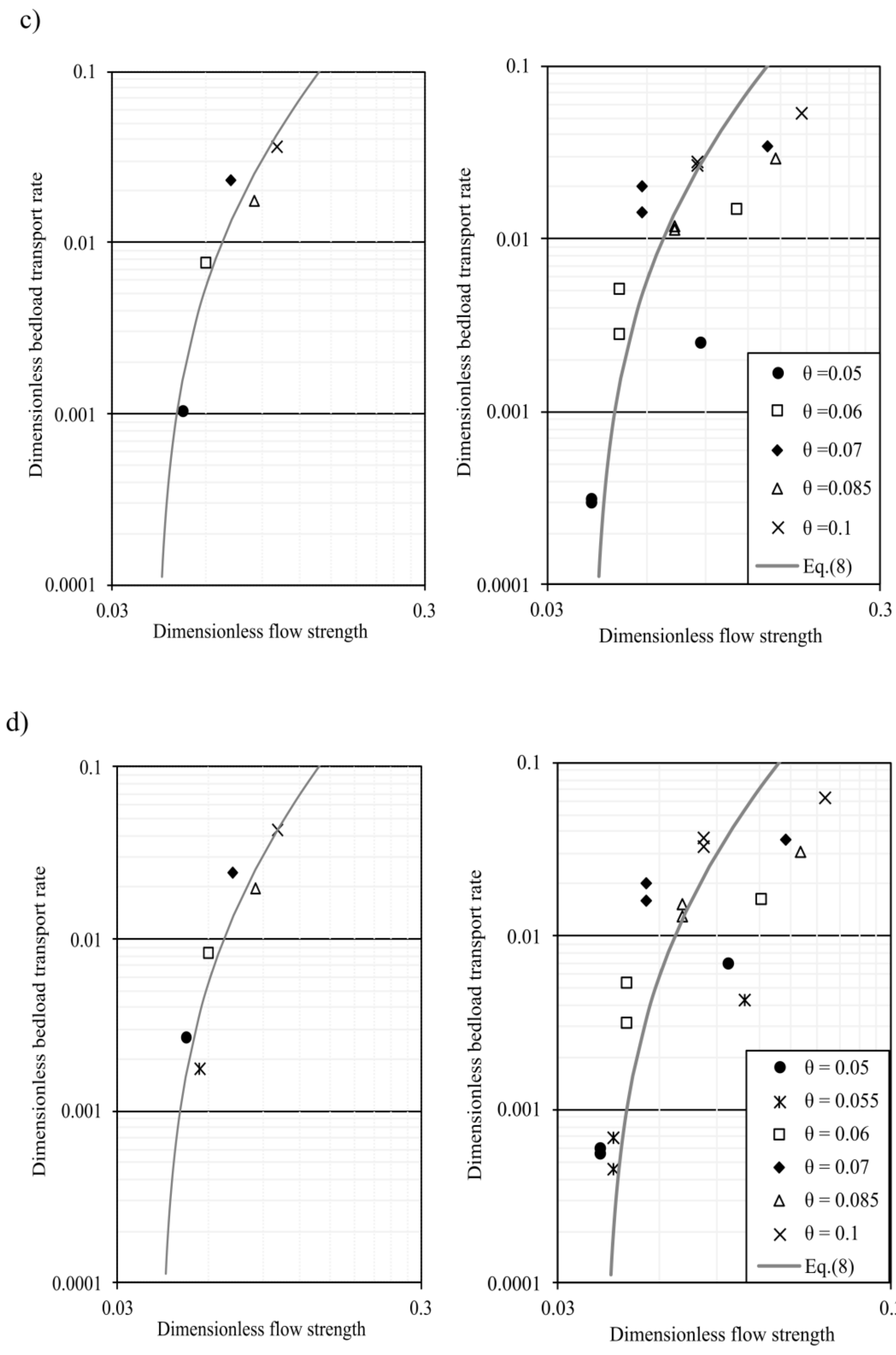

Figure 2.10. Comparison of the total dimensionless bedload transport rate (Left column in the figure) with dimensionless bedload transport rate in the left, middle, and right sections (Right column in the figure) for a) coverage ratio = 0, b) coverage ratio = 0.25, c) coverage ratio = 0.5, d) coverage ratio = 0.67, and e) coverage ratio = 1.

Figure 2.11 shows the effect of changing the coverage ratio on $(\phi_R + \phi_L)/\phi_M$ for different flow strengths. Figure 2.11 confirms the previous results regarding the coverage ratio and flow strength effect on the sediment transport distribution. The high values of $(\phi_R + \phi_L)/\phi_M$ for open channel flow (C = 0) and fully ice-covered (C = 1) demonstrate that sediment transport distribution is the most uniform in these two conditions. Also, high values of flow strength had a more uniform sediment transport distribution; that is, the value of $(\phi_R + \phi_L)/\phi_M$ is in the same range for θ = 0.07, 0.085, and 0.1. The presence of border ice caused a decrease in $(\phi_R + \phi_L)/\phi_M$, representing lower relative sediment transport close to the banks and greater relative sediment transport in the middle section. Once again, the effect of the coverage ratio extent on sediment transport distribution is more significant at lower flow strength than at higher flow strength.

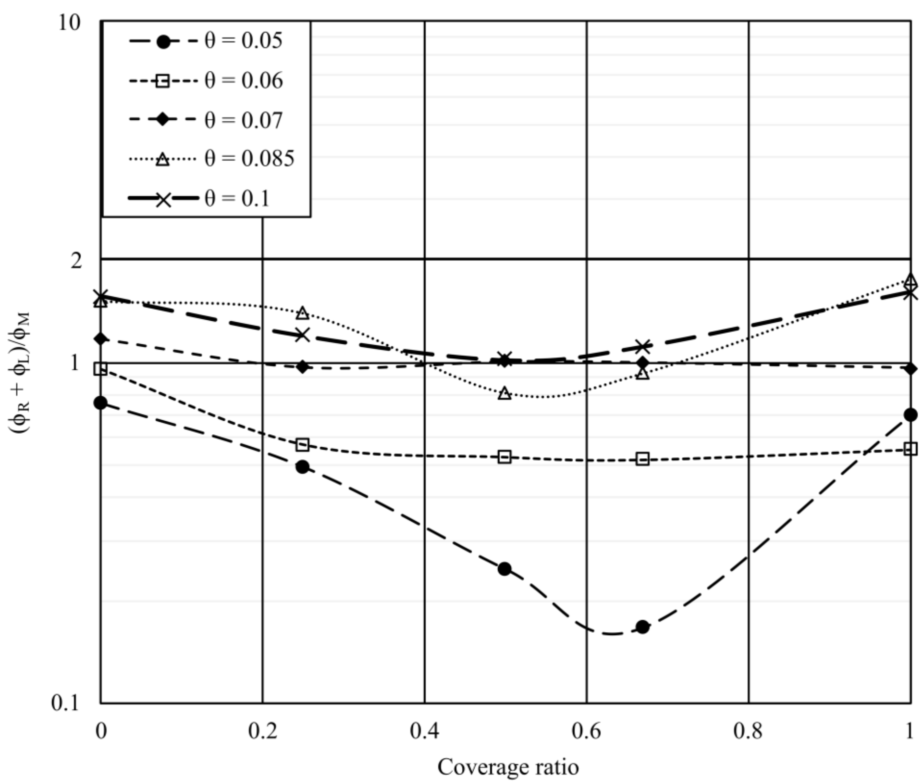

Figure 2.11. Coverage ratio effect on $(\phi_R + \phi_L)/\phi_M$ for different flow strengths.

2.5 Discussion

The current study enhanced the engineering ability to estimate the effect of ice cover on sediment transport and can be a benchmark for numerical studies on sediment transport in partially ice-cover rivers. Figure 2.12 shows an idealized schematic view of border ice growth in a river. Border ice starts forming along the river banks (Time 2). Once the initial border ice has formed, it grows horizontally inwards towards the center of the channel (Time 3 & 4) and vertically downwards as it thickens. It eventually forms a complete ice cover (Time 5). Border ice growth can occur due to two different mechanisms: thermal growth and frazil accretion, both vertically and laterally. This schematic does not represent the border ice growth process; instead, it is used to compare water depth and border ice width in different stages. In the case of a constant discharge throughout the period of border ice formation, increasing the coverage ratio results in additional flow resistance, which causes an overall decrease in water velocity and an overall increase in water depth, followed by an overall decrease in the bedload transport rate. Comparing partially ice-covered flow conditions shows that increasing the border ice coverage ratio (moving from Time 2 to Time 4) causes a decrease in $(\phi_R + \phi_L)/\phi_M$. That is, increasing C results in less uniform sediment transport distribution in a way that the relative bedload transport rate of the middle of the cross section increases and that of the side sections decreases. Prior to the current study, this type of flow redistribution beneath a partial ice cover was unquantified.

During the border ice growth period, late fall and early winter, discharge is typically relatively low compared to peak flows during the snowmelt-driven spring freshet. The applied shear stresses are, therefore, also typically lower than at peak flow. The likelihood of sediment transport beneath a partial ice cover is, therefore, greater in a river comprised of a bed material with a relatively low critical shear stress, which may include both non-cohesive and cohesive sediment. The current experimental results allow more accurate quantification of whether sediment transport will occur in any of a wide variety of rivers in northern climates, and more specifically allow which portions of a channel cross section would experience the most sediment transport to be estimated.

Border ice can influence sediment transport dynamics of a river in opposite ways. Firstly, border ice causes the frozen bank and bed material to be protected from being eroded by water, moving ice, and wind. Secondly, changes in water levels and velocities can cause border ice to be detached from the bank, causing the removal and transport of frozen bank and bed materials as well as any washload-size sediment originating from within the border ice itself (Turcotte et al., 2011). Border ice presence, therefore, has a complex effect on the sediment transport rate in northern rivers. In the current research, the process of border ice growth was not investigated, nor was the impact of these real-world sediment transport mechanisms explored. Instead, the focus was on providing the first quantitative results of bedload transport under partially ice-covered conditions.

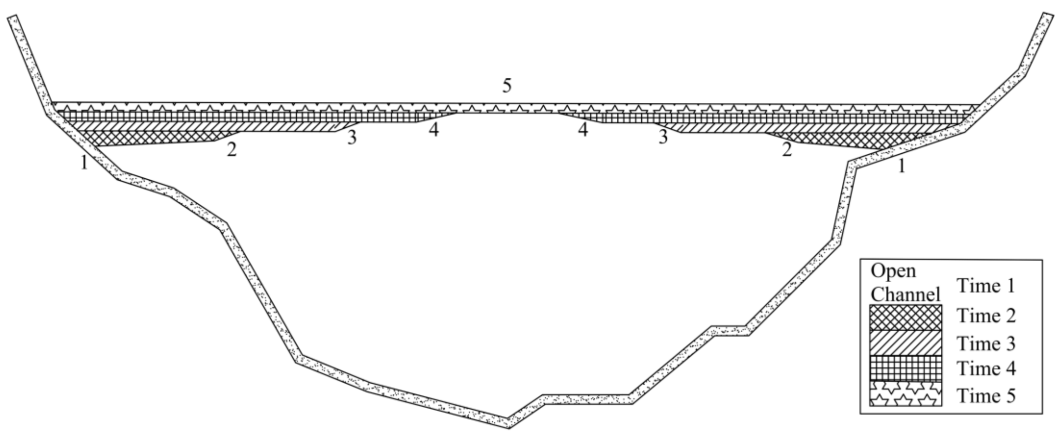

Figure 2.12. Schematic diagram of different stages of typical border ice growth.

Sediment transport redistribution caused by a partial ice cover has the potential to affect hydraulic structures, such as bridge piers. That is, designing the structures based on the total sediment transport rate is not always correct because ϕ_M is more than ϕ for the partially ice-covered period. Figure 2.13 shows that ϕ_M can be more than two times ϕ for a part of the year at relatively lower values of flow strength. Conversely, engineers interested in flow-induced riverbank erosion can note that the proportion of the channel's total sediment transport rate near the banks is reduced while a partial ice cover is present. The current results, therefore, allow engineers to have a more accurate estimate of sediment transport processes throughout the entire year, rather than relying on approximations during the winter.

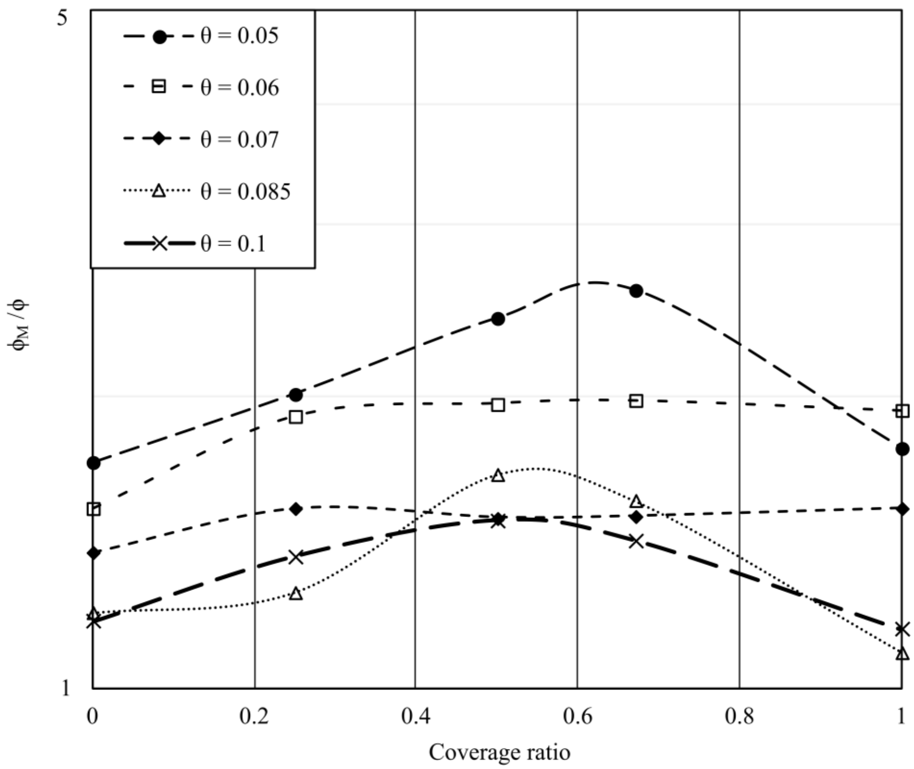

Figure 2.13. Coverage ratio effect on ϕ_M/ϕ for different flow strengths.

Blackburn and She (2019) presented developments to the river ice process model, River1D (She et al., 2009) to accommodate natural channel geometry and include freeze-up details such as border ice formation. The current experimental results would be difficult to incorporate into one-dimensional numerical models like this because of the cross-sectional averaging that occurs, while sediment transport redistribution takes place across the width of the channel. There may be more potential to incorporate the current experimental results into two dimensional river ice models like CRISSP2D (Shen, 2002) and RIVER2D (Steffler and Blackburn, 2002).

2.6 Conclusions

The main objective of the current research was to study sediment transport rate and distribution in partially ice-covered rivers. Sediment transport was studied in a controlled laboratory setting to find a formula to estimate the sediment transport rate in a partially ice-covered river, since sediment transport beneath a partial ice cover had not yet been studied. The experimental results were found to be comparable to previous studies. The general form of the Knack and Shen (2015) equation, suggested for open and fully ice-covered flow, can be used to estimate the total cross-section-averaged sediment transport rate for partially ice-covered flow. Empirical coefficients for this equation were calculated using the experimental results. However, this equation falls short in predicting the level of sediment transport redistribution that can occur beneath a partial ice cover. Results confirmed that for a given discharge, an increasing partial ice coverage ratio caused an overall decrease in the total sediment transport of the entire cross section.

Previous studies (Essel et al., 2021; Kimiaghalam et al., 2017; Peters, 2015) demonstrated that the presence of border ice caused redistribution in flow characteristics. The current study confirmed that border ice redistributes sediment transport as well. In order to quantify sediment transport redistribution, the coefficient of $(\phi_R + \phi_L)/\phi_M$ was defined, calculated, and compared for all the tests. At dimensionless flow strengths approaching 0.1, the effect of having different coverage ratios on sediment transport distribution across the channel was minor. At lower values of dimensionless flow strength, it was found that increasing the amount of border ice cover caused a pronounced redistribution of sediment transport, with the relative rate near the banks decreasing and the relative rate within the middle section increasing.

2.7 Acknowledgments

The authors would like to acknowledge Alexander Wall for his assistance with the experimental setup. This research was supported by the Natural Sciences and Engineering Research Council of Canada (NSERC-RGPIN-2018-06448).

Chapter 3 Paper 2: Sediment transport beneath a simulated partial ice cover: Effects of asymmetric border ice

3.1 Abstract

With the onset of winter in cold regions, border ice begins to form, impacting sediment transport rate and distribution. Understanding the effect of ice cover is crucial in regions with prolonged sub-freezing temperatures, as water bodies remain frozen for a considerable part of the year. While the existing literature includes many studies on sediment transport in open channel flow and several studies on completely ice-covered flow, there is limited research on sediment transport in partially ice-covered channels. Addressing this gap, the current study conducted laboratory experiments in a rectangular flume at the Hydraulics Research and Testing Facility, University of Manitoba, Canada. The investigation focused on examining the influence of asymmetric border ice, varying coverage ratios in asymmetric partially ice-covered flow, and changing flow strengths on bedload transport rate and distribution. Additionally, a comparison was made with symmetric partially ice-covered flow conditions. The findings indicate that the presence of asymmetric border ice indeed affected the bedload transport distribution within the channel, causing non-uniform bedload transport distribution across the channel width, with peak values concentrated in the center of the open flow section. Increased asymmetry in border ice leads to greater asymmetry in bedload transport rate distribution. Despite these pronounced differences in bedload transport rate across the channel width, the cross-section-averaged bedload transport rate could still be estimated utilizing the conventional equations, used for open channel flow, fully ice-covered flow, and symmetric partially ice-covered flow, with the effect of ice cover accounted for by incorporating an additional boundary in the calculation of the wetted perimeter, leading to adjustments in the flow strength.

Keywords: sediment transport; bedload; ice-covered channel; asymmetric border ice

3.2 Introduction

Throughout the winter season, ice is commonly found on almost all rivers in northern climates, leading to substantial changes in flow distribution, discharge, water levels, and sediment transport. When temperatures begin to decrease, border ice may form along the riverbanks and gradually extend toward the center of the channel, leading to the formation of a partial ice cover. Also, during midwinter thaw events, the main section of the channel may open up, creating a partial ice cover (Peters et al., 2017). Climate change has the potential to increase the duration of partially ice-covered flow in northern rivers by delaying freeze-up and increasing the frequency and duration of mid-winter thaws. Therefore, considering the influence of a partial ice cover becomes essential in fully understanding a river's sediment budget in specific cases. While previous studies have primarily concentrated on open channel flow and fully ice-covered flow, there has been limited investigation into partially ice-covered flow. It is important to gain insights into border ice impact on river flow, sediment transport, and geomorphology to improve our understanding of how rivers with partial ice covers change over time (Clark, 2013).

Partial ice cover research has mainly relied on experimental measurements due to limitations in field studies and numerical modeling. Field studies encounter challenges due to the transient nature of border ice growth and the fragility of thin ice, which can raise safety concerns in data collection (Nyantekyi-Kwakye et al., 2021). On the other hand, the lack of sufficient benchmarks for model validation makes numerical modeling challenging. As a result, experimental measurements have emerged as the favored method for understanding partial ice cover phenomena phenomena (Majewski, 1992; Peters et al., 2018;Kimiaghalam et al., 2017; Essel et al., 2021). These studies involve exploring the effects of border ice on flow characteristics by Peters et al. (2017), turbulent flow behavior by Essel et al. (2021), shear stress distribution by Kimiaghalam et al. (2017), and the influence of bed and ice roughness by Peters et al. (2018).

Bed sediment motion is a result of the forces applied to individual bed particles (lift, drag, and gravity). The presence of ice cover causes turbulence and a reduction in water drag on the bed (Ettema & Daly, 2004). This is mainly because of the additional boundary resistance from the ice cover, leading to raised water levels and a decrease in average velocity and sediment transport rate for the same flow rate. Furthermore, the presence of ice cover can cause lateral flow redistribution, resulting in a varying impact on sediment transport rates at specific locations along the spanwise direction. Therefore, the effect of ice cover on river bed and bank dynamics is complex and variable in different situations (Ettema & Daly, 2004). The analysis of partially ice-covered rivers is even more complex because of the concurrent presence of open water and ice cover.

There have been a limited number of studies exploring the impact of ice presence on sediment transport rate. Ettema and Daly (2004) provided qualitative insights into how ice cover affects sediment transport by developing a set of dimensionless parameters. (Lawson, 1986) conducted fieldwork, measuring suspended and bedload concentration data during winter and comparing them to data from the summer period. Experimental studies, e.g., (Wuebben, 1986, 1988), suggested open water theories applying to lower flow layers in ice-covered conditions. Shen and Wang (1995) supported conventional relations for bedload transport in ice-covered channels by conducting flume experiments with a floating cover and low-density chips. Additional experimental work has explored the effect of ice on sediment transport rate (Al-Abed, 1989; Muste et al., 2000). Ettema et al. (2000) conducted a study to assess sediment transport rate and bedforms under the influence of ice. They compared flume data from various studies, including Ettema et al. (1999), Sayre an Song (1979), Smith and Ettema (1995) with Meyer-Peter and Muller’s (1948) and Einstein’s (1950) formulas, making similar suggestions for sediment transport rate. Few numerical model studies have explored the effects of river ice cover on sediment transport and changes in the riverbed. Notable examples of such studies are those conducted by Carr and Tuthill (2012), Kolerski and Shen (2015), Manolidis and Katopodes (2014), Zhang et al. (1994), and Knack (2011). Knack and Shen (2018) illustrated the development of a coupled model, which integrates a sediment transport and bed change model with a hydro-thermal-ice dynamics model. To validate the model, laboratory experiments were conducted under open water conditions, as there was a lack of laboratory or quantitative field observations on bed changes under ice conditions.

Rouzegar and Clark (2023a) investigated the bedload transport rate in a partially ice-covered channel and showed that the conventional equation describing the bedload transport in open channel and fully ice-covered flow was applicable in estimating the total cross-section-averaged bedload transport for partially ice-covered flow. In this equation, the dimensionless bedload transport rate was related to flow strength, and an empirical coefficient for this equation was derived from experimental data. They also investigated the bedload transport distribution influenced by different extents of ice cover and compared the result with open channel and fully ice-covered flow. In a qualitative experimental study, Rouzegar and Clark (2023b) investigated the effect of asymmetric border ice on bedload transport distribution, considering that border ice in nature does not always follow a symmetric pattern. The current study aims to build on previous work, and for the first time quantify the effect of asymmetric border ice on bedload transport rate and distribution. Results are compared with symmetric border ice conditions as well as open channel flow conditions, and the dramatic differences in specific channel locations are highlighted.

3.3 Methodology

A 14-m-long, 1.2-m-wide flume was constructed using high-density overlay (HDO) plywood with a bed slope of 0.26% for the experiments (Figure 3.1). The simulated ice cover was made of flexible plastic bubble wrap. To achieve the desired ice coverage ratio (the ratio of the top width covered by ice to the total top width) and prevent lateral movement of the simulated ice during each partially ice-covered test, the bubble wrap was nailed to the flume wall at the appropriate elevation (Figure 3.2). A layer of uniform silica sand, 70 mm thick, with a median diameter (d50) of 1.3 mm, was evenly distributed along the entire flume length to simulate a sand bed. At the downstream end of the flume, a fixed step with dimensions of 1.2 m in width, 0.6 m in length, and a height equal to the sand height was installed. The purpose of this step was to create a separation between the movable sand and the sediment trap, which was positioned downstream of the step. The sediment trap was partitioned into a few separate bins oriented in the streamwise direction. This division of the sediment trap allowed for precise measurements of the bedload transport rate in both ice-covered and open sections of the channel. All experiments were carried out at room temperature, while actual border ice formation in the field occurs at temperatures near zero. The current research did not explore the impact of varying water temperatures. Further details of the experimental setup and procedure can be found in Rouzegar and Clark (2022, 2023a).

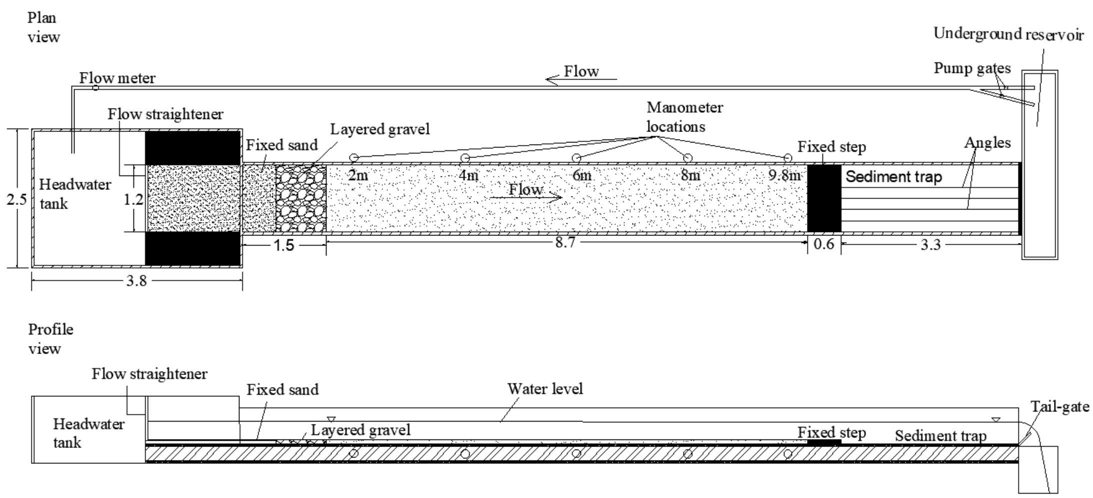

Figure 3.1. Schematic diagram of the experimental setup (all dimensions in meters).

Figure 3.2. Simulated ice covers for asymmetric partially ice-covered flow.

The bedload transport experiments were conducted under uniform flow conditions. This was accomplished by modifying the water depth and discharge to meet the specific requirements of each test, following the method outlined by Rouzegar and Clark (2023a). Throughout all experimental runs, the water surface slope and flow depth were assessed using five 39.4 mm diameter manometer tubes installed on the flume wall, equipped with a point gauge with an accuracy of ±0.2 mm. Also, confirmation of fully developed flow was obtained by utilizing a Nortek Vectrino acoustic Doppler velocimeter to measure vertical profiles of streamwise velocity at different distances along the flume length. The duration of each test was adjusted based on the bedload transport rate, resulting in shorter test durations for higher bedload transport rates and relatively longer durations for lower bedload transport rates.

After completing each experiment, sand in different sections of the sediment trap was collected separately. The collected sand was dried in an oven at a precise temperature of 110 ± 5 °C (230 ± 9 °F) and then allowed to cool in the air at room temperature for approximately 1 ± 1⁄2 h. Subsequently, the mass of dried sand was measured with an accuracy of ±0.2 g [30]. The sediment volume was calculated knowing that the bulk density of sand was 1.5 g/cm^3 ($\rho = \frac{G}{V}$), where G is the collected and dried mass of sediment [g], V is the volume of dried sediment [m^3], and ρ is the sand bulk density. The volumetric rate of bedload transport per unit width (q_b) was then calculated using Equation [3.1] (Khosravi et al., 2020; Nezu & Rodi, 1986; Tsai & Ettema, 1994):

$$q_b = \frac{V}{\mathrm{b}T} \quad [3.1]$$

where T is the sampling time [s] and b is the flume width [m].

In experiments with relatively short durations, the absence of upstream sediment supply throughout the tests has an observable impact solely at the upstream end of the channel, leaving the morphology in downstream sections and the channel's sediment transport rates unaffected (Binns & da Silva, 2009; Khosravi et al., 2020). The test durations in the current experiments were all set to ensure the foregoing conclusion was true.

Rouzegar and Clark (2023a) have investigated the effect of flow strength on bedload transport rate and distribution in a symmetric partially ice-covered channel. In the current study, seven tests were designed, including four different dimensionless flow strengths (0.05, 0.06, 0.07, 0.1), two different coverage ratios (0.5, 0.67), and three different shapes of asymmetric border ice, to explore the impact of such asymmetry on bedload transport rate and distribution. The test conditions are listed in Table 3.1.

Table 3.1. Experimental conditions (note: C = coverage ratio, Q = flow rate).

Test No.	C	Dimensionless Flow Strength (θ)	Q (m^3/s)	Water Depth (m)	Sand Bed Slope (%)	Border Ice Width-Right (m)	Border Ice Width-Left (m)
II-1	0.67	0.05	0.11	0.17	0.1	0.2	0.6
II-2	0.67	0.06	0.16	0.22	0.1	0.2	0.6
II-3	0.67	0.07	0.21	0.26	0.1	0.2	0.6
II-4	0.67	0.10	0.11	0.13	0.26	0.2	0.6
II-5	0.5	0.05	0.10	0.16	0.1	0	0.6
II-6	0.5	0.05	0.10	0.16	0.1	0.15	0.45
II-7	0.5	0.07	0.20	0.24	0.1	0.15	0.45

3.4 Results and Analysis

The influence of asymmetric border ice on bedload transport rate and distribution was investigated through a comprehensive experimental analysis of various factors and conditions.

3.4.1 Cross-Section-Averaged Bedload Transport Rate

For each test, dimensionless flow strength ($\theta = \frac{\tau_b}{\Delta\, \rho\, g\, D}$) and cross-section averaged dimensionless bedload transport rate ($\phi = \frac{q_b}{(\Delta\, g D^3)^{1/2}}$) were calculated (to calculate ϕ_{avg}, the total mass of dry sand within the entire sediment trap was taken into account.), where τ_b = average bed shear stress, τ = cross-sectional average shear stress ($\tau = \gamma R_h S$), R_h = the hydraulic radius, S = water surface slope, g = gravitational acceleration, D = particle diameter, and $\Delta = s - 1$ (s = specific gravity of sediment). The calculation of the shear stress at the channel bed (τ_b) involved multiplying the cross-sectional average shear stress (τ) by 1.2, as suggested by Peters (2015). Peters (2015) utilized a log-law fitting procedure for comparable hydraulic conditions within the same experimental setup. Rouzegar and Clark (2023a) further investigated the impact of ice cover on the flow dynamics, measuring the velocity profiles for each coverage ratio using a Nortek Vectrino II profiling acoustic Doppler velocimeter (ADV), and calculated the bed shear stress distribution by fitting the log-law to each velocity profile. Since the results obtained from Rouzegar and Clark's (2023a) analysis closely matched those reported by Peters et al. (2017), the consistency and reliability of the findings confirm the results used in this study. The wetted perimeter and area for different conditions of asymmetric border ice are shown in Figure 3.3.

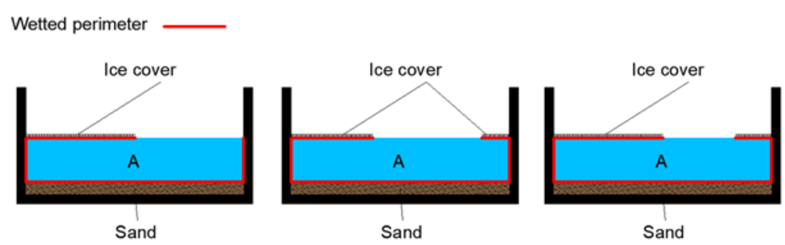

Figure 3.3. Wetted perimeter and area for channels with asymmetric border ice.

Figure 3.4 compares the cross-section-averaged dimensionless bedload transport rate derived from the current set of experiments involving asymmetric border ice with data from previous studies that examined symmetric partially ice-covered, fully ice-covered, and open channel flow conditions. The figure also includes the empirical equation proposed by Knack and Shen (2015) (Equation [3.2]). Remarkably, this empirical equation aligns fairly well with the data from the current experiments, implying that it has the capability to predict the cross-section-averaged dimensionless bedload transport rate in asymmetric partially ice-covered rivers, similar to Rouzegar and Clark's (2023a) findings for symmetric border ice conditions.

$$\phi = \alpha(\theta - \theta_c)^{\beta} \qquad [3.2]$$

where α and β = empirical coefficients and θ_c = critical dimensionless flow strength. Equation [3.2] was originally suggested by Chein and Wan (1999). Knack and Shen (2015) empirically determined appropriate values of α and β through a range of studies (yielding $\alpha = 25$ and $\beta = 2.1$).

It is worth noting that the experimental setup limitations, like pump capacity, measurable water depth, and measurable sand quantity, restricted the range of flow strengths. However, the available data within a limited range were considered sufficient for the study's purposes because extremely high water velocities prevent the formation of border ice during freeze-up.

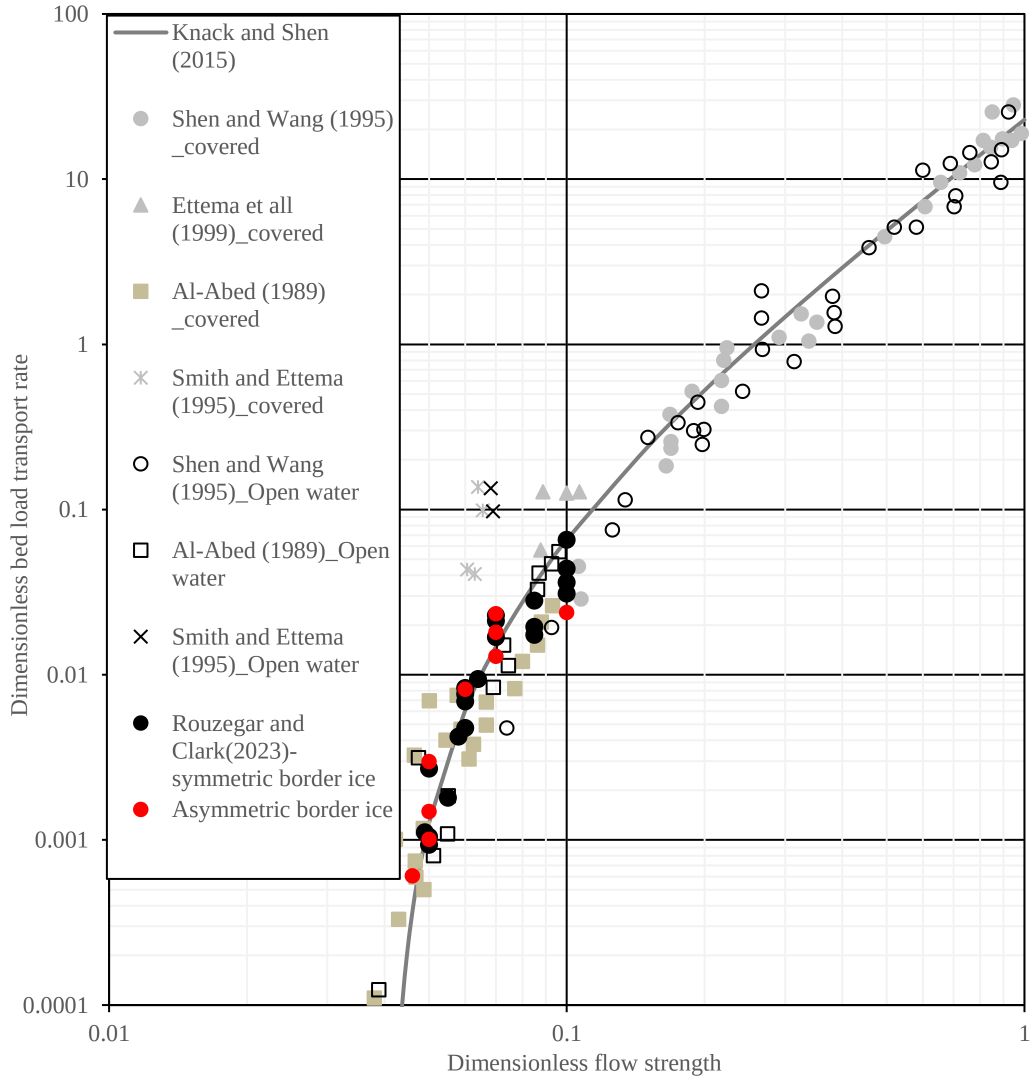

Figure 3.4. Comparison of experimental data to previous studies (Al-Abed, 1989; Ettema et al., 1999; Rouzegar & Clark, 2023b; Shen & Wang, 1995; Smith & Ettema, 1995) and Knack and Shen's (2015) equation.

3.4.2 Effect of Level of Asymmetry

The effect of the level of asymmetry in partially ice-covered flow was investigated through the examination of three different experiments, wherein varying B_r (border ice width on the right-hand-side of the channel) and B_l (border ice width on the left-hand-side of the channel) were considered. The data for the symmetric case is derived from the work of Rouzegar and Clark (2023a). A constant coverage ratio (C = 0.5) and flow strength (θ = 0.05) were maintained throughout all three tests to ensure comparability of results and facilitate the exclusive observation of the influence of the level of asymmetry. The asymmetric condition for each test is shown in Table 3.2. For each test, the dimensionless bedload transport rate in each bin (ϕ) and cross-section-averaged dimensionless bedload transport rate (ϕ_{avg}) were calculated, and ϕ/ϕ_{avg} was obtained.

Figure 3.5 illustrates the bedload transport rate distribution in the aforementioned experiments. In this figure, Y represents the distance from the flume wall, and b denotes the flume width. Also, thick lines correspond to the covered sections, while the dotted line indicates the open sections. Figure 3.5c illustrates the bed load transport distribution across the channel width in the presence of symmetric border ice, with the peak value located at the center of the channel and the minimum value observed in the corners. The presence of symmetric border ice causes lower relative bedload transport close to the banks and greater relative bedload transport in the middle section (Rouzegar & Clark, 2023b). Asymmetric border ice can cause even more redistribution in the bedload transport rate, leading to a non-uniform distribution of bedload transport across the channel width. That is, the peak values of bedload transport tend to be concentrated in the center of the open flow section rather than the center of the channel in symmetric border ice flow conditions (Figure 3.5a,b). The greater the level of border ice asymmetry, the more asymmetry in bedload transport rate distribution was observed. Also, the difference of ϕ/ϕ_{avg} in the open section and the covered section is more significant when the level of asymmetry increases.

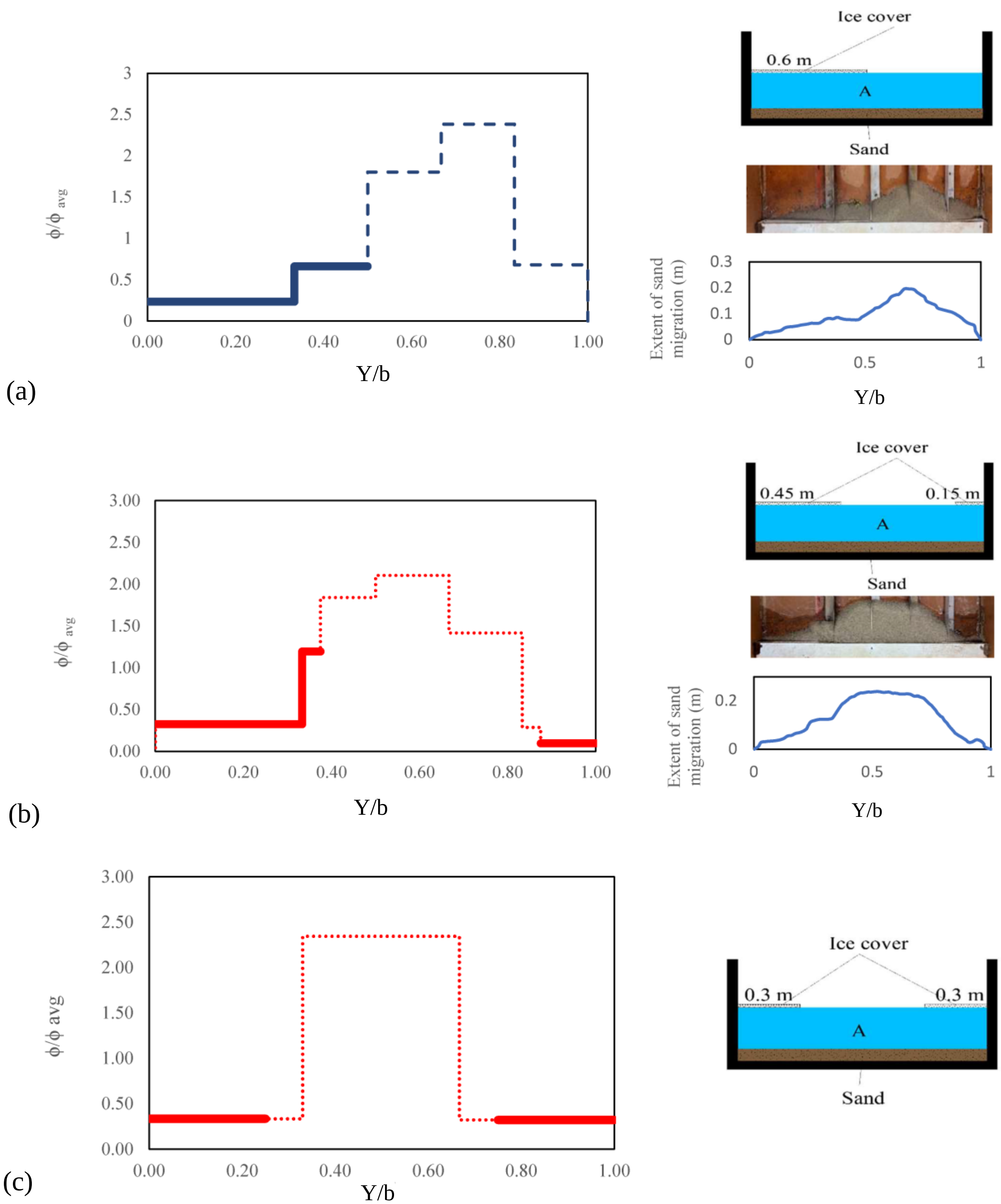

Figure 3.5. Comparison of bedload transport rate distribution for constant coverage ratio (C = 0.5) and flow strength (θ = 0.05) and different levels of asymmetry (a) B_r = 0, B_l = 0.6 m; (b) B_r = 0.15 m, B_l = 0.45 m; and (c) B_r = 0.3 m, B_l = 0.3 m.

Presuming that the sediment trap has been partitioned into three equally sized sections, labeled as R (right section), M (middle section), and L (left section) when observing in the downstream direction, for each section, the ratio of ϕ/ϕ_{avg} was calculated and is summarized in Table 3.2. As depicted in the figure adjacent to Table 3.2, the first test exhibits no ice cover in the right section, leading to the highest ϕ_R/ϕ_{avg} ratio among all tests. However, as the coverage ratio increases in the right section, the ϕ_R/ϕ_{avg} ratio decreases. Conversely, in the middle section, test 1 demonstrates the most substantial ice cover compared to the other tests, resulting in the lowest ϕ_M/ϕ_{avg} ratio, which then progressively increases from test 1 to 3. The same trend is observed for the left section. These results show that ice coverage leads to a proportionate decrease in bedload transport rate in the covered sections and a corresponding increase in bedload transport rate in the open flow section.

Table 3.2. Effect of level of asymmetry on bedload transport distribution.

Test No.	θ	B_r	B_l	C	ϕ_R/ϕ_{avg}	ϕ_M/ϕ_{avg}	ϕ_L/ϕ_{avg}
1	0.05	0	0.6	0.5	1.532	1.232	0.235
2	0.05	0.15	0.45	0.5	0.781	1.892	0.327
3	0.05	0.3	0.3	0.5	0.322	2.344	0.334

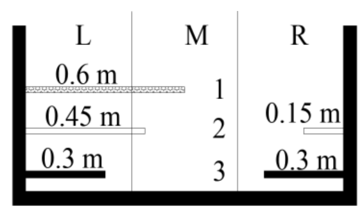

Figure 3.6 further separates out the experimental results of the three mentioned tests into the average, left, middle, and right sections, (i.e., (θ, ϕ_{avg}), (θ_L, ϕ_L), (θ_M, ϕ_M), (θ_R, ϕ_R)). In this figure, the data for the right section is represented by " ─ ", the middle section by "▲", the left section by " × ", and the average is denoted by " ● ". Additionally, test number 1 is depicted in red, test number 2 in blue, and test number 3 in green.

A comparison of data points reveals that when a section is predominantly covered by ice in each test, the additional boundary leads to reduced flow strength and, consequently, lower ϕ values. Conversely, for open sections, the trend is reversed, resulting in higher ϕ values. Moreover, all tests (θ, ϕ_{avg}) align with the predicted line, indicating that the equation effectively estimates the average-cross-section bedload transport rate. However, data points related to the right, middle, and left sections deviate from the line, potentially due to assumptions made in the calculation of the wetted perimeter, resulting in inaccuracies in flow strength estimation. Upon analyzing the data points, it becomes evident that for sections mainly covered by ice (L(1), L(2), L(3), R(2), R(3)), the assumed value for θ is underestimated due to an overestimation in the wetted perimeter calculation. Conversely, for open sections (M(1), M(2), M(3), R(1)), the value for θ is overestimated because of an underestimation in the wetted perimeter calculation. The reason for potential underestimation or overestimation in calculating the wetted perimeter for different sections individually is due to the exclusive consideration of the solid interface in the wetted perimeter calculation, while disregarding the water interface length between the higher momentum and lower momentum fluid.

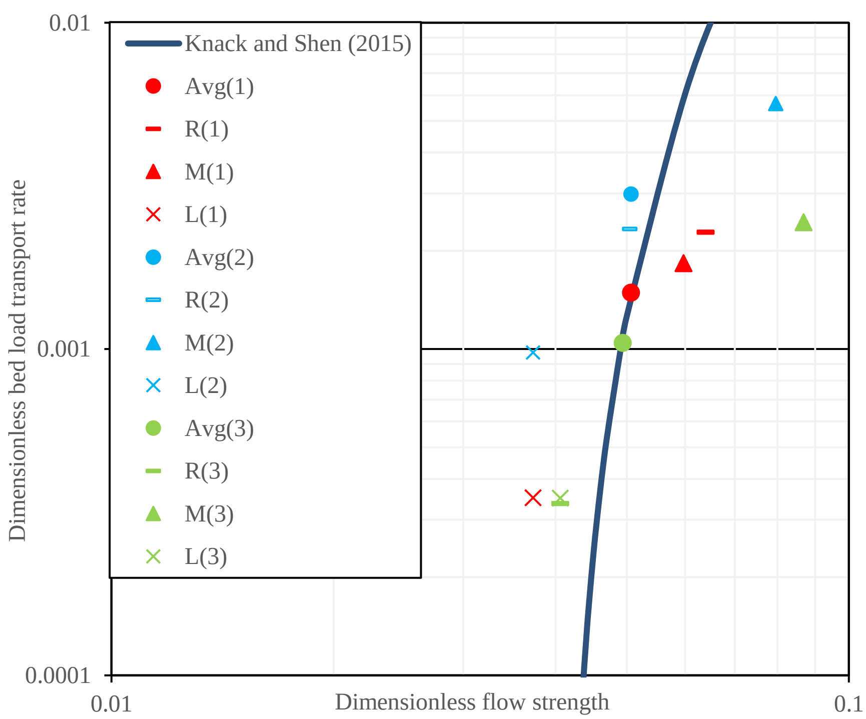

Figure 3.6. Comparison of dimensionless bedload transport rate in the left, middle, and right sections of the channel.

3.4.3 Effect of Coverage Ratio

The effect of the coverage ratio was investigated by comparing two groups of tests under symmetric (Rouzegar & Clark, 2023b) and asymmetric conditions (Figure 3.7). In each group of the test, flow strength was kept constant while varying the coverage ratio. The results showed that increasing the coverage ratio caused an increase in ϕ/ϕ_{avg} in the central section, while it caused a decrease in ϕ/ϕ_{avg} in the side sections for both symmetric and asymmetric conditions. These findings confirm that ice coverage contributes to a relative reduction in bedload transport rate in the covered sections and a relative increase in bedload transport rate in the open flow section. Also, as the coverage ratio increased, there was a greater redistribution in bedload transport, resulting in a less uniform f distribution along the cross-section.

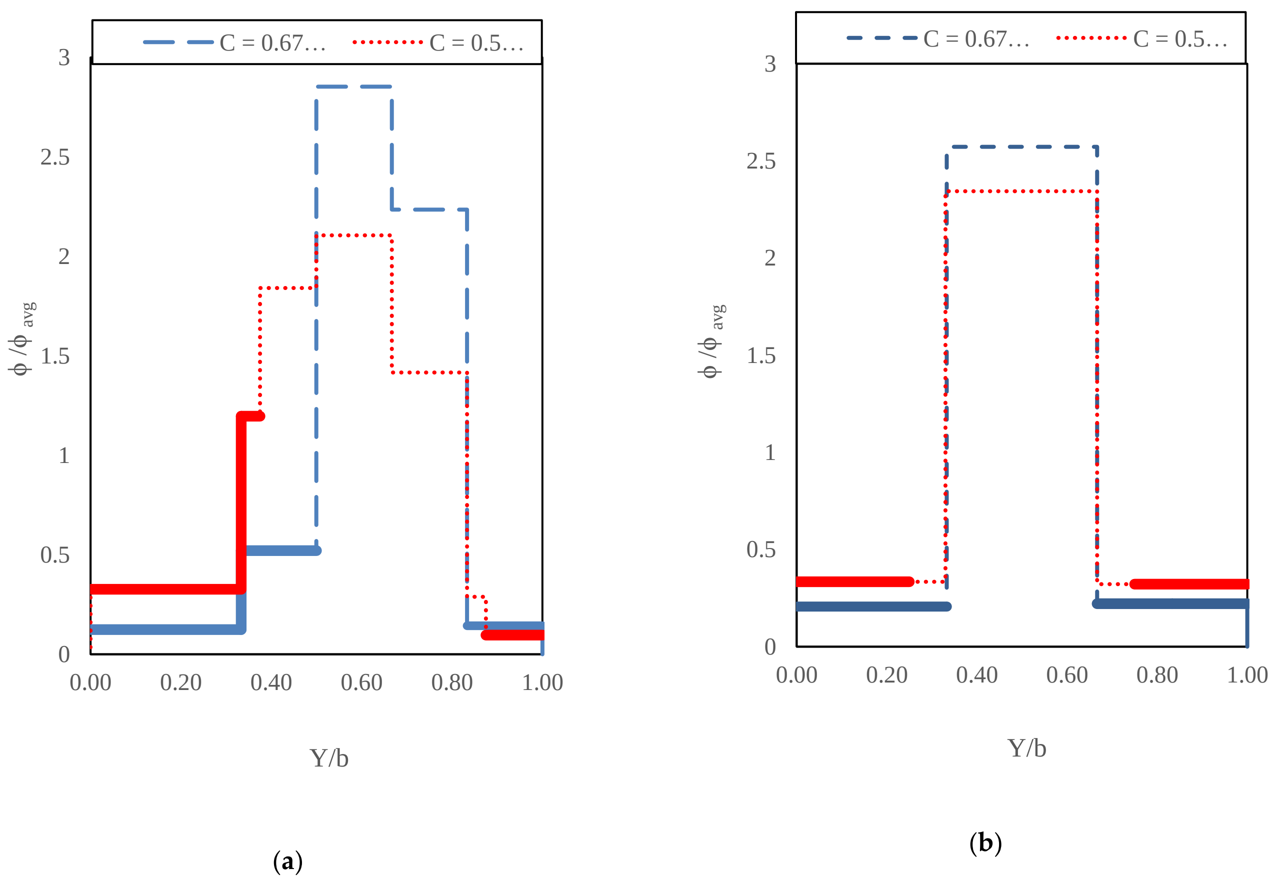

Figure 3.7. Comparison of bedload transport rate distribution for constant flow strength ($\theta = 0.05$) and different coverage ratios for (a) asymmetric border ice ($B_r/B_l = 1/3$); and (b) symmetric border ice ($B_r/B_l = 1$). (Note: Bold line corresponds to the ice-covered portion, and the dashed lines the open water portions.)

3.4.4 Effect of Flow Strength

Rouzegar and Clark (2023a) demonstrated that in rivers characterized by symmetric border ice for a constant coverage ratio and high dimensionless flow strength, the difference of bedload transport rate in the middle section and the side sections wasn't significant. However, at low dimensionless flow strengths, the relative bedload transport rates at the sides were significantly lower than those in the middle. This is presented in Figure 3.8, where the high flow strength experiment has open water and ice-covered value of ϕ/ϕ_{avg} of 1.41 and 0.84, respectively; while the lowest flow strength experiment covers a much greater range of ϕ/ϕ_{avg} from 2.57 to 0.2. Careful inspection of all the experiments will reveal that the flow wasn't perfectly symmetric, despite controlling the experimental conditions as carefully as possible.

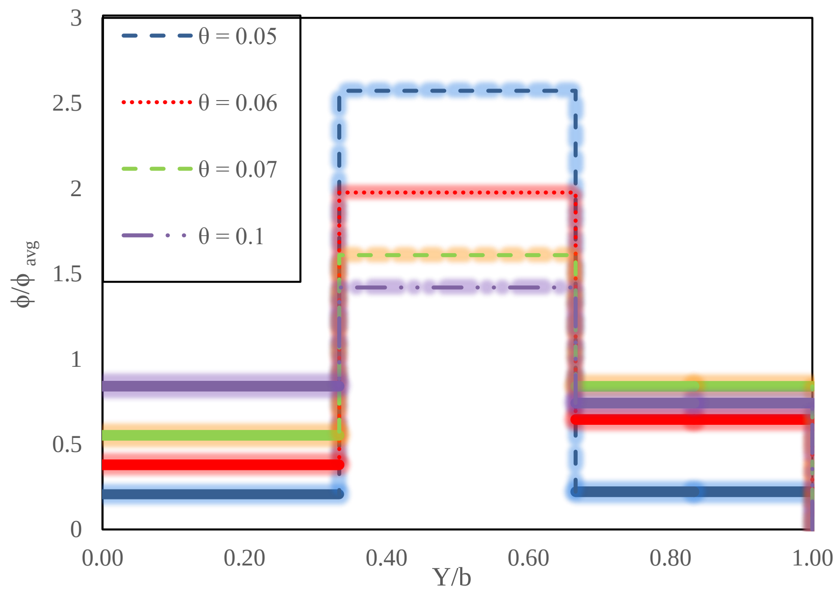

Figure 3.8. Comparison of bedload transport rate distribution for constant coverage ratios (C = 0.67) at different flow strengths in a symmetric partially ice-covered river. (Note: Bold line corresponds to the ice-covered portion, and the dashed lines the open water portions.).

The effect of flow strength in asymmetric partially ice-covered flow was studied by analyzing five distinct experiments, all maintaining a constant coverage ratio (C = 0.67), constant level of asymmetry ($B_r/B_l = 1/3$), and different flow strengths. Figure 3.9 shows the bedload transport rate distribution in these experiments. On the left-hand side of the figure, sediment trap pictures were included to visually demonstrate the continuous data. Additionally, a blue line was included to aid in identifying the extent of the deposited sediment. Similar to symmetric experiments, the effect of border ice on bedload transport rate distribution is more noticeable in the low flow strength. That is, the range of ϕ/ϕ_{avg} spans from 0.12 to 2.85 at the lowest flow strength and from 0.59 to 1.65 at the highest flow strength. Furthermore, the impact of asymmetry in border ice is more significant at lower flow strength. Examining the figures on the left-hand side, at the lowest flow strength, the maximum extent of migration occurred in the middle of the open section. In contrast, for other cases, the maximum value was located in the middle of the channel, and the effect of asymmetry was less noticeable. The figure on the right-hand side demonstrates similar results for ϕ/ϕ_{avg}. Focusing on the middle sections, specifically the regions where 0.33 < Y/b < 0.5 (ice-covered flow) and 0.5 < Y/b < 0.67 (open flow), at the lowest flow strength the difference in ϕ/ϕ_{avg} between these two sections was significant (ϕ/ϕ_{avg} =0.52 and 2.85). However, this difference is not as noticeable at the highest flow strength (ϕ/ϕ_{avg} =1.05 and 1.65), and the distribution appears to be more symmetrical. It is worth noting that each experiment had a different duration, resulting in a variable total sediment volume.

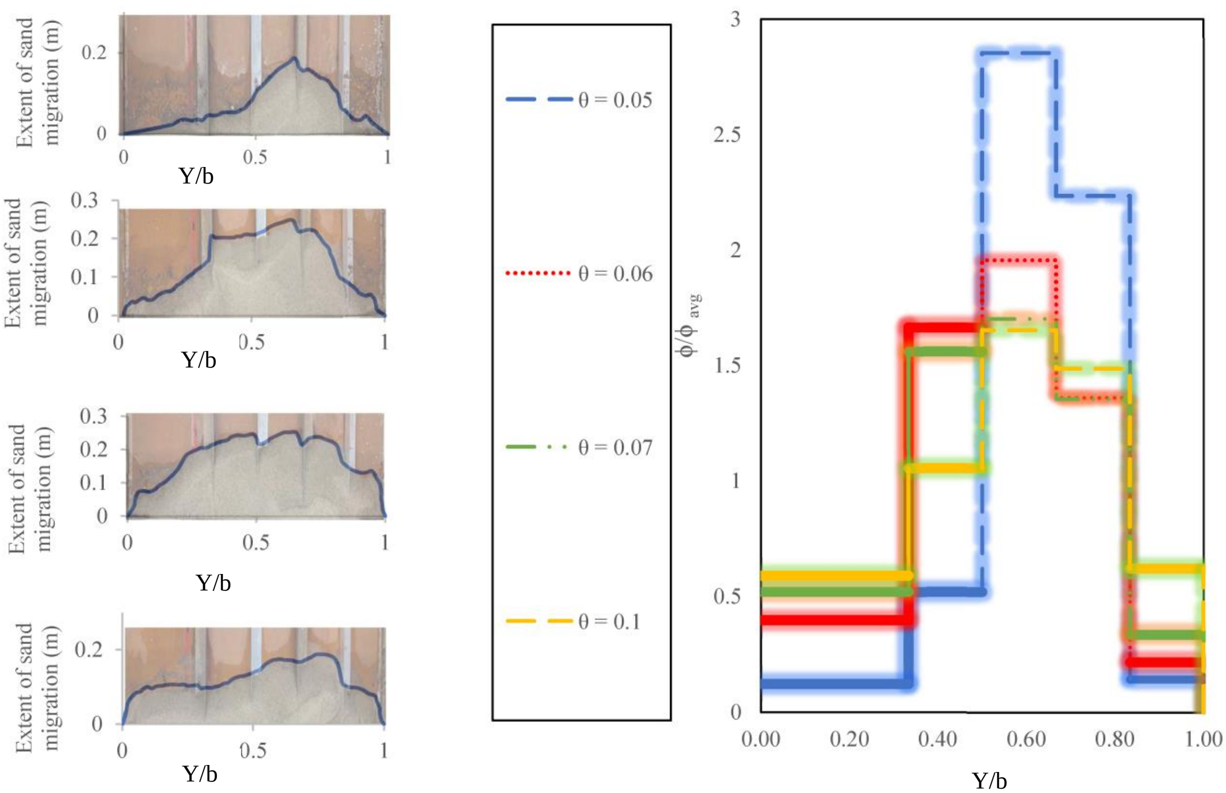

Figure 3.9. Comparison of bedload transport rate distribution for constant coverage ratios (C = 0.67), constant asymmetric level (B_r/B_l = 1/3), and different flow strength in an asymmetric partially ice-covered river, (Note: Bold line corresponds to the ice-covered portion, and the dashed lines the open water portions.).

3.5 Discussion

The presence of border ice introduces a complex dynamic to sediment transport rates in northern rivers. The findings from the current experiments serve as a benchmark for numerical investigations into sediment transport in rivers with partial ice cover. These results offer a more accurate quantification of sediment transport likelihood in a diverse range of northern climate rivers. Specifically, they enable the estimation of which portions of a channel cross-section would experience the highest sediment transport. In this study, the research did not delve into the process of border ice growth, nor did it explore the real-world impact of sediment transport mechanisms. Instead, the primary focus was on presenting the initial quantitative results related to bedload transport under asymmetric partially ice-covered conditions that might happen in real-world situations and then comparing the result with the symmetric conditions.

The initiation of border ice occurs along the riverbanks. Following the initial formation, this border ice horizontally extends towards the center of the channel while simultaneously thickening as it grows vertically downwards. In addition to the freeze-up season, the main section of the channel may open up and result in a partial ice cover during midwinter thaw events (Figure 3.10). It is important to note that partial ice cover is not always symmetrical in real-world scenarios. Asymmetry can arise due to variations in the river cross-section, leading to uneven water velocity distribution across the channel and resulting in asymmetric partial ice cover. Meandering rivers, for instance, exemplify this situation, where both the velocity profile within the cross-section and along the river’s length are not symmetric, potentially giving rise to asymmetric partial ice cover (Figure 3.10). Although the current research did not specifically consider meandering rivers, the findings indicate that asymmetric border ice conditions can significantly impact sediment transport rate redistribution. Consequently, a potential avenue for future research involves extending this study to include different types of rivers, such as meandering rivers, to further explore the effects of asymmetric border ice on sediment transport.

a)

b)

Figure 3.10. Asymmetric partially ice cover in meandering river: (a) Dauphin River, Manitoba, Canada, Dec 2014 (freeze-up season) (Images courtesy of S. Clark and A. Wall); (b) Bulkley river, British Columbia, Apr 2023 (beak-up season) (Images courtesy of USGS).

The growth of border ice involves two primary mechanisms: thermal growth and frazil accretion, commonly known as buttering. Border ice expands through these processes, resulting in diverse surface textures based on the chosen growth method. Irregular undersurfaces may be observed, especially in frazil accretion or freeze-up jam formation.

Consequently, investigating the impact of varying ice roughness on sediment transport rates presents an intriguing avenue for future research.

Blackburn and She (2019) improved the River1D river ice model for natural channel geometry and freeze-up, incorporating border ice formation. Integrating current experimental results into River1D is challenging due to cross-sectional averaging, particularly with sediment transport redistribution across asymmetric ice cover. Alternatively, better integration potential exists in two-dimensional river ice models, like CRISSP2D by Shen (2002) and RIVER2D by Steffler and Blackburn (2002).

3.6 Conclusions

This research aimed to investigate bedload transport rate and distribution in channels with asymmetric partial ice cover. Controlled laboratory experiments were conducted to achieve this objective, examining bedload transport under various conditions. The study specifically assessed the applicability of the Knack and Shen's (2015) formula for estimating the total cross-section-averaged bedload transport rate in asymmetric partially ice-covered rivers. Remarkably, the experimental findings for asymmetric border ice aligned with Knack and Shen's (2015), originally developed for open channel and fully ice-covered flow, as well as the findings of Rouzegar and Clark (2022) for symmetric partially ice-covered flow. This indicates that the empirical equation may be suitable for predicting cross-section-averaged bedload transport in rivers with different types of border ice cover. However, this equation lacks precision in predicting the extent of sediment transport redistribution beneath a partial ice cover.

According to Rouzegar and Clark (2023a), the presence of symmetric border ice results in lower relative bedload transport near the banks and higher relative bedload transport in the middle section of the channel. However, the situation becomes even more complex with asymmetric border ice, leading to further redistribution in the bedload transport rate and causing a non-uniform distribution of bedload transport across the channel width. Furthermore, this redistribution is more pronounced at higher flow strengths and less noticeable at lower flow strengths. Our ability to model this variation in bedload transport rate likely hinges on the ability to accurately predict the boundary shear stress distribution throughout the entire wetted perimeter of the channel. This may be easier when using a two dimensional numerical model. The experimental results from this study comprise the only data source for potential assessment or validation of numerical model ability to predict bedload transport rate in channels with asymmetric border ice.

Author Contributions: Conceptualization, M.R.; Methodology, M.R.; Validation, M.R.; Formal analysis, M.R.; Investigation, M.R.; Resources, S.P.C.; Data curation, M.R.; Writing—original draft, M.R.; Writing—review & editing, S.P.C.; Supervision, S.P.C.; Funding acquisition, S.P.C. All authors have read and agreed to the published version of the manuscript.

Funding: This research was supported by the Natural Sciences and Engineering Research Council of Canada (NSERC-RGPIN-2018-06448).

Data Availability Statement: Data available on request from the authors.

Acknowledgments: The authors would like to acknowledge Alexander Wall for his assistance with the experimental setup.

Conflicts of Interest: The authors declare no conflict of interest.

Chapter 4 Paper 3: An experimental study into the bedform morphology in partially ice-covered channels

4.1 Abstract

The advent of winter in cold climates often leads to the formation of border ice along riverbanks, a phenomenon that can persist over substantial portions of the winter, thereby influencing the dynamics and geomorphological structure of river channels. Bed morphology and dunes play a crucial role in sediment transport and influencing flow resistance. Consequently, accurately predicting dune dimensions is vital for anticipating the behavior of rivers. Despite extensive studies on bedforms within open channel flows, research on partially ice-covered and fully ice-covered flows remains limited. This investigation, conducted in a rectangular flume at the University of Manitoba's Hydraulics Research & Testing Facility in Canada, delved into how border ice affects bed morphology and bedform features. For each experimental condition, including open channel, symmetric and asymmetric border ice, and fully ice-covered flows, bedform dimensions were assessed against theoretical equations found in the literature. This analysis confirmed the suitability of these equations for describing bedform characteristics in partially ice-covered rivers. Furthermore, the impact of border ice extent, variations in flow strengths, and asymmetry of border ice on bedform features were also investigated. The occurrence of bedforms within the channel width was notably influenced by the presence, positioning, and varying extents of partial ice cover. The influence of ice coverage on the distribution of bed feature formation was markedly pronounced at lower flow strengths, whereas it became minimal at higher flow strengths.

Keywords: Bedform, Sediment transport, Ice-covered channel, Border ice, River morphology

4.2 Introduction

Investigating the influence of ice cover on fluvial systems in cold regions is paramount for a comprehensive understanding of their hydraulic, sediment transport, and geomorphological characteristics. During the winter months, the formation of ice, particularly border ice along the river's banks, initiates a series of alterations in hydraulic conditions, including modifications to flow distribution and velocity profiles. Border ice then progressively extends toward the channel's center, increasing the width of partial ice cover that significantly influences riverine behavior (Peters et al., 2017). With climate change potentially extending the duration of partial ice cover through later freeze-ups and more frequent mid-winter thaws, understanding the implications of border ice becomes increasingly pertinent. Such knowledge is crucial for accurately modeling the morphodynamic responses of rivers to partial ice cover and for devising effective management strategies for these unique fluvial environments (Clark, 2013; Peters, 2015).

Research focusing on partially ice-covered rivers remains limited despite the considerable effects of such conditions on hydrodynamic processes and sediment dynamics. The inherent challenges associated with field investigations in these environments, such as the transient nature of ice growth and the associated safety hazards, necessitate a reliance on controlled experimental studies. These studies have provided valuable insights into the flow modifications induced by ice cover, including changes in turbulent flow behavior, shear stress distribution, and the influence of different features like bed and ice roughness (Peters et al., 2018; Kimiaghalam et al., 2017; Majewski, 1992).

Bedforms in rivers with sand beds are often the foremost factors influencing flow resistance. The processes of their formation, growth, and kinematics govern sediment transport (Venditti et al., 2016). Understanding bedform behavior is essential for deciphering the processes within present-day channels, and it also sheds light on the characteristics of ancient, now-absent channels on Earth and beyond. Both the task of forecasting dune features based on observed flow traits and the challenge of deducing historical flow conditions from dunes captured in the geological record depends on the correlation between flow properties and the dimensions of dunes. Dune sizes estimated via the direct approach serve as quantitative indicators of roughness height for calculating flow resistance and estimating scour depths. Additionally, numerous equations for sediment transport incorporate the dimensions of dunes (Bradley & Venditti, 2017).

Research on sediment transport and bed morphology in ice-covered rivers remains sparse. Wuebben (1986, 1988) conducted an experimental study on sediment transport and bedform dynamics under conditions of floating cover and demonstrated that theories applicable to open water could be extended to the lower flow layer in ice-covered situations, where bed resistance predominantly dictates the flow characteristics. Ettema and Daly (2004) conducted a comprehensive qualitative analysis, formulating a series of dimensionless parameters anticipated to impact sediment transport and bedform dimensions in icy environments. Further investigations into the interplay between ice processes and fluvial sediment dynamics have been reviewed by Turcotte et al. (2011) and Ettema (2008), highlighting the significant effects of ice cover on river morphology. However, the challenging nature of fieldwork in such conditions has led to a scarcity of detailed empirical data, constraining extensive quantitative analysis. Numerical modeling studies addressing the influence of ice cover on sediment transport and riverbed alterations are limited but noteworthy. Contributions from Carr and Tuthill (2012), Kolerski and Shen (2015), and Knack and Shen (2018) stand out in this regard. Specifically, Knack and Shen (2018) developed an integrated model that combines sediment transport and bedform dynamics with hydro-thermal-ice processes. Due to the absence of detailed field observations under ice conditions, the validation of this model relied on laboratory experiments conducted in open water, underscoring the need for empirical studies to enhance the understanding of sediment dynamics in ice-affected rivers. Rouzegar and Clark (2023a, 2023c) explored bedload transport under conditions of symmetric and asymmetric border ice, finding that existing models for open channel and fully ice-covered flows could effectively estimate average bedload transport in scenarios of partial ice cover. They highlighted how the presence, variability in extent, and positioning of border ice influence the redistribution of bedload transport rates. Furthering this line of inquiry, Rouzegar and Clark (2023d) qualitatively investigated the effect of border ice on bedforms. The current research aims to quantitatively assess the influence of border ice on bedform configurations for the first time. This investigation will evaluate the effects of partial ice cover on bedforms through laboratory simulations of symmetric and asymmetric border ice conditions, comparing these outcomes to those observed in open channel and in fully ice-covered flows. The anticipated outcomes of this research will offer valuable empirical data to enhance the calibration and validation of numerical models, such as the work of Knack and Shen (2018) in investigating and determining bedform dimensions.

4.3 Methodology

4.3.1 Experimental setup

The physical experiments were conducted at the Hydraulics Research & Testing Facility at the University of Manitoba. A rectangular flume (Figure 4.1) measuring 14 m in length and 1.2 m in width was constructed using high-density overlay (HDO) plywood, featuring a bed slope of 0.26%. Discharge in the flume's supply pipe was measured using a Dynasonic ultrasonic flow meter (with ±1% accuracy). This supply pipe led to a head tank designed with greater width and depth than the flume, dissipating turbulence generated by the discharge pipe. To condition the flow, water passed through a honeycomb flow straightener. Gravel of varying diameter lined the flume bed at the upstream end, facilitating rapid boundary layer development to promote fully developed flow conditions along a greater length of the flume. The occurrence of fully developed flow was verified by measuring vertical profiles of streamwise velocity at different distances along the flume length using a Nortek Vectrino acoustic Doppler velocimeter. Five manometer tubes with a diameter of 39.4 mm were installed on the flume wall to measure the water surface profile, utilizing a point gauge with an accuracy of ±0.2 mm. An initial uniform layer of silica sand, 70 mm thick, with a median diameter (d_{50}) of 1.3 mm, was placed throughout the flume length. Steel rails along the flume walls accommodated a leveling device on rollers to ensure a smooth and flat sand bed at the start of each experiment. Adjusting the slope of the flume rails and adding or removing sand allowed for changes in the sand bed slope, while maintaining a minimum sand depth of 70 mm. Control of the downstream water level was achieved through a bottom-mounted, hinged gate.

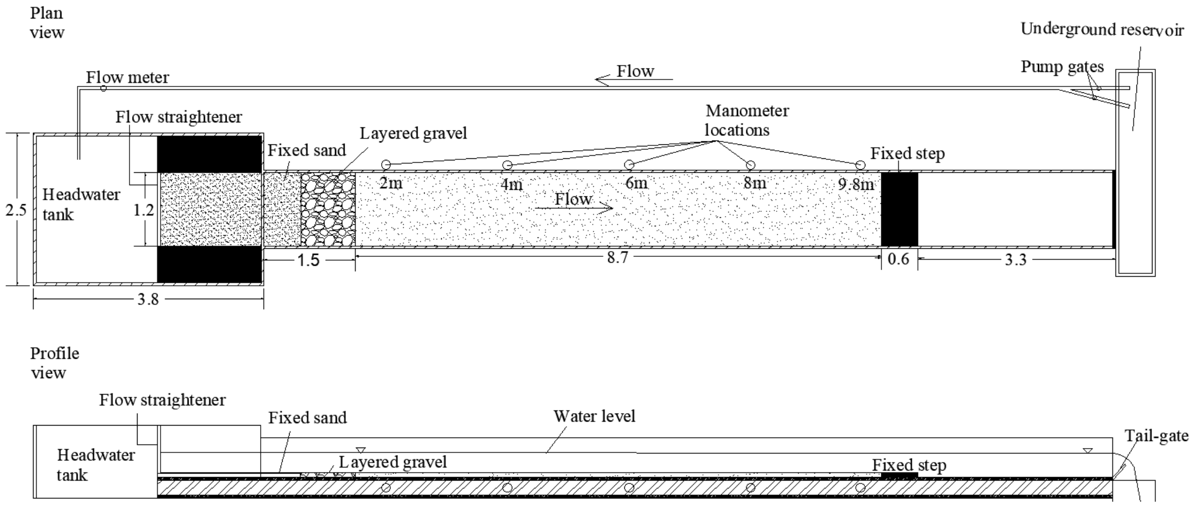

Figure 4.1. Schematic diagram of the experimental setup (all dimensions in meters).

Plastic bubble wrap was utilized to simulate a smooth, partial ice cover (Figure 4.2). Several lines were marked along the bubble wrap, positioned at appropriate distances to represent the distinct ice coverage ratios employed in the present study. Nailing the bubble wrap to the flume wall at the designated elevation along the corresponding line ensured the desired ice coverage ratio and prevented lateral movement of the simulated ice during each partially ice-covered test. For fully ice-covered conditions, the bubble wrap was affixed to the upstream end of the flume. For additional details and images of the experimental setup, refer to Rouzegar and Clark (2022). The test conditions are listed in Table 4.1, where the coverage ratio, C (which measures the proportion of the top width covered by ice relative to the overall top width), was used to quantify the extent of the ice coverage.

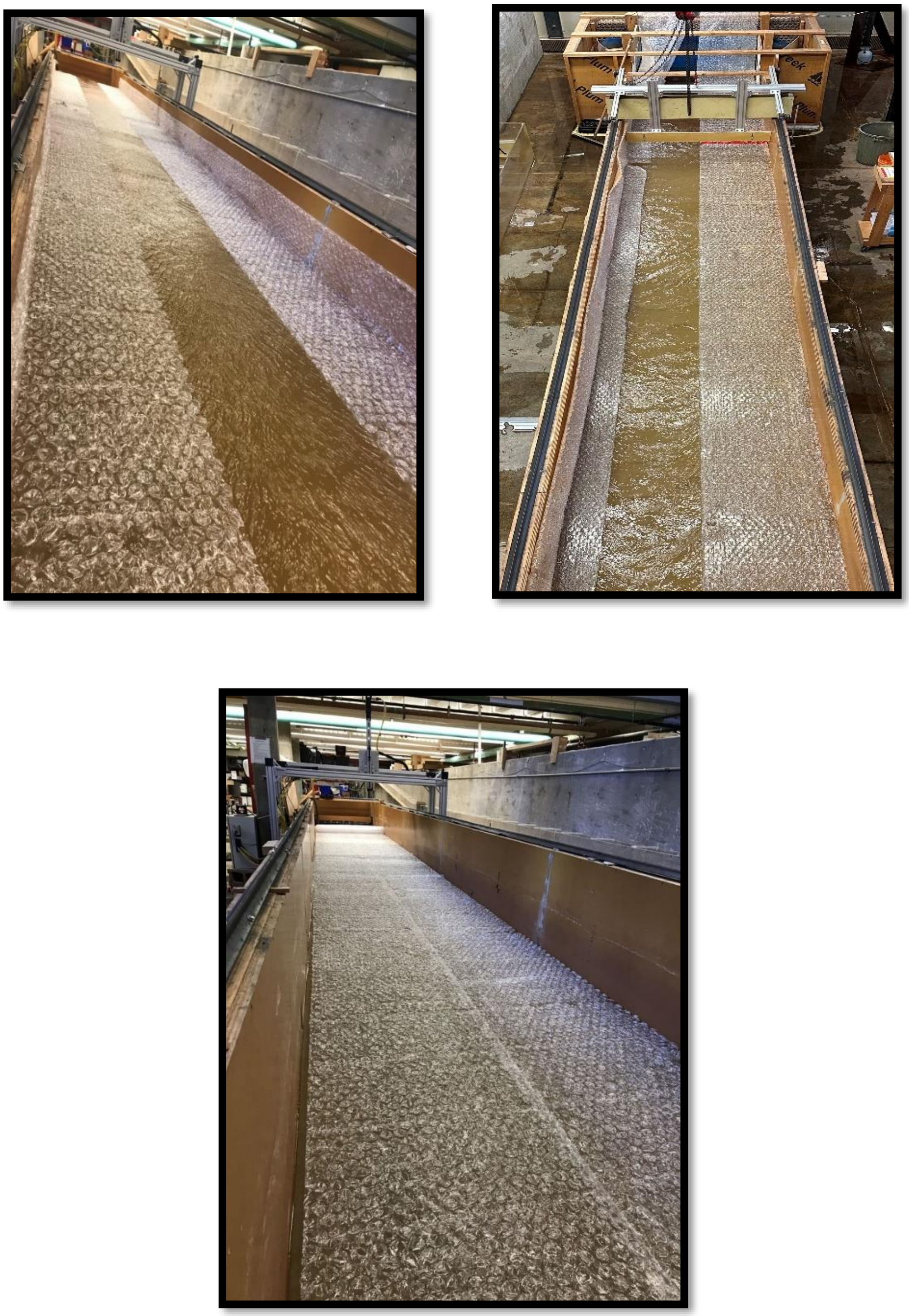

Figure 4.2. Simulated ice-covers for a) symmetric partially ice-covered flow, b) asymmetric partially ice-covered flow, and c) fully ice-covered flow.

Table 4.1. Experimental conditions (note: C = coverage ratio, Q = flow rate)

	C	Border Ice Width-Right (B_r) (m)	Border Ice Width-Left (B_l) (m)	Dimensionless flow strength (θ)	Q (m^3/s)	Water depth (m)	Slope (%)
Open channel	0	N/A	N/A	0.05	0.06	0.10	0.10
	0	N/A	N/A	0.06	0.09	0.13	0.10
	0	N/A	N/A	0.07	0.13	0.16	0.10
	0	N/A	N/A	0.085	0.05	0.07	0.26
	0	N/A	N/A	0.10	0.07	0.08	0.26
Fully ice-covered	1	N/A	N/A	0.05	0.13	0.20	0.10
	1	N/A	N/A	0.06	0.18	0.26	0.10
	1	N/A	N/A	0.064	0.21	0.28	0.10
	1	N/A	N/A	0.085	0.10	0.13	0.26
	1	N/A	N/A	0.10	0.13	0.16	0.26
Symmetric partial ice	0.25	0.15	0.15	0.05	0.08	0.13	0.10
	0.25	0.15	0.15	0.06	0.12	0.17	0.10
	0.25	0.15	0.15	0.07	0.16	0.20	0.10
	0.25	0.15	0.15	0.085	0.06	0.08	0.26
	0.25	0.15	0.15	0.10	0.08	0.10	0.26
Symmetric partial ice	0.50	0.3	0.3	0.05	0.10	0.16	0.10
	0.50	0.3	0.3	0.06	0.14	0.20	0.10
	0.50	0.3	0.3	0.07	0.20	0.24	0.10
	0.50	0.3	0.3	0.085	0.08	0.10	0.26
	0.50	0.3	0.3	0.10	0.10	0.12	0.26
Symmetric partial ice	0.67	0.4	0.4	0.05	0.11	0.17	0.10
	0.67	0.4	0.4	0.06	0.16	0.22	0.10
	0.67	0.4	0.4	0.07	0.21	0.26	0.10
	0.67	0.4	0.4	0.085	0.08	0.11	0.26
	0.67	0.4	0.4	0.10	0.11	0.13	0.26
Asymmetric partial ice	0.67	0.2	0.6	0.05	0.11	0.17	0.1
	0.67	0.2	0.6	0.06	0.16	0.22	0.1
	0.67	0.2	0.6	0.07	0.21	0.26	0.1
	0.67	0.2	0.6	0.10	0.11	0.13	0.26
	0.5	0	0.6	0.05	0.10	0.16	0.1
	0.5	0.15	0.45	0.05	0.10	0.16	0.1
	0.5	0.15	0.45	0.07	0.20	0.24	0.1

4.3.2 Experimental procedure and data acquisition

All experiments were conducted under uniform flow conditions by adjusting the discharge and water depth to the specified values for each test. A standardized procedure was adhered to in order to achieve uniform flow within the laboratory setting. The bed was leveled to the desired slope, and the tailgate was initially raised to prevent flow before the commencement of each experiment. Additional details can be found in Rouzegar and Clark (2023a).

After each experiment, water was gradually drained from the flume. To quantify the bedforms, images of the deformed bed were acquired using a Canon EOS Rebel T7i camera paired with a Canon EFS 18-55 mm lens. Various scenarios were explored and compared to identify the optimal number of photos that ensure sufficient overlap. These scenarios involved experimenting with different quantities of photos and capturing them from diverse angles. Following Agisoft Software (2016) guidelines, it is recommended to maintain an 80% forward overlap for images within a single flight line and a 60% side overlap for adjacent flight lines when capturing aerial imagery. In each test, 40 to 50 photos were captured. Eight markers were strategically placed on the flume walls to aid in both image alignment and point cloud scaling/referencing (Figure 4.3).

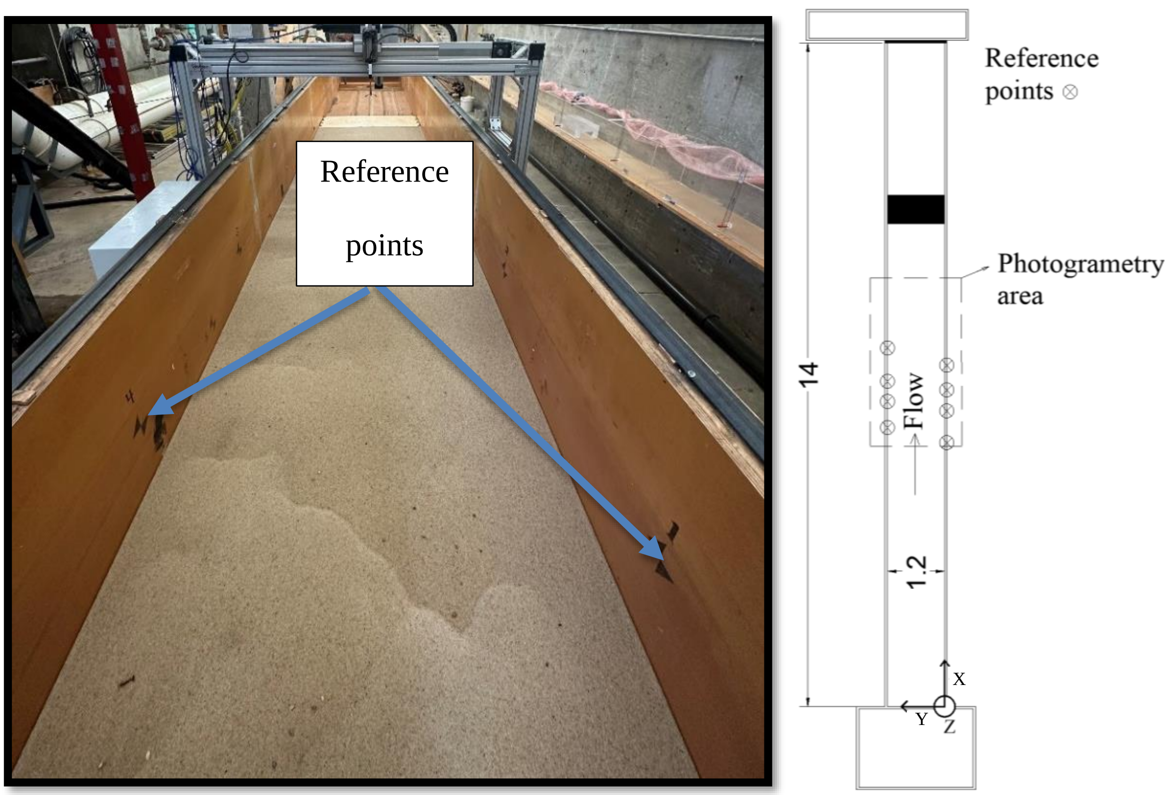

Figure 4.3. Reference points locations and coordinate system in the flume.

Each set of images was processed to generate three-dimensional point clouds utilizing Agisoft Photoscan Professional Version 1.6.6. Additional information about Agisoft usage can be found in the work of (Rouzegar & Clark, 2023d).

4.3.3 Bed elevation data processing

Coordinates were obtained from Agisoft, and the analysis focused on the longitudinal profile along the flume, measured at 15 distinct points 0.075 m apart, starting from the flume wall. A filtering method was required to remove the noise from the data, which was performed in different steps. First, data were filtered based on valid data criteria. In other words, data with 'Y' values outside the valid range (0-1.2 m) and data with 'Z' values lower than the flume bed were considered invalid. In the next step, high-frequency fluctuations linked to the presence of very small bed forms were eliminated from the bed elevation profile. This refinement was achieved by utilizing a Fourier transform technique (A. Singh et al., 2012). Following this, local maxima and minima were identified in the filtered signal, and the differences between consecutive maxima and minima's 'Z' values were computed to ascertain bedform heights. Ultimately, bedform heights surpassing a specified threshold (threshold = 2 * d_{50}) were extracted based on Singh et al.’s (2012) methodology. Wavelengths were calculated by determining the streamwise distance between consecutive crests and consecutive throughs 'X' values, with subsequent computation of their average value (Figure 4.4). In Figure 4.5, all the steps outlined for a sample experiment are presented.

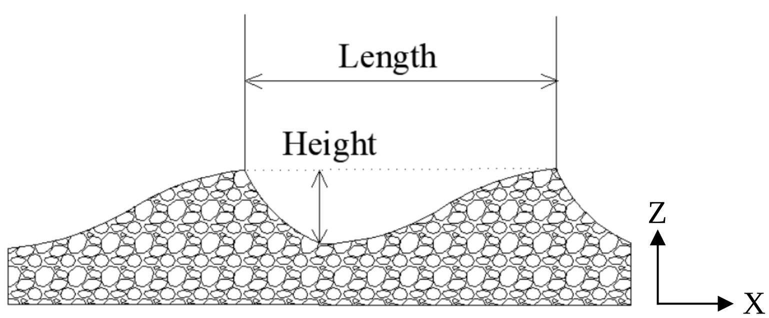

Figure 4.4. Schematic of bedform height and length definition.

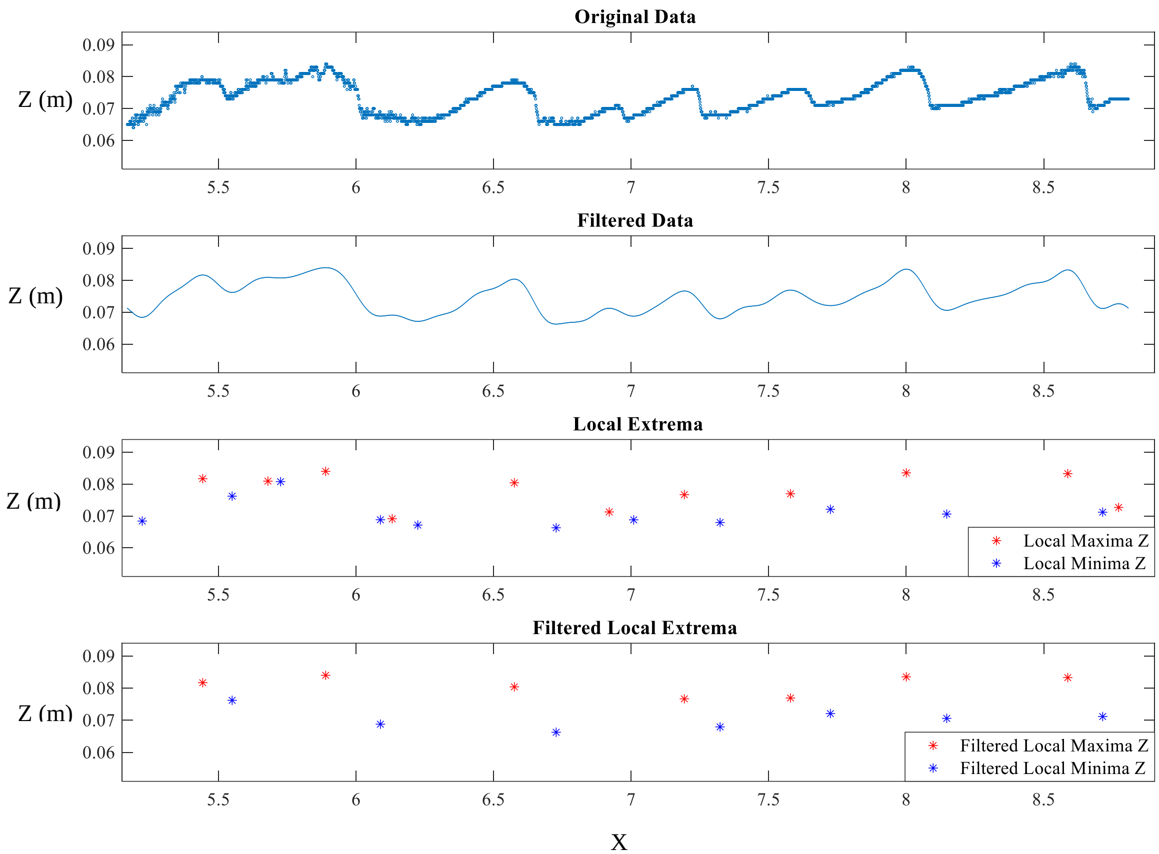

Figure 4.5. Step-by-Step analysis of bedform profiles: measuring heights and lengths.

4.4 Results and Analysis

For each test, the average shear stress along the entire wetted perimeter was determined using Equation [4.1], where τ represents the average shear stress, γ is the specific weight of water, R_h denotes the hydraulic radius, and S is the slope of the water surface. The shear stress at the channel bed (τ_b) was determined by multiplying the cross-sectional average shear stress (τ) by 1.2 (Equation [4.2]), a methodology recommended by Peters (2015), who applied a log-law fitting to similar hydraulic conditions within the same experimental setup. Further exploration into the effects of ice cover on flow dynamics was undertaken by Rouzegar and Clark (2023a), who measured velocity profiles across various coverage ratios using a Nortek Vectrino II profiling acoustic Doppler velocimeter (ADV) and derived the bed shear stress distribution by applying the log-law to each velocity profile. The alignment of their findings with those of Peters et al. (2017) reinforces the reliability and coherence of the data, validating their application in this research.

$$\tau = \gamma R_h S \qquad [4.1]$$

$$\tau_b = 1.2\tau \qquad [4.2]$$

Subsequently, for each experiment, the dimensionless flow strength (θ) was computed using Equation 3, where g signifies gravitational acceleration, D is the average diameter of the sand particles, and Δ is defined as s - 1, with s indicating the specific gravity of the sediment.

$$\theta = \frac{\tau_b}{\Delta\,\rho\,g\,D} \qquad [4.3]$$

Subsequent steps involved a detailed examination of how border ice influences bedforms, incorporating an in-depth analysis of diverse factors and conditions.

4.4.1 3D profiles (symmetric border ice)

Figure 4.6 presents a visual comparison of 3D bedform patterns under a range of hydraulic conditions, including open channel flow, symmetric partially ice-covered, and fully ice-covered. This figure is systematically arranged such that each row represents a specific coverage ratio, demonstrating the impact of ice coverage on bedform characteristics, while each column indicates a particular flow strength, revealing the influence of θ on bedform morphology

Analyzing the bedform patterns at a constant θ value while varying the coverage ratios shows that an increase in the coverage ratio typically corresponds to more occurrences of significant bedforms. Delving into the details for various flow strengths, the following observations are made: At the minimal flow strength of θ = 0.05, bedforms are barely noticeable, almost resembling a flat surface. At the flow strength of θ = 0.07, it is observed that the open channel flow (C = 0) shows the most uniform bed migration across the channel width amongst all of the various coverage ratios tested. In this condition, the bedforms are more two-dimensional, with dunes aligning nearly perpendicular to the flow and extending across nearly the entire flume cross-section, including close to the flume walls. However, with an increase in the coverage ratio, the bedform uniformity seen in open channel flows diminishes, leading to the emergence of more complex, three-dimensional bedform structures. Moreover, under higher coverage ratios, there's a noticeable absence of bedforms beneath the ice-covered portions of the channel, indicating that bedform generation is hindered by ice coverage and tends to occur further from the flume walls.At a higher flow strength of θ = 0.1, consistent with observations across other flow strengths, an increase in coverage ratio results in more significant bedforms. However, a distinctive feature of this higher flow regime is the pronounced irregularity in the shapes of bedforms across all coverage ratio scenarios. Interestingly, these irregular bedforms are found not only in the open flow portions of the channel but also within the ice-covered portions of the channel and adjacent to the flume walls, contrasting conditions at lower flow strengths where such areas typically lacked bedform formation. Therefore, the impact of changing the coverage ratio is less significant at higher flow strengths. This observation aligns with the findings of Rouzegar and Clark (2023a) regarding the rate of bedload transport.

Additionally, when holding the coverage ratio (C) constant to explore the effects of varying flow strengths (θ), it is found that higher flow strength results in more pronounced bedforms, an increase in the irregularity in bedform shapes, and a shift towards more complex, three-dimensional bedforms.

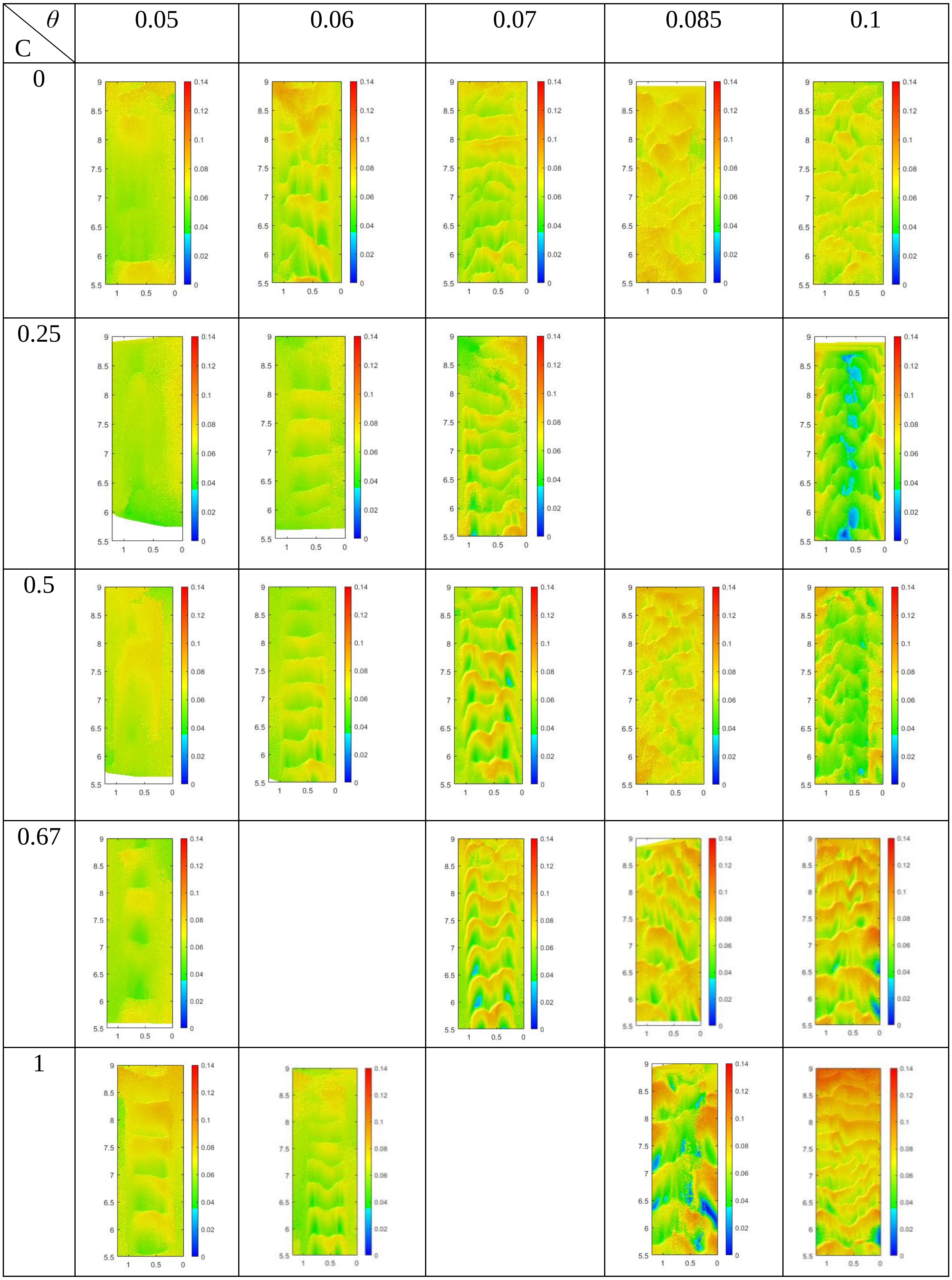

Figure 4.6. Plan view of bedform patterns within open channel, symmetrically partial ice-covered, and fully ice-covered flow conditions, depicted across a range of flow strengths. The color bar legend indicates variations in bedform elevation (Z), with each color

4.4.2 3D Profiles (asymmetric border ice)

Figure 4.7 compares symmetric and asymmetric border ice cases with identical flow strength ($\theta = 0.07$) and coverage ratio ($C = 0.67$) but different border ice positions. In the symmetric condition (Figure 4.7a), the border ice widths on both the right (B_r) and left (B_l) are set to 0.4. In contrast, the asymmetric conditions, shown in Figure 4.7b and Figure 4.7c, feature varied border ice widths, with B_r and B_l measuring 0.15 and 0.45 meters in Figure 4.7b and 0.2 and 0.6 meters in Figure 4.7c, respectively.

Results from experiments with symmetric border ice demonstrate that the presence of border ice can suppress bedform presence beneath the ice cover, resulting in bedforms having an offset from the flume wall. As illustrated in Figure 4.7a, the offsets on both the right and left sections are the same, approximately 0.18 m, due to the equal border ice widths in the right and left sections. In contrast, in the case of asymmetric border ice, the offset in the right and left sides are not identical because of the unequal border ice widths on the two sides. For instance, in Figure 4.7b, the right side exhibits a 0.1 m offset corresponding to a 0.15 m border ice width, whereas the left side shows a 0.2 m offset under a 0.45 m border ice width. A similar trend is observed in Figure 4.7c, with a 0.15 m offset on the right ($B_r = 0.2$ m) and a 0.3 m offset on the left ($B_l = 0.6$ m). This emphasizes the influence of both the position and extent of border ice on the resulting bedforms characteristics.

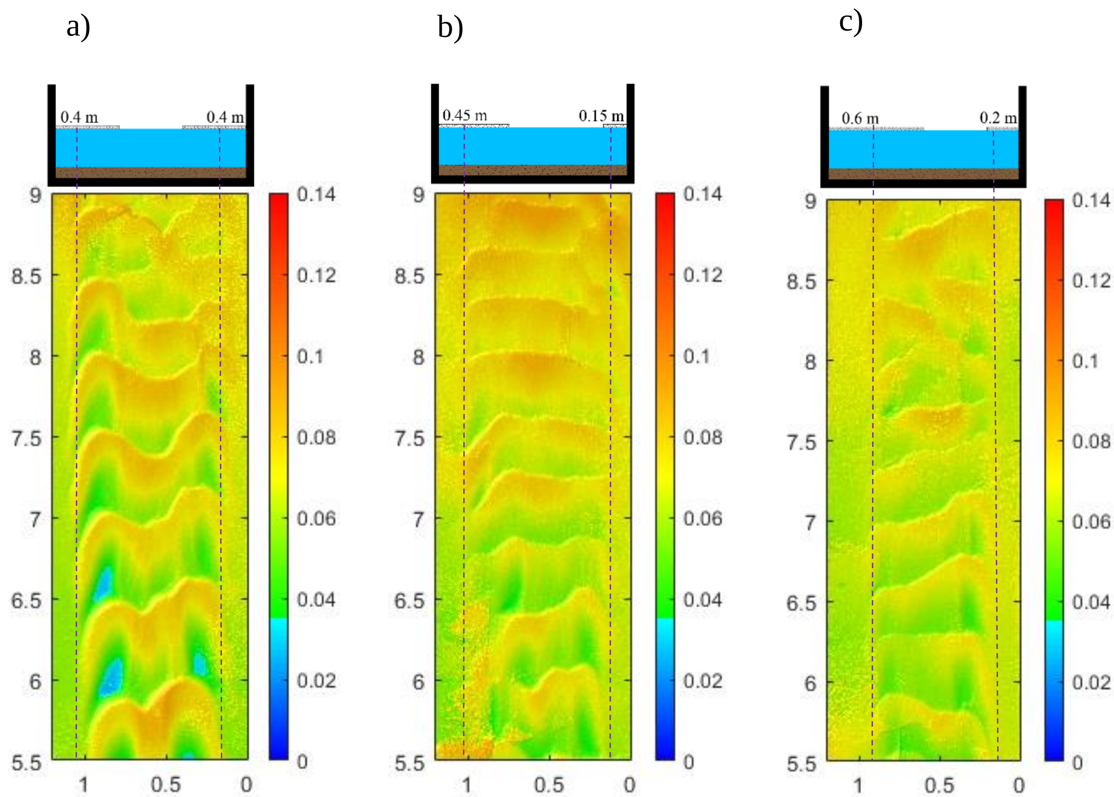

Figure 4.7. Comparison of bedform patterns in a) symmetric, b) asymmetric partially ice-covered flow with B_r = 0.15 m and B_l = 0.45 m, and c) asymmetric partially ice-covered flow with B_r = 0.2 m and B_l = 0.6 m (all dimensions are in meters).

Figure 4.8 shows the effect of flow strength variations on bedform morphology under an asymmetric border ice condition, while keeping a constant coverage ratio of C = 0.67 and specific border ice width of B_r = 0.2 and B_l = 0.6. Observations across these scenarios reveal that the presence of border ice tends to inhibit bedform formation beneath the ice-covered areas, leading to distinct offsets from the flume wall. These offsets vary in the right and left sides, reflecting the asymmetrical widths of the border ice.

Similar to findings in symmetric border ice conditions, when the coverage ratio is held constant and flow strengths are varied, an increase in flow strength leads to more pronounced bedform formation. This rise in flow strength is associated with an increase in the irregularity of bedform shapes and a shift towards more three-dimensional bedforms. Again, at a higher flow strength of θ = 0.1, the presence of border ice has a diminished effect on bedform morphology.

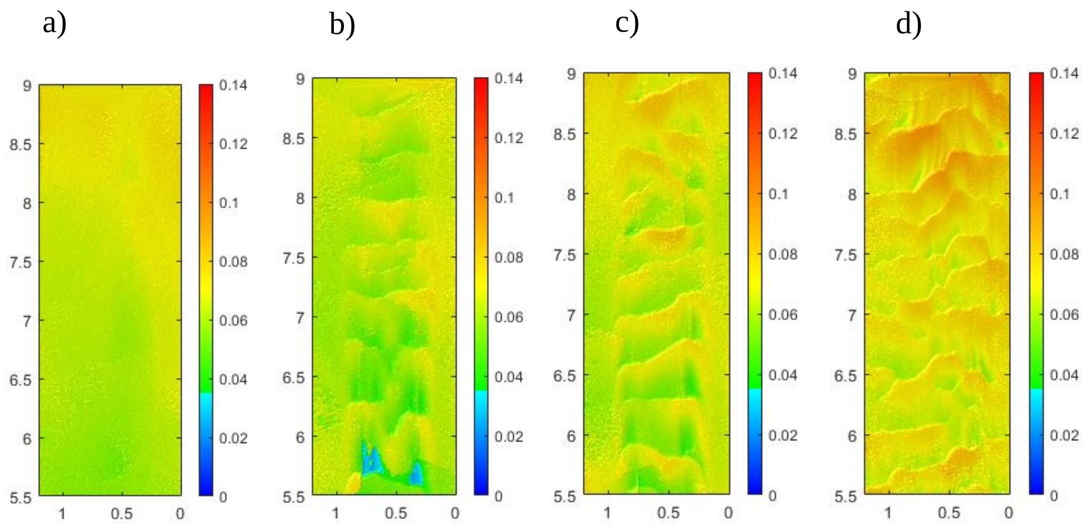

Figure 4.8. Comparison of bedform patterns in asymmetric partially ice-covered flow with distinct B_r = 0.2 m and B_l =0.6 m and varied flow strengths a) θ = 0.05, b) θ = 0.06, c) θ = 0.07, and d) θ = 0. 1 (all dimensions are in meters).

4.4.3 Longitudinal bed profiles

After generating a Digital Elevation Model (DEM) for all cases, the point coordinates were extracted from Agisoft. Longitudinal profiles at seven distinct distances from the flume wall (Figure 4.9) were then plotted and compared.

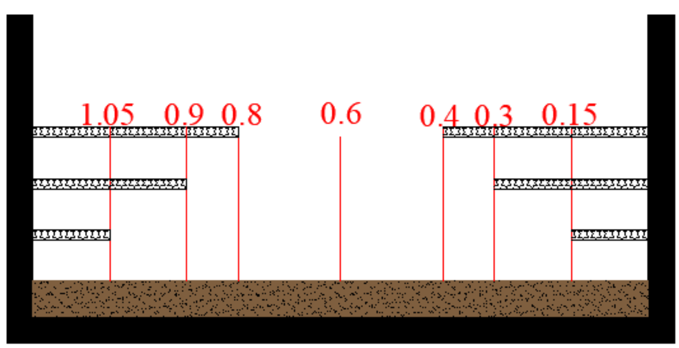

Figure 4.9. Longitudinal profile locations across the channel width (all dimensions are in meters).

4.4.3.1 Comparison of longitudinal profile across the channel width

Longitudinal profiles at varying distances from the flume wall were plotted and analyzed on a single graph to explore the effect of border ice on bedforms across the channel width. Figure 4.10 displays these comparisons for various coverage ratios (C = 0, 0.25, 0.5, 0.67) individually. The figure uses data from one side of the flume only, due to symmetry. It was confirmed that the results are quite similar for the opposite side of the flume. A constant flow strength of $\theta = 0.07$ was used in all cases. The choice of $\theta = 0.07$ was made based on the 3D profile analyses, which indicated that this dimensionless flow strength resulted in the most significant differences. Bedform changes were less evident at lower flow strengths, and at higher flow strengths, the impact of varying border ice extent was minimal.

Figure 4.10a depicts the conditions of open channel flow. All the profiles uniformly demonstrate a consistent pattern with an average bedform height of 0.01 m, with the exception occurring at Y = 0.15 m, where the average bedform height slightly decreases to 0.006 m. This exception highlights the sidewall effect, which causes a reduction in sediment transport near the wall and consequently results in a reduced formation of bedforms.

Figure 4.10b displays the condition with a coverage ratio of C = 0.25. In this case, the ice-covered area (Y = 0.15) experiences bedforms that are slightly less pronounced, resulting from reduced sediment transport, whereas the open areas see more sediment transport, leading to more distinct bedforms. The observed trend illustrates that more pronounced bedforms become evident moving from the flume wall toward the centerline. In Figure 4.10b, the edge of the border ice at Y = 0.15 m exhibits more significant bedforms, with an average height of 0.012 m, compared to Figure 4.10a, where the average bedform height at the same location is measured 0.006 m. This difference is due to the Y = 0.15 m area displaying properties similar to the open sections, particularly in terms of increase in sediment transport leading to more noticeable bedform configurations.

In Figure 4.10c and Figure 4.10d, corresponding to coverage ratios of C = 0.5 and C = 0.67, respectively, it is shown that the areas under cover exhibit less pronounced bedforms, whereas the open areas display more distinct bedforms. For a coverage ratio of 0.5, the peak bedform height was H = 0.027 m observed at Y = 0.3 m, at the edge of the border ice. Along the channel, bedform heights were measured as H = 0.018 m at Y = 0.15 m, H = 0.022 m at Y = 0.4 m, and H = 0.021 m at Y = 0.6 m, indicating the highest value at the border ice edge. This observation is consistent with the findings by Peters et al. (2017), who examined shear stress distribution and discovered that at C = 0.5, the highest shear stress values were at the ice edge, with a local minimum at the channel's centerline. This pattern contrasts with other coverage ratios, where the minimum shear stress occurred at the corners, and the maximum shear stress was found at the center.

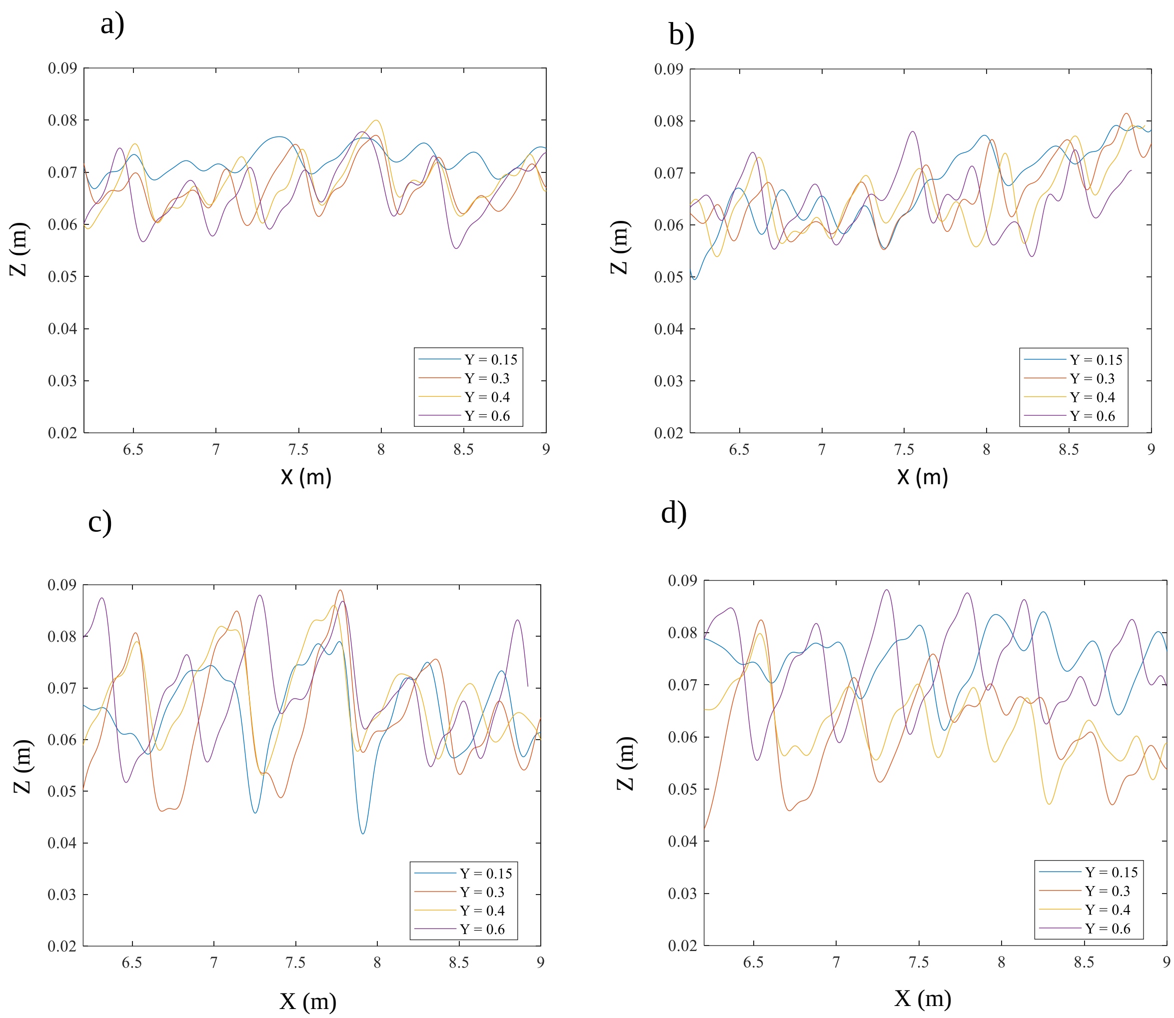

Figure 4.10. Longitudinal profile comparison at different distances from the flume wall for a) C = 0, b) C = 0.25, c) C = 0.5, d) C = 0.67 (all dimensions are in meters).

4.4.3.2 Comparison of longitudinal profiles for diverse border ice coverage ratios

Figure 4.11 gives more details by showing the longitudinal profile at the distance of Y = 0.3 m from the flume wall for different cases of coverage ratio (0, 0.25, 0.5, 0.67) and similar flow strength (θ = 0.07). The selection of θ = 0.07 was based on its ability to highlight significant changes in 3D profiles, making it ideal for assessing border ice effects. Increasing the coverage ratio resulted in the development of more pronounced bedforms with greater heights. The figure demonstrates that at coverage ratios of C = 0 and 0.25, the bedforms are notably smaller, with average heights of 0.01 m and 0.013 m, respectively. However, with higher coverage ratios of C = 0.5 and 0.67, the bedforms show a significant increase in size, with average heights reaching 0.027 m and 0.022 m, respectively. Moreover, at a coverage ratio of C = 0.5, the Y = 0.3 m position is at the border ice edge, leading to a significant differentiation between the bedform sizes at C = 0.25 and C = 0.5.

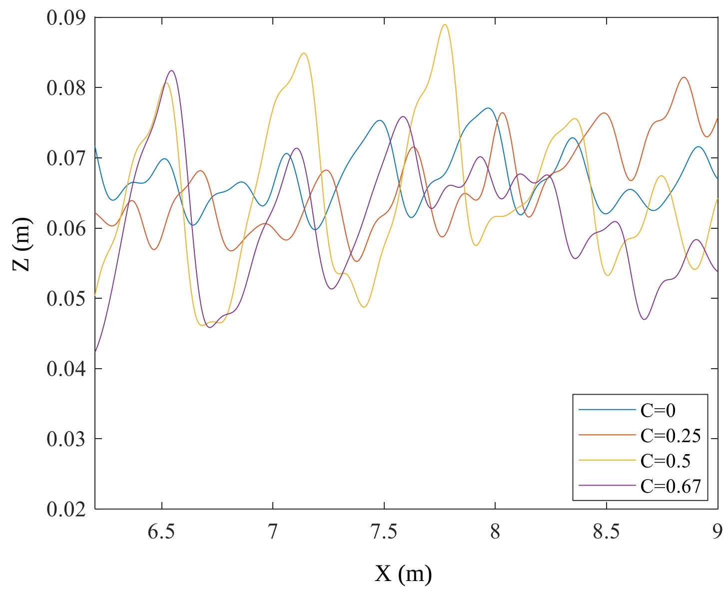

Figure 4.11. Longitudinal profile comparison at θ =0.07 and y=0.3 m from the Flume Wall for different coverage ratios (all dimensions are in meters).

4.4.4 Effect of coverage ratio on bedform dimensions

After determining the bedform heights for each scenario, the average bedform height was computed for every case. This involved computing the mean value of all bedform heights across the flume's width, obtained from the longitudinal profiles presented in the methodology section. Figure 4.12 indicates the relationship between average bedform height and the coverage ratio under a range of flow strengths. At lower θ values (i.e. 0.05 and 0.06), there is minimal formation of bedforms. Specifically, with a flow strength of 0.05 and coverage ratios of 0.25 and 0.5, bedforms are almost absent, leading to an average bedform height that approaches zero. For higher flow strengths with θ values of 0.07, 0.085, and 0.1, an increase in coverage ratios is associated with a rise in the average height of bedforms.

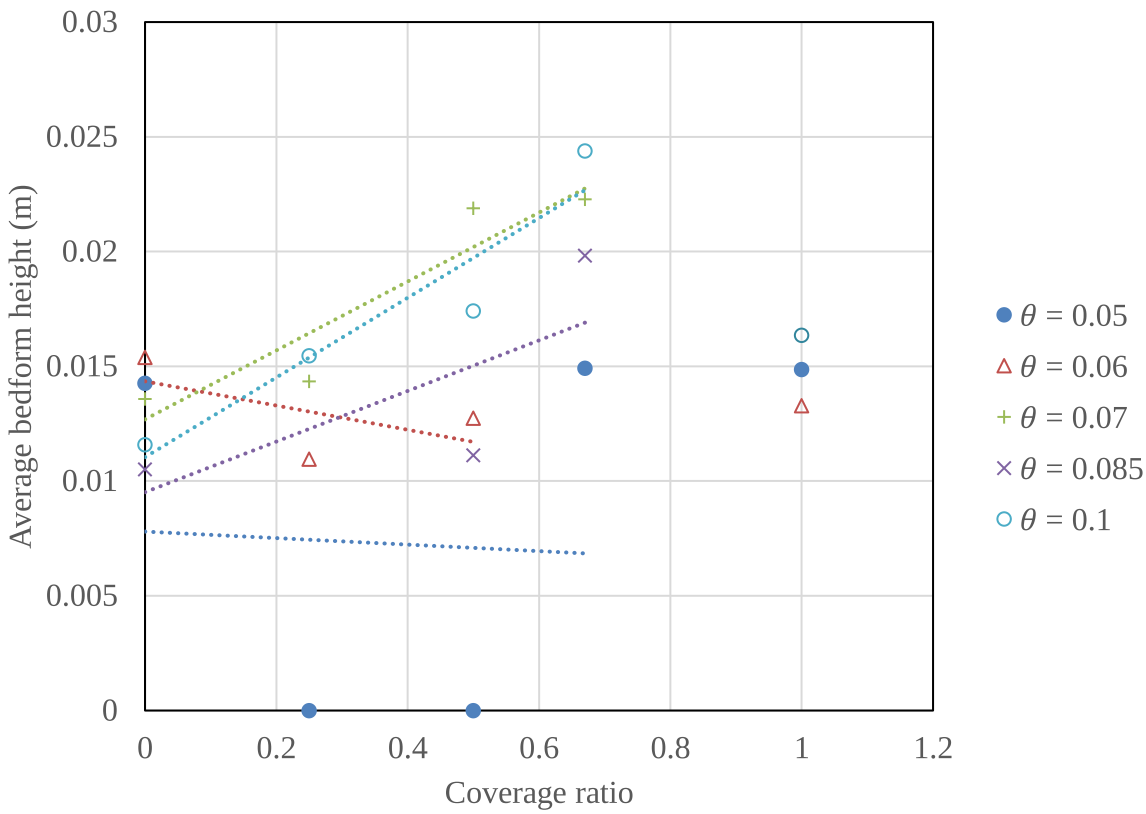

Figure 4.12. effect of increasing coverage ratio on bedform height for different flow strengths

To assess the impact of varying extents of border ice on bedform dimension within the channel width, average bedform height for different longitudinal profiles at various distances from the flume wall was calculated and plotted for different coverage ratios for both θ equals 0.07 and 0.1 (Figure 4.13). It was observed that, within partially ice-covered channels, an increase in coverage ratio generally led to an increase in bedform height for a fixed longitudinal position (y), a trend consistent for both θ values examined.

For $\theta = 0.07$ at a constant coverage ratio, moving from the vicinity of the flume wall towards the centerline led to an increase in bedform heights, transitioning from ice-covered regions to open water areas. However, for $\theta = 0.1$, for a constant coverage ratio, no special trend is noticeable moving from the flume wall to the centerline. This pattern highlights the increased complexity and irregularity of bedform profiles at higher flow strengths, where the influence of border ice extent changes on bedform dimensions becomes less pronounced. It's important to highlight that during the transition from partially ice-covered to fully ice-covered flow conditions, there's a significant decrease in the average bedform height across the entire channel width, making the bedform heights closely resemble those in open channel flow scenarios with a coverage ratio of 0. This observation indicates that, for the same flow strength, bedform development is notably more pronounced in partially ice-covered conditions than in either open channel flows or fully ice-covered situations.

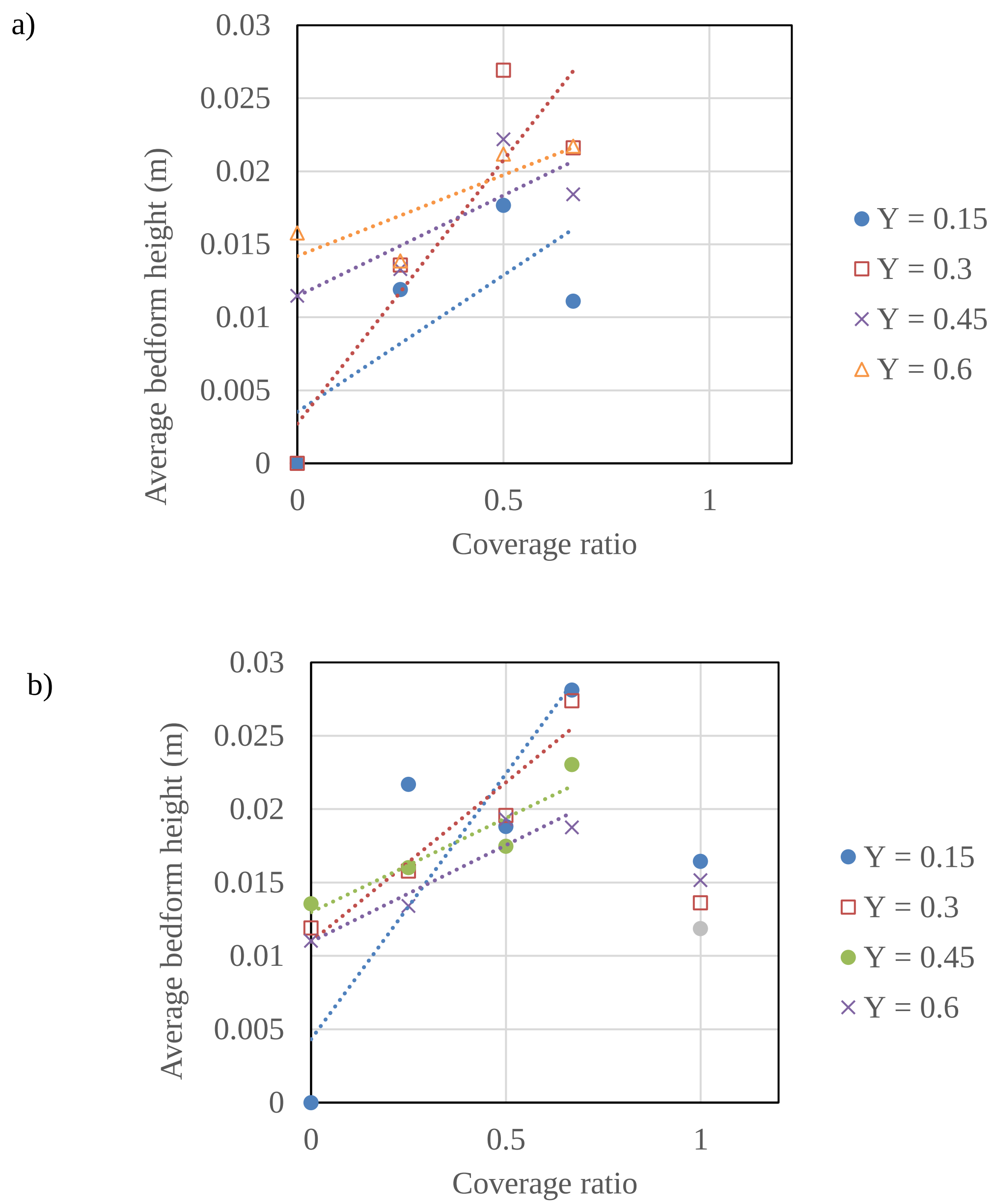

Figure 4.13. Effect of coverage ratio on bedform heights for a) θ =0.07, b) θ =0.1

4.4.5 Dune scaling relations

In a 2017 study, Bradley and Venditti compiled a comprehensive dataset of dune dimensions and flow characteristics, drawing from various sources that included laboratory flume experiments and field observations. They charted the dune height and length data on a graph, deducing that these parameters conform to a power law (Equation [4.4]), which is similar to Flemming's (1988) equation (Equation [4.5]):

$$H = 0.0513\ L^{0.7744} \qquad [4.4]$$

$$H = 0.0677\ L^{0.8098} \qquad [4.5]$$

In the current research, all dune heights and lengths from the depicted longitudinal profiles in the methodology section for all cases were calculated and are presented in Figure 4.14.

As the data from previous studies represented in this graph predominantly feature heights greater than 1 cm, heights less than 1 cm were excluded to ensure better comparability with these studies. Additionally, it allows the analysis to concentrate on larger-scale bedforms, while deliberately excluding smaller-scale variations (Venditti et al., 2016). The resulting data align with the ranges observed in previous studies, indicating that the proposed equations apply to partially and fully ice-covered flows as well as open channel flows.

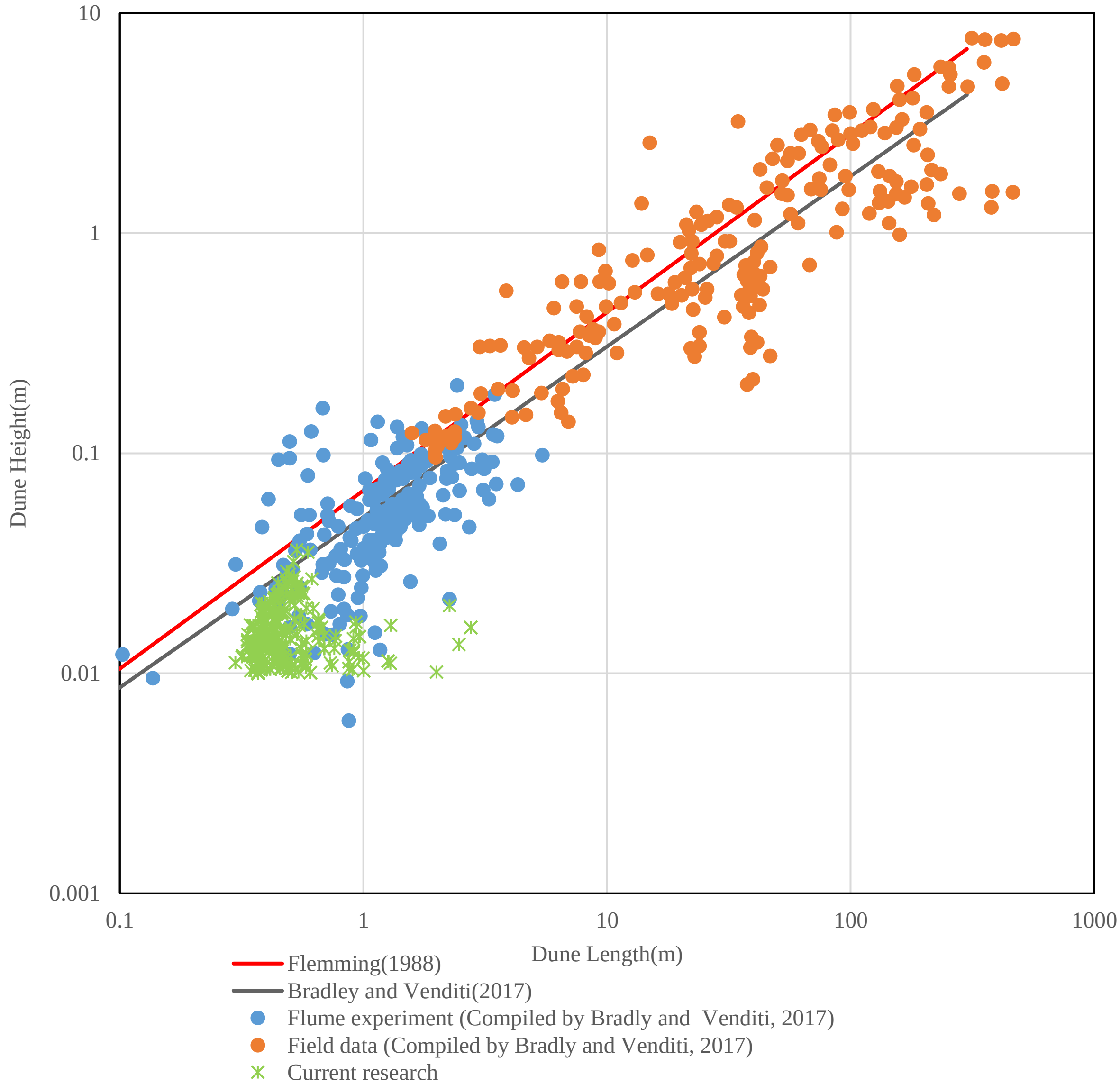

Figure 4.14. Visualization of dune height as a function of its length

Bradley and Venditti's plotted data indicated an upper limit of H = h/2.5, aligning with Alle's (1982) findings where almost no data points exceeded this threshold. Contrarily, the upper limit in the current study aligns with Yalin' s (1964) theory, suggesting H = h/6 as the maximal growth limit for dunes. Furthermore, the data points to a lower growth boundary, with scarcely any values below the h/H = 20 ratio (Figure 4.15a).

Regarding the lengths of dunes, both the current study's data and Bradley and Venditti's (2017) compiled dataset indicate that the L = 5h relation suggested by Yalin (1964)aligns with the central tendency of the data. In alignment with the constraints identified by Allen (1982), the data predominantly falls within the limits of L/h = 16 and L/h = 1 (Figure 4.15b)

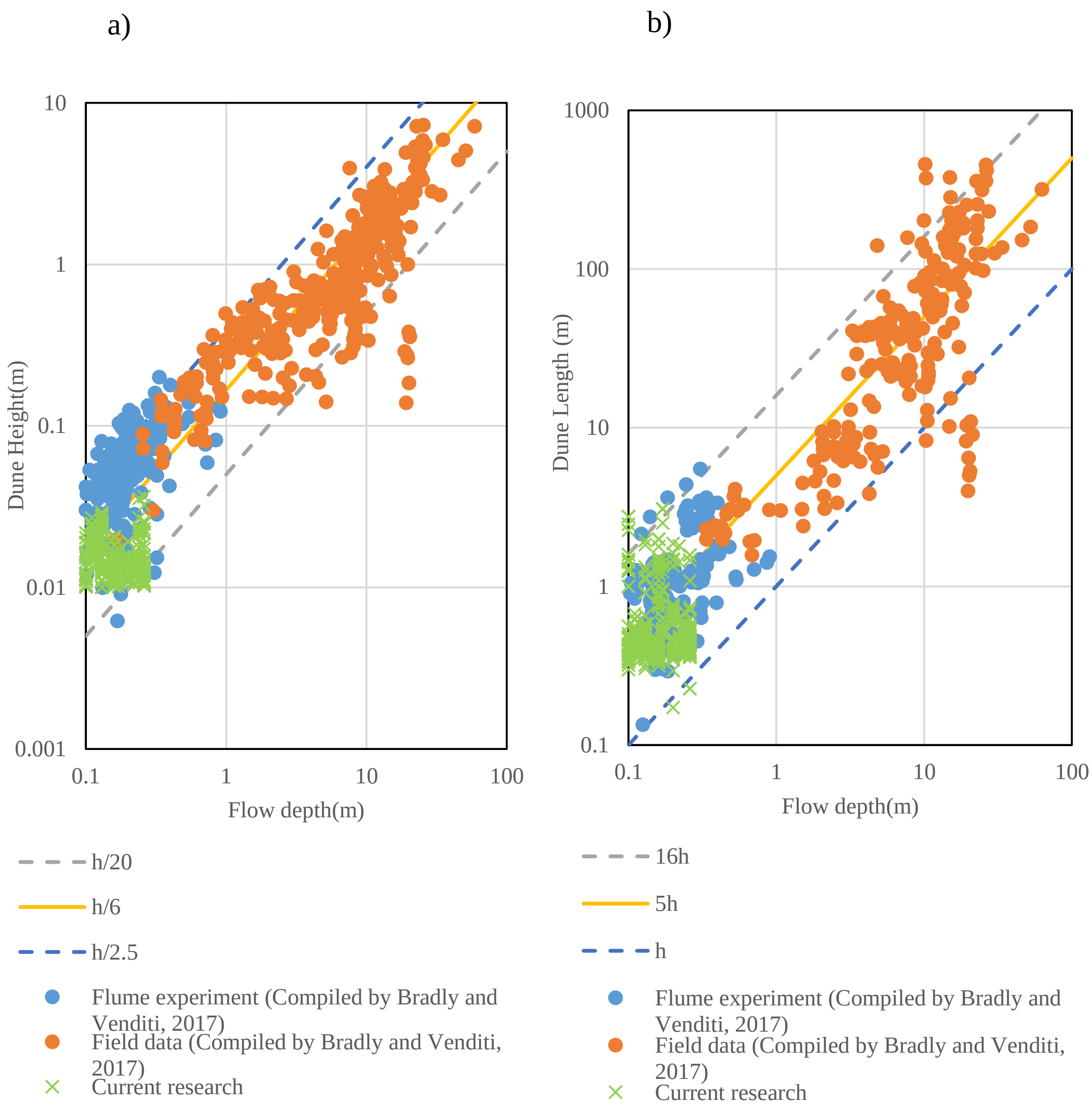

Figure 4.15. (a) Dune height versus flow depth. (b) Dune length versus flow depth. The dashed lines denote the boundaries identified by Allen (1982), and the solid lines illustrate the simplified scaling relations H = h/6 and L = 5h as defined by Yalin (1964).

4.5 Discussion

The present study has advanced the engineering capabilities for predicting the effect of ice cover on sediment transport, serving as a benchmark for future numerical investigations into sediment dynamics in rivers with partial ice coverage. Peters's (2015) research illustrates the effect of border ice on river flow, revealing a shift that results in decreased flow beneath ice-covered areas and enhanced flow in open areas. Building on this, Rouzegar and Clark (2023a, 2023c) further investigated how border ice affects the sediment transport rate within rivers, a crucial aspect of river dynamics and morphology.

Expanding on these insights, the current study delves into the broader implications of flow redistribution caused by ice cover, particularly focusing on its effects on bedforms. The findings suggest that the redistribution of flow not only influences sediment transport but also contributes to more prounounced bedform formation and an increase in the height of bedforms in open water areas. This elevation in bedform height is more than just a morphological change; it significantly influences the flow resistance encountered in open water sections of the river. An increase in flow resistance could trigger a series of further changes in how water is distributed across the river, introducing a new level of complexity to the flow dynamics. This complexity is particularly relevant in environments subject to seasonal ice cover, making the study of these flow dynamics a rich area for further research.

Figure 4.16a presents the distribution of bed load transport rates as detailed by Rouzegar and Clark (2023c), while Figure 4.16b displays the distribution of bedform heights across the channel width, derived from the current study, under identical experimental conditions. This setup features asymmetric border ice conditions with B_r = 0.2 m and B_l = 0.6 m, a flow strength of 0.07, and a coverage ratio of 0.67. On the right side of the figure, a detailed plan view of the flume is provided, showcasing both the sediment trap and the channel itself, providing a valuable reference for correlating the sediment transport rates indicated in the trap with the bedform patterns in the flume. The graphs reveal a consistency between the sediment transport rate distribution and bedform formation. In areas near the sides and under the border ice where sediment transport rates are lower, fewer bedforms are observed, mirroring the reduced sediment activity. Conversely, in the central area, which simulates open channel flow conditions, an elevated sediment transport rate leads to more pronounced bedform development. Continuing the experiment over an extended period could result in an increase in bedform size within the open channel sections, potentially increasing flow resistance and reducing the flow rate in these areas, and following this, less bedform formation and less increase in bedform height.

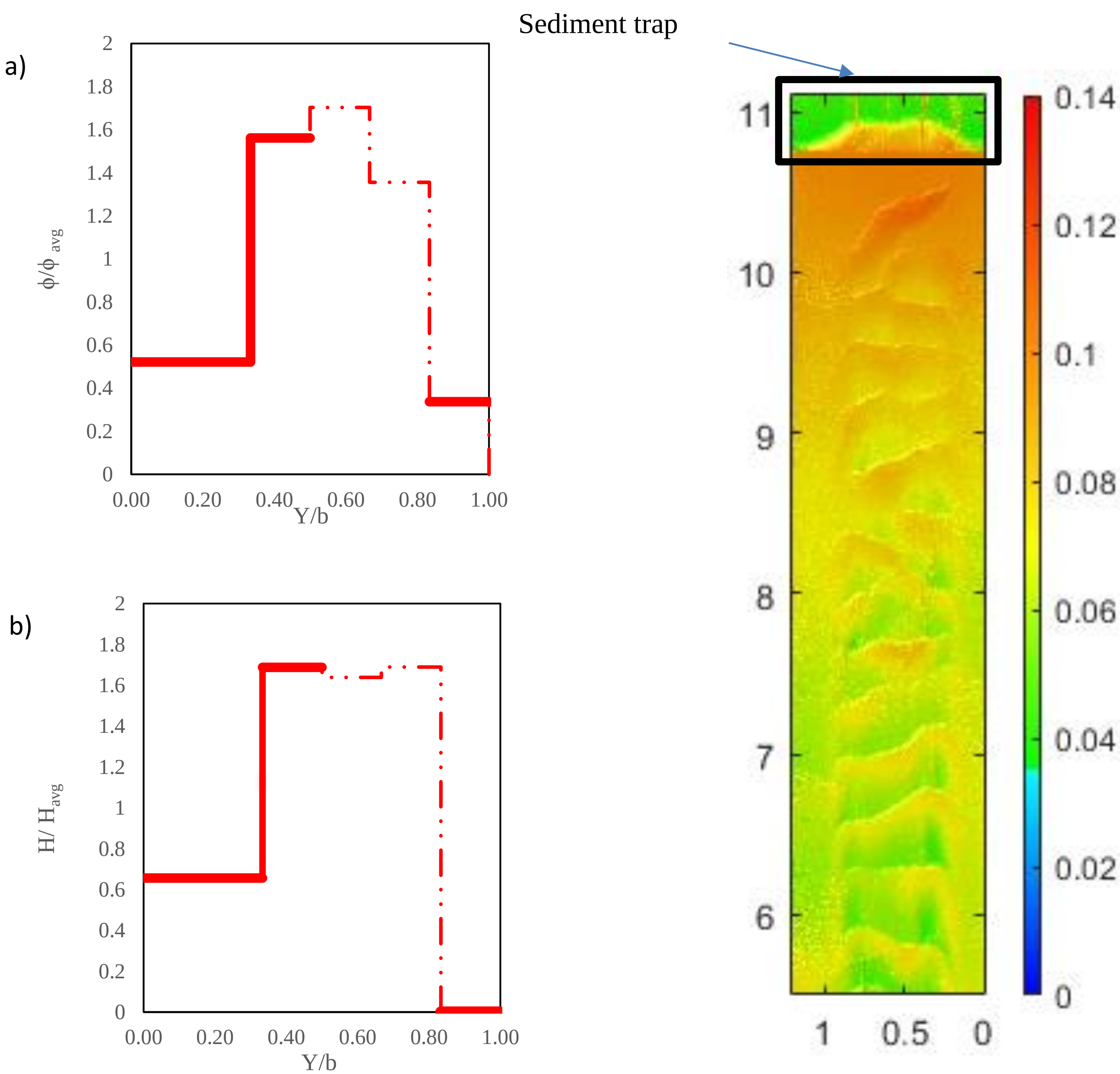

Figure 4.16. Comparative analysis of a) bedload transport rate distribution and b) bedform height variations across the channel width

In open channel flow conditions, observations of the velocity profile in the channel cross-section show two substantial counter-rotating vortices near the bed at each corner. A distinct pattern emerges in channels with partial ice coverage, revealing strong counter-rotating secondary circulations at the channel's center, accompanied by eight corner vortices (Figure 4.17). These core secondary circulations were driven by streamwise vorticity originating from the edges of the ice cover. With a decrease in ice coverage, there's a notable increase in the interactions between the core circulations and the corner vortices beneath the ice, leading to their eventual unification. The interaction between the central circulation and corner vortices forms a crucial connection linking the sections under ice cover with those of open water. Such a dynamic connection is likely to facilitate increased momentum, heat, and sediment transport in channels with partial ice cover compared to open channel flows (Essel et al., 2021). Additionally, this interaction can lead to an enhanced formation of bedforms, starting from the location at the vicinity of the border ice edge and extending into the open water area. Specifically, the current study's findings highlight that at a coverage ratio of 0.5, the peak of bedform height was observed right at the border ice edge, highlighting the significant influence that the ice boundary plays in dictating the contours of the underwater topographies within these transition zones.

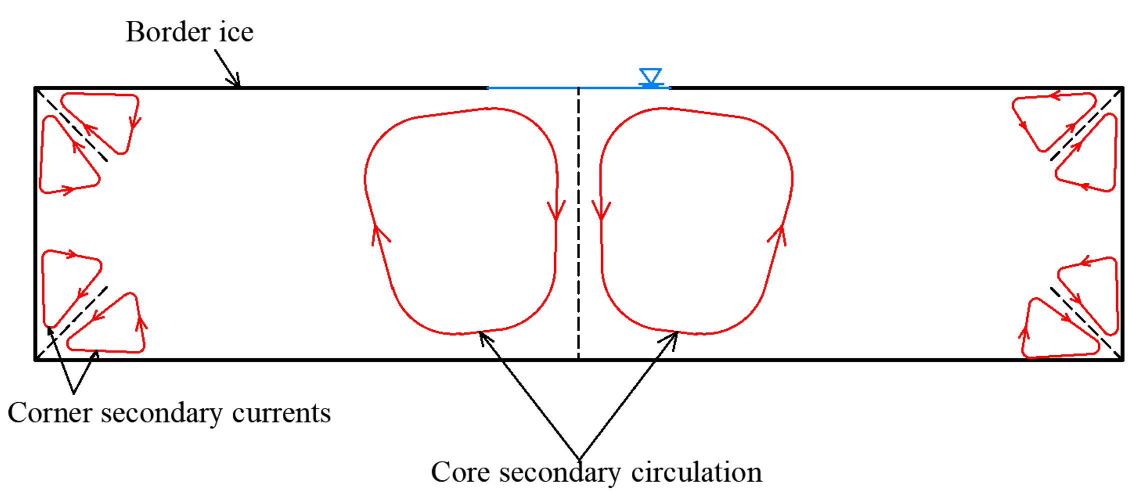

Figure 4.17. Schematic of secondary currents in the cross-section of partially ice-cover flow (modified from Essel et al. (2021).

4.6 Conclusions

The primary focus of this research was to analyze the bed morphology and formation of bedforms in rivers affected by partial ice cover. Through controlled laboratory experiments, the study aimed to determine how changes in the ice coverage ratio influence the height and wavelength of emerging bedforms. Bedform dimensions were evaluated across various experimental setups, including open channel conditions, symmetric and asymmetric border ice configurations, and fully ice-covered flows, and compared with theoretical models from existing literature. This comparison validated the applicability of these theoretical models for characterizing bedform dynamics in rivers with partial ice cover.

Additionally, the study examined how the extent of border ice, changes in flow strength, and the asymmetry of ice formations affect bedform characteristics. The formation of bedforms within the channel was notably influenced by the presence, positioning, and different degrees of partial ice cover. Specifically, the initiation point of bedforms relative to the flume wall was observed to shift further away as the ice coverage ratio increased. Additionally, bedform heights were found to be diminished beneath ice cover while being more pronounced in open water areas. Moreover, an increase in bedform height was observed adjacent to the ice edge, particularly for an ice coverage ratio of 0.5, where the maximum bedform height was recorded right at the ice boundary.

In cases of asymmetric border ice, bedforms occurred in an asymmetric pattern, affected by the ice coverage ratio. The influence of ice cover on the distribution of bedforms was particularly pronounced at lower flow strengths, diminishing with higher flow strengths where bedform patterns became more irregular and less predictable.

4.7 Acknowledgments

The authors would like to acknowledge Alexander Wall for his assistance with the experimental setup. This research was supported by the Natural Sciences and Engineering Research Council of Canada (NSERC-RGPIN-2018-06448).

Chapter 5 Conclusions and Future Work

5.1 Summary and Conclusions

The primary objective of this research was to investigate sediment transport and bed morphology in partially ice-covered rivers, a topic of significant importance in the context of alluvial rivers in cold climates. This pioneering study marks the first time that such an in-depth investigation has been conducted under these specific conditions, emphasizing the novelty and the critical advancements made in understanding these complex systems. The interaction between sediment dynamics and ice cover, especially during substantial shifts in flow conditions, plays a crucial role in modifying riverbeds. To address this, controlled laboratory experiments were conducted to explore bedload transport rate and bed morphology under various partially ice-covered conditions.

The thesis begins with a comprehensive literature review in **Chapter 1**, discussing key topics, including the formation of border ice, the hydraulic characteristics of partially ice-covered rivers, and the theories governing sediment transport and bed morphology.

Chapter 2 delves into studying the bedload transport rate and distribution in partially ice-covered rivers. It also examines the effects of varying extents of ice cover and changes in flow strengths on bedload transport distribution, comparing these with conditions observed under fully ice-covered and open channel flows. The experimental results suggest that the general form of the Knack and Shen's (2015) equation, intended for open and fully ice-covered flow, is applicable for estimating the total cross-section-averaged bedload transport rate in partially ice-covered conditions. However, this equation does not adequately capture the redistribution of bedload transport under partial ice cover. The results further demonstrated that an increase in the partial ice coverage ratio reduces the total bedload transport across the channel for a constant discharge.

Prior studies, such as those by (Essel et al., 2021; Kimiaghalam et al., 2017; Peters, 2015) have shown that the presence of border ice causes significant redistribution in flow characteristics. This study corroborates those findings, showing that the presence of border ice also redistributes bedload transport. A coefficient $(\phi_R + \phi_L)/\phi_M$ was defined and calculated to quantify this redistribution, revealing that differences in coverage ratios minimally affected bedload transport distribution at dimensionless flow strengths near 0.1. However, at lower flow strengths, an increase in border ice significantly altered bedload distribution, decreasing transport rates near the banks and increasing them in the central channel.

The results presented in Chapter 2 fulfill Research Objective 1 and establish a significant benchmark in the study of fluvial dynamics. This research is pioneering, being the first to be documented in a peer-reviewed journal that provides a comprehensive analysis of sediment transport in partially ice-covered rivers. Historically, investigations into this subject have been limited to either open channel flow or fully ice-covered flow scenarios. This study breaks new ground by examining the effects of border ice on sediment dynamics and transport rates, a topic that has not been explored previously.

The novelty of this research is highlighted by adapting previously established equations, which were limited to open and fully ice-covered flows, for use under partially ice-covered conditions. This adaptation includes the derivation of an empirical coefficient specifically tailored to these conditions. Moreover, this study is the first to explore and quantify the redistribution of bedload transport due to the presence of border ice, significantly enhancing our understanding of how partial ice cover influences riverine sediment transport. These groundbreaking insights not only fulfill a crucial research gap but also set a new precedent for future investigations into the complex interplay of ice dynamics and sediment transport in cold climate rivers.

Chapter 3 focused on investigating the bedload transport rate and distribution in channels featuring asymmetric partial ice cover. The research examined how asymmetric border ice, varying coverage ratios, and different flow strengths influence bedload transport. The study also included comparisons with symmetrically partially ice-covered flow conditions to gauge differences. A key part of the investigation was assessing the suitability of the Knack and

Shen's (2015) formula for estimating the total cross-section-averaged bedload transport rate in rivers with asymmetric partial ice cover.

The findings revealed that asymmetric border ice significantly alters bedload transport distribution within the channel, leading to a non-uniform distribution across the channel width, with peak transport rates typically concentrated in the center of the open flow section. The degree of asymmetry in border ice was directly linked to a corresponding asymmetry in bedload transport rate distribution. Moreover, this redistribution was found to be more pronounced at higher flow strengths and became less noticeable at lower flow strengths.

Despite the marked variability in bedload transport across the channel, the study confirmed that the cross-section-averaged bedload transport rate could still be effectively estimated using Knack and Shen's (2015) equation with modifications to account for the effects of ice cover. This involved incorporating an additional boundary in the calculation of the wetted perimeter, which necessitated adjustments in flow strength. This approach ensures that even in the presence of significant asymmetrical partial ice coverage, reliable estimations of bedload transport can be achieved, enhancing the understanding and management of sediment dynamics in ice-affected rivers.

This chapter continues the investigation on the effects of border ice on sediment transport rate and distribution in partially ice-covered channels by focusing on the impact of border ice asymmetry. These findings contribute directly to Research Objective 2, marking this study as a peer-reviewed journal publication that provides detailed insights into the impact of asymmetric border ice on sediment transport. By systematically examining different conditions of border ice, this research formulates and quantifies the bedload transport rates under these varying conditions for the first time, significantly advancing our understanding of sediment dynamics under partial ice coverage and its implications for river management.

Chapter 4 focuses on analyzing bed morphology and bedforms in rivers influenced by partial ice cover. The study aimed to determine how changes in the ice coverage ratio influence bedform height and wavelength. Bedform dimensions were assessed in various experimental setups, including open channel conditions, symmetric and asymmetric border ice configurations, and fully ice-covered flows, and they were compared with theoretical models from the existing literature. This comparison confirmed the applicability of these models for characterizing bedform features under partial ice cover. The study further examined how the extent of border ice, flow strength variations, and border ice asymmetry impact bedform characteristics. The presence of border ice notably affected bedform formation, with initiation points shifting further from the flume wall as ice coverage increased. Bedform heights were diminished under ice cover and were more pronounced in open water areas, with an increase in bedform height observed adjacent to the ice edge, especially at an ice coverage ratio of 0.5.

In cases of asymmetric border ice, bedforms displayed an asymmetric pattern influenced by the ice coverage ratio. The impact of ice cover on bedform distribution was especially marked at lower flow strengths, diminishing with higher flow strengths where bedform patterns became more irregular and less predictable. This comprehensive study provides vital insights into sediment transport dynamics and bed morphology in cold climate rivers, enhancing our understanding and informing future river management and engineering efforts.

Notably, prior to this research, there had been no studies on bedform dimensions in partially ice-covered conditions. This novel study simulates the effects of border ice and its impact on bedform dimensions for the first time, comparing the results with equations previously established for open channel and fully ice-covered flow conditions. Including both symmetric and asymmetric border ice configurations, this research provides unprecedented insights into bedform distribution across the channel width in partially ice-covered rivers. This is significant, as bedform dimensions can crucially affect flow characteristics in cold regions. Contributing directly to Objective 3 of this research, this chapter establishes a foundational understanding of how partial ice cover influences riverine landscapes, offering new perspectives that are essential for advancing river management strategies in cold climates.

5.2 Limitations

This study represents the first in-depth investigation of bedload transport in partially ice-covered rivers. To ensure the feasibility and manageability of the experiments, several simplifications were made. These limitations highlight areas for potential improvement and future research.

1. **Experimental Setup Constraints**

Pump Capacity: The limited pump capacity resulted in restricted flow rates, which may not fully represent natural river conditions.

Measurable Amount of Sand: The amount of sand that could be collected in the sediment trap, transported, and weighed was constrained by the laboratory setup and the physical capabilities of the personnel involved. Handling large quantities of sand posed practical challenges and influenced the scope of the experiments.

Measurable Time: The duration of experiments was limited to short-term studies to minimize the effects of not having an upstream sediment supply, potentially affecting the long-term applicability of the results.

2. **Actual Border Ice Rigidity**

The use of bubble wrap as a substitute for border ice presented a limitation. While bubble wrap is a relatively soft and easily deformable material, actual border ice is more rigid and less flexible, potentially affecting the accuracy of the experiments.

3. **Thermal Effects**

Thermal effects, which can significantly influence water viscosity and sediment transport dynamics, were not considered in this study. Future research could incorporate thermal variations to better simulate real-world conditions.

4. Uniform Flow Conditions

The experiments were conducted under uniform flow conditions, which do not account for the natural variations and turbulence found in real river scenarios. Incorporating non-uniform flow conditions would enhance the realism and applicability of the findings.

5. Uniform Sand Particles

The study used uniform sand particles, limiting the applicability of the results to different sediment sizes and distributions. The experimental conditions, especially the particle size, restricted the bedform to dunes, with no ripples occurring in the experiments. Future studies should consider a range of sediment sizes to better understand their impact on bedload transport and bedform.

6. Anchor Ice Formation

Anchor ice formation, a significant factor in sediment transport by ice, was not considered in this study. Investigating the role of anchor ice in sediment dynamics would provide a more comprehensive understanding of the processes involved.

5.3 Future Work

Laboratory Studies

1. **Expand Experimental Scope:** Additional experiments should be conducted with the same apparatus that was used for the test series in this thesis to further explore the influence of variables such as aspect ratio, bed roughness, and border ice roughness on bedload transport rate and bed morphology. These experiments would provide deeper insights into how these factors interact to affect sediment dynamics.

2. **Comprehensive Long-Term Experimental Studies with Upstream Sand Supply:** Future studies should integrate long-term experiments with a consistent upstream sand supply to assess the sustained impact of border ice on riverbed evolution and bedload transport. This approach is essential to understanding the long-term

development of bedforms and the time required to reach equilibrium under varied sediment dynamics scenarios. Experiments should include periodic pauses to analyze bed formation over time, offering insights into how the presence of border ice influences sediment dynamics over extended periods. Continuous sediment input is necessary for these long-term experiments due to the significantly higher overall movement of sediment, which provides a more realistic assessment of natural river conditions.

3. **Investigation of Bedform Movement Velocity in Channel Width:** Future studies should also focus on investigating the velocity of bedform movement across different sections of the channel width. Understanding how bedforms migrate and their interaction with varying flow conditions and ice cover will provide a more comprehensive understanding of sediment dynamics in partially ice-covered rivers.

Numerical Modeling

4. **Model Validation and Expansion:** The experimental results obtained from this study provide a valuable basis for validating two-dimensional numerical models designed to simulate river ice dynamics. These models can be utilized to simulate various conditions of partially ice-covered flow, allowing parameters to be adjusted over a broader range than is feasible with experimental methods. This approach will enhance our understanding of sediment transport and bed morphology dynamics in rivers with partial ice cover.

5. **Dynamic Numerical Analysis:** There is a need to employ numerical models to dynamically investigate how the growth of border ice affects sediment transport and bed formation. By simulating these processes, the models will provide a dynamic view of how sediment behavior and riverbed morphology evolve as border ice develops, offering valuable insights into these interactions' transient and complex nature.

References

Agisoft Software. (2016). Agisoft PhotoScan User Manual. *Professional Edition, Version 1.2*.

ASTM C-128-15. (2015). Standard test method for density, relative density (specific gravity) and absorption of fine aggregates. West Conshohocken, PA, USA: ASTM International.

Allen, J. R. L. (1978). Computational models for dune time-lag: calculations using Stein's rule for dune height. In *Sedimentary Geology*, 20, 165-216.

Al-Abed, N.M.A. (1989). *Sediment Transport under Ice Covered Channels. (Ph.D. Dissertation*). University of Kashmir, Srinagar, India.

Ashton, G. (1986). *River and lake ice engineering*. Water Resources Publications, LLC.

Barton, J. R., & Lin, P. N. (1995). A Study of the Sediment Transport in Alluvial Channels.

Binns, A. D., & da Silva, A. M. (2009). On the quantification of the bed development time of alluvial meandering streams. Journal of Hydraulic Engineering, 135(5), 339e438.

Blackburn, J., & She, Y. (2019). A comprehensive public-domain river ice process model and its application to a complex natural river. Cold Regions Science and Technology, 163, 44e58.

Bradley, R. W., & Venditti, J. G. (2017). Reevaluating dune scaling relations. In *Earth-Science Reviews*, 165, 356–376. https://doi.org/10.1016/j.earscirev.2016.11.004

Carr, M. L., & Tuthill, A. M. (2012). Modeling of Scour-Inducing Ice Effects at Melvin Price Lock and Dam. *Journal of Hydraulic Engineering*, *138*(1), 85-92. https://doi.org/10.1061/(asce)hy.1943-7900.0000483

Chein, N. & Wan, Z. (1999). *Mechanics of sediment transport*, ASCE Press, Reston, VA, USA.

Chen, J., Wang, Z., Li, M., Wei, T., & Chen, Z. (2012). Bedform characteristics during falling flood stage and morphodynamic interpretation of the middle-lower Changjiang (Yangtze) River channel, China. *Geomorphology*, *147–148*. https://doi.org/10.1016/j.geomorph.2011.06.042

Chow, V. Te. (1959). Open-Channel Hydraulics. Ven Te Chow. McGraw-Hill, New York, 1959.

Clark, S. (2013). Border and Skim Ice. In S. Beltaos (Ed.), *River Ice Formation*. Committee on River Ice Processes and the Environment: Edmonton, AB, Canada**,** 77–106.

Coleman, H. W., & Steele, W. G. (1999). Experimentation and uncertainty analysis for engineers (2nd ed.). New York: John Wiley & Sons.

Einstein, H. A. (1950). *The bed load function for sediment transport in open channels*, Technical Bulletin 1026, U.S. Department of Agriculture, Washington, D.C., U.S.

Essel, E. E., Clark, S. P., Dow, K., & Tachie, M. F. (2021). Experimental and numerical investigation of three-dimensional open channel with simulated partial ice-covers. *Journal of Hydraulic Research*, *59*(6), 977-988. https://doi.org/10.1080/00221686.2020.1862322

Ettema, R., Braileanu, F., & Muste, M. (1999). Laboratory study of suspended sediment transport in ice-covered flow Laboratory Study of Suspended Sediment Transport in Ice-Covered Flow. IIHR Report No. 404, Iowa Institute of Hydraulic Research, University of Iowa, Iowa City, Iowa.

Ettema, R., Braileanu, F., & Muste, M. (2000). Method for estimating sediment transport in ice-covered channels. *Journal of Cold Regions Engineering*, *14*(3).

Ettema, R., & Daly, S. F. (2004). *Sediment transport under ice*. U.S. Army Crops of Engineers Report ERDC/CRREL TR-0420, Engineer Research and Development Center, Cold Regions Research and Engineering lab, Hanover, NH.

Ettema, R. (2008). Ice Effects on Sediment Transport in Rivers. In *Sedimentation Engineering: Processes, measurements, modeling, and practice*, 613-648. https://doi.org/10.1061/9780784408148.ch13

Flemming, B. W. (1988). Zur klassifikation subaquatischer, strömungstransversaler Transportkörper. Bochumer geologische und geotechnische Arbeiten, 29(93-97), 44-47.

García, M. H. (2007). ASCE manual of practice 110-Sedimentation engineering: Processes, measurements, modeling, and practice. Examining the Confluence of Environmental and Water Concerns - Proceedings of the World Environmental and Water Resources Congress 2006. https://doi.org/10.1061/40856(200)94

Gill M.A. (1971). Height of sand dunes in open channel flows. *Journal of the Hydraulics Division, 97(12), 2067-2074.* https://doi.org/10.1061/jyceaj.0003169

Hirayama, K. (1986). Growth of ice cover in steep and small rivers. *8th International Symposium on Ice*, 451–464.

Julien, P. Y. (1995). *Erosion and Sedimentation.* New York: Cambridge University Press.

Julien, P. Y., & Klaassen, G. J. (1995). Sand-Dune Geometry of Large Rivers during Floods. *Journal of Hydraulic Engineering*, *121*(9). https://doi.org/10.1061/(asce)0733-9429(1995)121:9(657)

Kämäri, M., Alho, P., Veijalainen, N., Aaltonen, J., Huokuna, M., & Lotsari, E. (2015). River ice cover influence on sediment transportation at present and under projected hydroclimatic conditions. *Hydrological Processes*, *29*(22). https://doi.org/10.1002/hyp.10522

Karim, F. (1995). Bed Configuration and Hydraulic Resistance in Alluvial-Channel Flows. *Journal of Hydraulic Engineering*, *121*(1). https://doi.org/10.1061/(asce)0733-9429(1995)121:1(15)

Karim, F. (1999). Bed-Form Geometry in Sand-Bed Flows. *Journal of Hydraulic Engineering*, *125*(12). https://doi.org/10.1061/(asce)0733-9429(1999)125:12(1253)

Kempema, E. W., & Ettema, R. (2011). Anchor ice rafting: observations from the Laramie River. *River research and applications*, *27*(9), 1126-1135.

Khosravi, K., Chegini, A. H. N., Cooper, J. R., Daggupati, P., Binns, A., & Mao, L. (2020). Uniform and graded bed-load sediment transport in a degrading channel with non-equilibrium conditions. International Journal of Sediment Research, 35(2), 115e124.

Kimiaghalam, N., Clark, S., & Dow, K. (2017). Estimation of shear stress distribution in a partially-covered channel. CGU HS Committee on River Ice Processes and the Environment, *19th workshop, Hydraulics of Ice-covered Rivers,* July 9-12, 2017, Whitehorse, Yukon, Canada.

Kimiaghalam, N., Clark, S. P., & Dow, K. (2018). Flow characteristics of a partially-covered trapezoidal channel. *Cold Regions Science and Technology*, *155*. https://doi.org/10.1016/j.coldregions.2018.08.016

Knack, I. (2011). *Mathematical modeling of river dynamics with thermal-ice-sediment processes (Ph.D. Dissertation).* Department of Civil and Environmental Engineering, Clarkson University, Potsdam, NY, U.S.

Knack, I., & Shen, H. T. (2015). Sediment transport in ice-covered channels. *International Journal of Sediment Research*, *30*(1), 63–67. https://doi.org/10.1016/S1001-6279(15)60006-3

Knack, I.M., & Shen, H.T. (2018). A numerical model for sediment transport and bed change with river ice. *Journal of Hydraulic Research. 56*(6), 844-856. https://doi.org/10.1080/00221686.2017.1414719

Knight, D. W., Demetriou, J. D., & Hamed, M. E. (1984). Boundary shear in smooth rectangular channels. *Journal of Hydraulic Engineering*. *110*(4), 405-422. https://doi.org/10.1061/(asce)0733-9429(1984)110:4(405)

Kolerski, T., & Shen, H. T. (2015). Possible effects of the 1984 St. Clair river ice jam on bed changes. *Canadian Journal of Civil Engineering*, *42*(9). https://doi.org/10.1139/cjce-2014-0275

Lane, E. W., & Eden, E. W. (1940). Sand Waves in the Lower Mississippi River. *Proceedings of Western Society of Professional Engineers, 45*(6), 281–291.

Lawson, D. E., Chacho, E.F. Jr., Brockett, B.E., Wuebben, J.L., Collins, C.M., Arcone, S.A., & Delaney, A.J. (1986). *Morphology, hydraulics, and sediment transport of an ice- covered river: Field techniques and initial data*. U.S. Army Crops of Engineering CRREL Report 86-11, U.S. Army Cold Regions Research and Engineering Laboratory, Hanover, NH.

Lefebvre, A., Paarlberg, A. J., & Winter, C. (2016). Characterising natural bedform morphology and its influence on flow. *Geo-Marine Letters, 36*(5). https://doi.org/10.1007/s00367-016-0455-5

Majewski, W. (1992). Laboratory investigation of the flow in open channels with partial ice cover. *Proceedings of the 11th International Symposium on Ice,* (pp. 335–345), June 15-19, 1992, Banff, Alberta, Canada.

Majewski, W., & Baginska, M. (1988). Hydraulic Conditions in open channels with ice cover. *Proceedings of the 9th International Symposium on Ice* , 112–121.

Manolidis, M., & Katopodes, N. (2014). Bed scouring during the release of an ice jam. *Journal of Marine Science and Engineering*, *2*(2), 370-385, https://doi.org/10.3390/jmse2020370

Matousek, V. (1984). Regularity of the Freezing-up of the Water Surface and Heat Exchange between Water Body and Water Surface. *Proceedings of the 7th International Symposium on Ice*, 187–200.

Meyer-Peter, E. & Muller, R. (1948). Formulas for bed-load transport. *Proceedings of the 2nd Meeting of IAHR*, (pp. 39–64), June7, 1948, Stockholm, Sweden.

Miles, T. M. (1993). A Study of Border Ice Growth on the Burntwood River. University of Manitoba.

Munson, B. R., Okiishi, T. H., Huebsch, W. W., Rothmayer, & P, A. (2013). Fundamentals of Fluid Mechanics Seventh Edition. In *Instrumentation, Measurements, and Experiments in Fluids*.

Muste, M., Braileanu, F. & Ettema, R. (2000). Flow and sediment transport measurements in a simulated ice-covered channel. *Water Resources Research*, *36*(9), 2711–2720.

Newbury, R. (1986). The Nelson River: A Study of Subarctic River Processes. John Hopkins University.

Nezu, I., & Rodi, W. (1986). Open-channel flow measurements with a laser Doppler anemometer. Journal of Hydraulic Engineering, 112(5), 335e355.

Nezu, I., & Nakagawa, H. (1993). *Turbulence in open-channel flows*. Rotterdam, Netherlands: A.A. Balkema.

Nyantekyi-Kwakye, B., Essel, E. E., Dow, K., Clark, S. P., & Tachie, M. F. (2021). Hydraulic and turbulent flow characteristics beneath a simulated partial ice-cover. *Journal of Hydraulic Research*. *59*(3), 392-403. https://doi.org/10.1080/00221686.2020.1780493

Olsen, O. J., & Florey, Q. L. (1952). Sedimentation studies in open channels: Boundary shear and velocity distribution by membrane analogy, analytical and finitedifference methods. Denver, CO, USA: U. S. Bureau of Reclamation, Design and Construction Division.

Pajunen, V., Lotsari, E., Välimäki, J., Wolff, F., Kärkkäinen, M., Blåfield, L., & Eltner, A. (2024). The impacts of low flow, ice-cover and ice thickness on sediment load in a sub-arctic river – Modelling sediment transport with particle image velocimetry calibration data sets. *Earth Surface Processes and Landforms*. https://doi.org/10.1002/esp.5809

Peters, M. (2015). *An experimental study of the hydraulic characteristics beneath a partial ice cover (M. S. thesis)*. Department of Civil Engineering, University of Manitoba, Winnipeg, Manitoba.

Peters, M., Clark, S. P., Dow, K., Malenchak, J., & Danielson, D. (2018). Flow characteristics beneath a simulated partial ice cover: Effects of ice and bed roughness.

Journal of Cold Regions Engineering, *32*(1). https://doi.org/10.1061/(asce)cr.1943-5495.0000143

Peters, M., Dow, K., Clark, S. P., Malenchak, J., & Danielson, D. (2017). Experimental investigation of the flow characteristics beneath partial ice covers. *Cold Regions Science and Technology*, *142*, 69–78. https://doi.org/10.1016/j.coldregions.2017.07.007

Raudkivi, A. J. (1998). Loose boundary hydraulics. In *Loose boundary hydraulics*. https://doi.org/10.1139/l91-110

Rouzegar, M., & Clark, S. P. (2022). Sediment transport rate estimation in partially ice-covered channels. In 26th IAHR international symposium on ice, June 19-23, 2022, Montreal, Canada.

Rouzegar, M., & Clark, S. P. (2023a). Experimental investigation of sediment transport in partially ice-covered channels. *International Journal of Sediment Research*, 38, 769–779. https://doi.org/10.1016/j.ijsrc.2023.06.003

Rouzegar, M. & Clark, S.P. (2023b) Experimental Investigation of Asymmetric Border Ice Effect on Sediment Transport. *Proceedings of the 40th IAHR World Congress*, Vienna, Austria, 21–25 August 2023.

Rouzegar, M., & Clark, S. P. (2023c). Sediment Transport Beneath a Simulated Partial Ice Cover: Effects of Asymmetric Border Ice. *Water (Switzerland)*, *15*(23). https://doi.org/10.3390/w15234153

Rouzegar, M., & Clark, S. P. (2023d). Experimental investigation of border ice effect on bedform development. *CGU HS Committee on River Ice Processes and the Environment 22nd Workshop on the Hydraulics of Ice-Covered Rivers*, 9–12.

Sayre, W. W., & Song, G. B. (1979). Effects of ice covers on alluvial channel flow and sediment transport processes. IIHR Report No. 218. USA: Iowa Institute of Hydraulic Research, University of Iowa, Iowa City, Iowa.

She, Y., Hicks, F., Steffler, P., & Healy, D. (2009). Constitutive model for internal resistance of moving ice accumulations and Eulerian implementation for river ice jam formation. Cold Regions Science and Technology, 55(3), 286e294.

Shen, H. T. (2002). Development of a comprehensive river ice simulation system. In Proceedings of the 16th IAHR international symposium on ice, IAHR (pp. 142e148). December 2e6, 2002, Dunedin, New Zealand.

Shen, H. T., & Wang, D. S. (1995). Under cover transport and accumulation of frazil granules. Journal of Hydraulic Engineering, 121(2), 94e215.

Singh, B. (1960). Transport of bed-load in channels with special reference to gradient and form [Doctoral dissertation]. Imperial College London.

Singh, A., Guala, M., Lanzoni, S., & Foufoula-Georgiou, E. (2012). Bedform effect on the reorganization of surface and subsurface grain size distribution in gravel bedded channels. *Acta Geophysica*, *60*(6), 1607–1638. https://doi.org/10.2478/s11600-012-0075-z

Smith, B. T. & Ettema, R. (1995). *Ice-Cover influence on flow and bedload transport in dune-bed channels*, IIHR Report No. 374, Iowa Institute of Hydraulic Research, University of Iowa, Iowa City, Iowa.

Steffler, P., & Blackburn, J. (2002). River2D: Two-Dimensional depth averaged model of River Hydrodynamics and fish Habitat, introduction to depth averaged modeling and User's manual (p. 120). Edmonton, Alberta, Canada: University of Alberta.

Sturm, T. W. (2010). *Open Channel Hydraulics* (2nd ed.). McGraw-Hill.

Teal, M. J., Ettema, R., & Walker, J. F. (1994). Estimation of mean flow velocity in ice-covered channels. *Journal of Hydraulic Engineering*. https://doi.org/10.1061/(ASCE)0733-9429(1994)120:12(1385)

Tsai, W.F., & Ettema, R. (1994). Modified eddy viscosity model in fully developed asymmetric channel flows. *Journal of Engineering Mechanics*, *120*(4), 720-732. https://doi.org/10.1061/(ASCE)0733-9399(1994)120:4(720)

Tsang, G. (1970). Change of Velocity Distribution in a Cross-Section of a Freezing River and the Effect of Frazil Ice Loading on Velocity Distribution. *1st International Symposium on Ice*, 1–11.

Turcotte, B., Morse, B., Bergeron, N. E., & Roy, A. G. (2011). Sediment transport in ice-affected rivers. *Journal of Hydrology*, *409*(1-2), 561–577.

Van Rijn, L. C. (1984). Sediment Transport, Part III: Bed forms and Alluvial Roughness. *Journal of Hydraulic Engineering*, *110*(12). https://doi.org/10.1061/(asce)0733-9429(1984)110:12(1733)

Vanoni, V. A., & Brooks, N. H. (1957). *Laboratory studies of the roughness and suspended load of alluvial streams* (Vol. 11). US Army Engineer Division.

Venditti, J. G., Lin, C. Y. M., & Kazemi, M. (2016). Variability in bedform morphology and kinematics with transport stage. *Sedimentology*, *63*(4). https://doi.org/10.1111/sed.12247

Wazney, L., Clark, S. P., & Wall, A. J. (2018). Field monitoring of secondary consolidation events and ice cover progression during freeze-up on the Lower Dauphin River, Manitoba. Cold Regions Science and Technology, 148, 159e171.

Wuebben, J. L. (1986). A laboratory study of flow in an ice-covered sand bed channel *Proceedings of the 8th International Symposium on Ice, IAHR*, (pp. 3–14), August 7-31, 1986, Iowa City, USA.

Wuebben J. L. (1988). Effects on an ice cover on flow in a movable bed channel, *Proceedings of the 9th International Symposium on Ice, IAHR*, (pp. 137–146), August 23-27, 1988, Sapporo, Japan.

Yalin, M. S. (1964). Geometrical Properties of Sand Wave. *Journal of the Hydraulics Division*, *90*(5). https://doi.org/10.1061/jyceaj.0001097

Yang, X., Zhang, B. & Shen, H.T. (1993). Simulation of wintertime fluvial processes in lower Yellow River. *Journal of Sedimentary Research*. 2, 36–43.

Zabilansky, L. J., Hains, D. B., & Remus, J. I. (2007). Increased bed erosion due to ice. *Proceedings of the International Conference on Cold Regions Engineering*. https://doi.org/10.1061/40836(210)16

Zhang, B., Yang, X., & Shen, H. (1994). Simulation of wintertime fluvial processes in lower Yellow River. *Journal of Hydrodynamics*, *6*(1).